REPUBLIC OF TURKEY
YILDIZ TECHNICAL UNIVERSITY
GRADUATE SCHOOL OF NATURAL AND APPLIED SCIENCES

X-BAND ISOFLUX MICROSTRIP PATCH ANTENNA ARRAY DESIGN FOR LOW EARTH ORBIT SATELLITES

Elif ALPAGU

MASTER OF SCIENCE THESIS
Department of Electronics and Communications Engineering
Program of Communications

Advisor
Prof. Dr. Ahmet KIZILAY

July, 2019

REPUBLIC OF TURKEY
YILDIZ TECHNICAL UNIVERSITY
GRADUATE SCHOOL OF NATURAL AND APPLIED SCIENCES

X-BAND ISOFLUX MICROSTRIP PATCH ANTENNA ARRAY DESIGN FOR LOW EARTH ORBIT SATELLITES

A thesis submitted by Elif ALPAGU in partial fulfillment of the requirements for the degree of **MASTER OF SCIENCE** is approved by the committee on 16.07.2019 in Department of Electronics and Communications Engineering, Program of Communications.

Prof. Dr. Ahmet KIZILAY
Yildiz Technical University
Advisor

Approved By the Examining Committee

Prof. Dr. Ahmet KIZILAY, Advisor
Yildiz Technical University

Doç.Dr.Hamid TORPİ, Member
Yildiz Technical University

Phd. Lecturer Peyman MAHOUTİ, Member
Istanbul Arel University

I hereby declare that I have obtained the required legal permissions during data collection and exploitation procedures, that I have made the in-text citations and cited the references properly, that I haven't falsified and/or fabricated research data and results of the study and that I have abided by the principles of the scientific research and ethics during my Thesis Study under the title of X-Band Isoflux Microstrip Patch Antenna Array Design for Low Earth Orbit Satellites supervised by my supervisor, Prof. Dr. Ahmet KIZILAY. In the case of a discovery of false statement, I am to acknowledge any legal consequence.

Elif ALPAGU

İmza

Dedicated to my mother(Hanım), my father(Abubekir)
and my siblings (Perihan, Müslime, Hülya, Hayat and Ali Osman)

ACKNOWLEDGEMENTS

I would like to thank my supervisor Prof. Dr. Ahmet KIZILAY for his guidance, advice and encouragement through my thesis. I am also grateful to Sezgin ÖRDEK for him technical assistance and giving motivation.

I would like to thank Alpçen TÜFEKÇİ and Yağmur FİDANER for controlling my thesis and giving advice to me about the typin. I would also like to thank to especially to Aktif Neser Elektronik Ltd. for their software support.

The measurements were made in the Laboratory of the RF-Microwave R&D [Yıldız Technical University RF LAB].

Finally, I would like to thank my family for their love, support and patience.

Elif ALPAGU

TABLE OF CONTENTS

LIST OF SYMBOLS

Z_0	Characteristic Impedance
ϵ_r	Dielectric Constant
ϵ_0	Dielectric Constant in Free Space
ϵ_{eff}	Effective Dielectric Constant
η	Intrinsic number
δ	Loss Tangent
f	Operating Frequency
k	Propagation Number or Wave Number
h	Thickness of the Substrate
λi	Wavelength in Free Space
W	Width of the Patch

LIST OF ABBREVIATIONS

AF	Array Factor
AR	Axial Ratio
CP	Circularly Polarized
GEO	Geostationary Earth Orbit
LEO	Low Earth Orbit
LHCP	Left Hand Circularly Polarized
LOS	Line Of Sight
MEO	Medium Earth Orbit
RF	Radio Frequency
RHCP	Right Hand Circularly Polarized

LIST OF FIGURES

ABSTRACT

X-Band Isoflux Microstrip Patch Antenna Array Design for Low Earth Orbit Satellites

Elif ALPAGU

Department of Electronics and Communications Engineering
Master of Science Thesis

Advisor: Prof. Dr. Ahmet KIZILAY

The Low Earth Orbit (LEO) levels are used by different satellite types such as communication satellites, earth monitoring satellites, scientific satellites and observation satellites. The orbiting time of satellites is restricted due to their limited energy. For this reason, the loads located on satellite should be designed to have low mass and they should consume the limited energy efficiently.

The antennas are basic loads on LEO satellites. Various antenna types are used in space applications such as parabolic, helical and array antennas. However, antennas with specialized specifications are needed within the increase in technology. The main ones are the small size for satellites and the desired beam forming. The microstrip patch antennas can be used for the small size feature. The microstrip patch antennas are simple to design, easy to construct and fabricate, cheap and have low mass and height.

Agility in beam forming is achieved by antennas operate with different patterns. These are the directional beam, the multi-directional beams and the wide-angle beams commonly known as isoflux. The goal of the isoflux pattern of the antenna is to compansate the distance variation from the satellite to the ground along the surface curvature of the earth to provide constant power density over the ground covered by the antenna radiation pattern.

In this work, a microstrip patch antenna array with isoflux radiation pattern is presented for LEO satellites. The proposed antenna is designed to be used in X-Band. The feeding network for the array antenna is designed. The antenna array is simulated

by the CST Microwave Studio 2018.

Keywords: Isoflux radiation pattern, Microstrip patch aray, LEO satellite, X band, Antenna array

ÖZET

Alçak Yörünge Uyduları için X-Bant Eş Akılı Mikroşerit Anten Tasarımı

Elif ALPAGU

Elektronik ve Haberleşme Mühendisliği Bölümü
Yüksek Lisans Tezi

Danışman: Prof. Dr. Ahmet KIZILAY

Alçak yörünge (LEO) katmanları; iletişim uyduları, dünya izleme uyduları, bilimsel uydular ve gözlem uyduları gibi farklı uydu tipleri tarafından kullanılır. Uyduların sınırlı enerjilerinden dolayı yörüngede kalma süreleri azdır. Bu sebeple, uydu üzerinde bulunan yükler düşük kütleli olacak şekilde dizayn edilmeli ve sınırlı enerjiyi verimli bir şekilde kullanmalıdırlar.

Antenler, LEO uydularında bulunan temel yüklerdir. Uzay uygulamalarında parabolik, helis ve dizi antenler gibi çeşitli anten tipleri kullanılmaktadır. Bununla beraber, teknolojinin artması ile özel tekniklere sahip antenlere ihtiyaç duyulmaktadır. Başlıca bu antenler, küçük boyutlu uyduların geliştirilmesi için küçük boyutlu ve istenilen ışıma örüntüsü oluşturması beklenen antenlerdir. Küçük boyut dizaynı için mikroşerit antenler kullanılabilir. Mikroşerit yama antenlerin tasarımı basit, yapımı ve üretimi kolay, ucuz ve düşük kütle ve yüksekliğe sahiptirler.

İstenilen ışıma örüntüsü oluşturabilmek , yönlü ışıma, çok-yönlü ışıma ve eş akılı olarak bilinen geniş-açılı ışıma gibi farklı ışıma örüntüsü oluşturabilen antenler ile sağlanabilir. Eş akılı ışıma örüntüsüne sahip antenin amacı, dünyanın yüzey eğiminden kaynaklı uydunun yeryüzüne olan değişken mesafesi ile orantılı olarak kapsama alanı boyunca güç yoğunluğunu eşitleyerek sağlamaktır.

Bu çalışmada LEO uyduları içim eş akılı ışıma örüntüsüne sahip mikroşerit yama anten dizisi sunulmuştur. Önerilen anten, X-Band'ında kullanılmak üzere tasarlanmıştır. Anten dizisine ait besleme hattı tasarlanmıştır. Anten dizisi CST Mikrodalga Studio

2018 tarafından simüle edilmiştir.

Anahtar Kelimeler: Eş akılı yayılım paterni, mikroşerit anten, LEO uydu, X-Band, Dizi Anten

1 Introduction

1.1 Literature Review

In space applications, many studies are carried out for using limited energy efficiently. The isoflux pattern has wide coverage pattern. The purpose of this pattern is to compensate the gain that changes according to the antenna's elevation angle when the satellite's elevation angle increases. In this context, many studies are focused on isoflux pattern. To provide wide coverage pattern and to form isoflux pattern some studies are focused on only one antenna . The choke ring, the microstrip antenna with cavity, the compact antenna with parasitic elements,helix antenna and the metasurface antenna were performed in these studies [1–5]. On the other hand, array antenna studies are performed to form isoflux pattern [6–10]. The L-probe-fed U-slotted microstrip antenna array and reflect-array are studied in the literature [6, 7]. In some studies, optimization studies were performed and suitable array antenna sequences have been proposed. The particle swarm optimization, harmony search optimization, genetic algorithm were performed in these studies [8–10].

1.2 Objective of the Thesis

The objective of the thesis to design, simulate and fabricate a microstrip patch antenna array with isoflux radiation for LEO satellites. Circular polarization is preferred to minimize antenna losses. Since it is a satellite antenna, circular polarization is preferred and an array antenna is used to create an Isoflux pattern. It is aimed to select an antenna that works in X-band and makes circular polarization. An appropriate antenna feeding technique is selected to improve bandwith and avoid parasitic radiation. To create an isoflux pattern by minimizing the number of antenna is planned in this thesis.

1.3 Hypothesis

The numbers of satellites needed for covering all the points in the coverage area on the Earth are minimized by exploiting isoflux antennas [7]. Although there are many studies on isoflux patern antennas, studies on isoflux microstrip patch antenna array is not common.

2
General Technical Information

2.1 What Is an Antenna?

There are several definitions of what the antenna is and what it is used for. Antenna is generally metallic device and it can radiate or receive radio waves. The other definition of the antenna is a device between space and device. This device can be coaxial cable or waveguide. It can transmit electromagnetic waves from the source to the antenna or it can receive electromagnetic waves from the receiver to the antenna. Generally, antenna can be defined as device that converts electrical signals to electromagnetic waves, or vice versa as shown in Figure 2.1 [11].

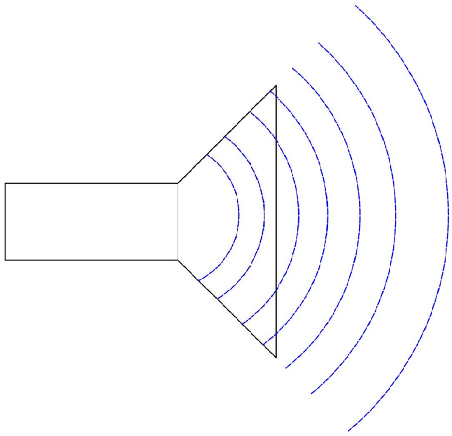

Figure 2.1 An example an Antenna Structure

An example an antenna structure can be observed in Figure 2.1. Antenna transmitting mode is represented by a Thevenin equivalent circuit as shown in Figure 2.2.

In Figure 2.2, the source is represented by an ideal generator, the transmission line is represented by a transmission line which has characteristic impedance Z_0 and antenna is represented by a load Z_A;

$$Z_A = (R_L + R_r + jX_A) \tag{2.1}$$

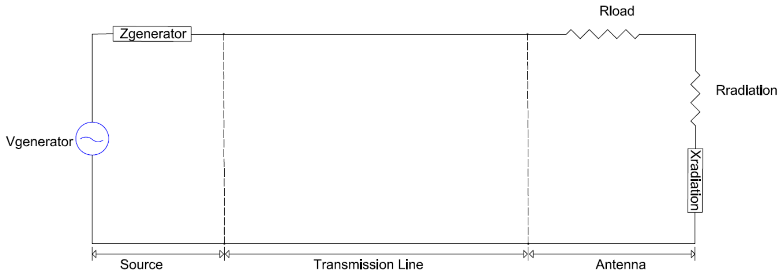

Figure 2.2 Thevenin Equivalent Circuit of Antenna

The dielectric and conduction losses are represented by the load R_L. When an antenna radiates, it is represented by the radiation resistance R_r and imaginary radiation resistance is X_A.

2.2 Antenna Fundamentals

In antenna applications, some undesirable problems can occur. If the impedance matching between the transmission line and the antenna cannot be achieved, a certain part of the power may be reflected to the antenna. Losses may occur when the appropriate polarized antenna is not selected for the applications. To avoid similar problems, the basic antenna parameters should be known. In this section, important antenna parameters will be mentioned.

2.2.1 Radiation Pattern

The other name of the radiation pattern is "antenna pattern". It indicates how well the antenna transmits or receives in a specific direction. This direction will be simulated as a function of space coordinates which are azimuth angle (horizontal diagram) and elevation angle or zenith angle (vertical diagram) in Figure2.3. Azimuth angle and elevation anglere are presented by ϕ and θ respectively [12].

In figure 2.3 an antenna is placed at the origin of the three-dimensional space coordinates which are spherical coordinates. Parts of the radiation pattern are called as lobes. They are major (main), minor, side and back lobes which are indicated in Figure 2.4 [11].

The maximum radiation's direction is called as major lobe. The major lobe is called as main lobe. The other lobes are called minor lobe. The side lobe and back lobes are undesirable radiation. The radiation intensity of these lobes are less than main lobe. The back lobe occurs behind the beam of an antenna [12].

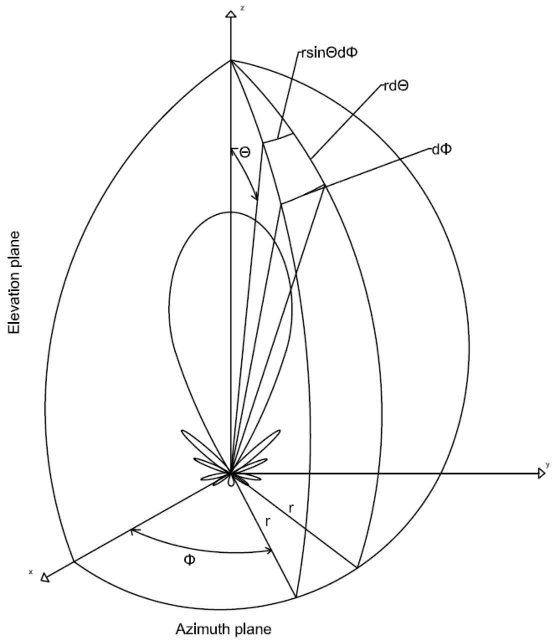

Figure 2.3 Three-dimensional coordinate system

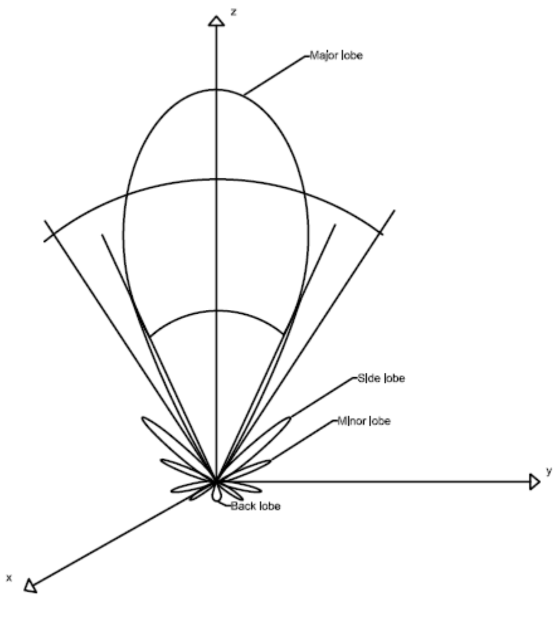

Figure 2.4 Radiation lobes

2.2.2 Beamwidth

The beamwidth is the angle between two points of maximum pattern on the opposite sides. There are lots of beamwidth on the antenna. The most important is Half-Power Beamwidth which is known as HPBW. HPBW can be defined as an angle which is half power intensity of the maximum radiated pattern. The other important beamwidth is First Null Beam Width which is known as FNBW. FNBW is an angle between two points which are first nulls of the pattern on main lobe [11].The beamwidth is shown as in Figure 2.5.

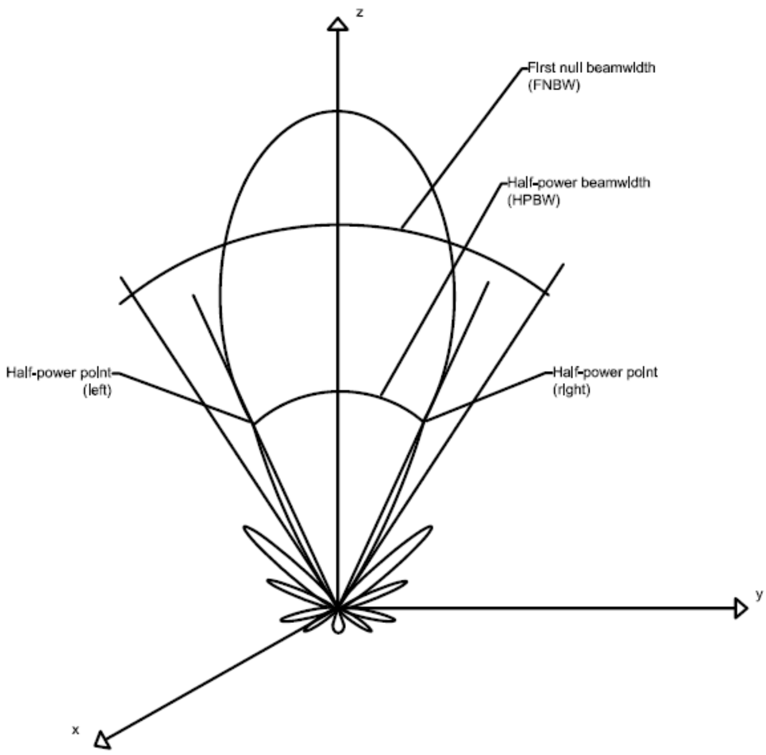

Figure 2.5 FNBW and HPBW

2.2.3 Directivity

The directivity is the ratio of the maximum radiation intensity in a constant direction to the average radiation intensity in all directions [11]. The other definition is the ratio of the power intensity in the direction of antenna's maximum radiation to the power intensity of an isotropic antenna with the same power and in the same distance. Directivity is also called as gain, if antenna is lossless [13].

$$D = \frac{U_{\max}}{U_{\text{ave}}} \tag{2.2}$$

The directivity is represented by D in Equation (2.1) and it is dimensionless. U_{max} is maximum radiation intensity and its unit is W/unit solid angle. U_{ave} is average radiation intensity and its unit is W/unit solid angle.

2.2.4 Antenna Efficiency

The antenna efficiency is also known as radiation efficiency. It is the ratio of the radiated power of the antenna to the electrical power given to the antenna.

$$e = \frac{P}{P_{\text{in}}} \tag{2.3}$$

Antenna efficiency is represented by e and it is dimensionless. P is the power radiated by antenna. P_{in} is input power [13].

2.2.5 Gain

The antenna gain indicates that how well an antenna radiate or receive a signal in the specified direction. The gain is related to directivity and efficiency.

$$G = e.D \tag{2.4}$$

Generally, the relative gain is used to calculate the gain. To determine relative gain a reference antenna should be used. The gain of the selected antenna must be known or recalculated. The reference antenna can be chosen as a horn, dipole, isotropic or any other antennas. In general isotropic antenna is preferred.

2.2.6 Bandwidth

The bandwidth can be defined as a frequency range which is include important fundamentals of the antenna in acceptable range. These parameters don't change in this bandwidth and provide desires features. The acceptable range will be determined by user's intended purpose. Generally the parameter S_{11} is used for this purpose. The parameter S_{11} is known as the reflection coefficient or return loss and it shows that how much power is reflected from the antenna. The acceptable range for the parameter S_{11} is generally determined as value of the below -10dB [11]. -14dB S_{11} value is chosen as the acceptable range in this project for the unit element because it is a satellite antenna. The bandwith is shown as in Figure 2.6.

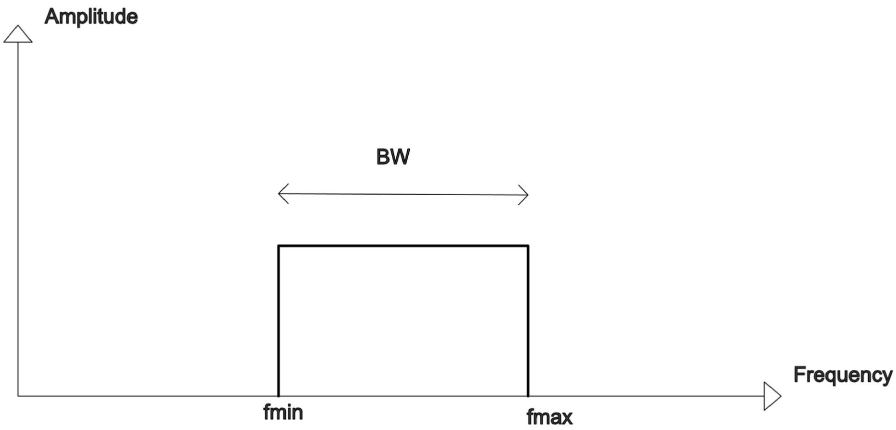

Figure 2.6 The Bandwidth

2.2.7 Polarization

The wave that is radiated from the antenna has electrical and magnetic field components. These two components are perpendicular to each other. Polarization is defined by the electrical field components's the direction. The polarization depends on the position of the antenna. In Figure 2.7, the direction of the electrical field components varies according to the position of the antenna, so the antenna polarization also changes according to the position of the antenna [11, 13].

The polarization is expressed as the rotation in the direction of propagation and axial ratio parameters. The rotation in the direction of the propagation is traced in clockwise and counterclockwise which are shown in Figure 2.8. The axial ratio (AR) is ratio of the major axis to minor axis.

Polarization can be divided into three categories; linear, circular and elliptical. They are indicated in Figure 2.9. If the polarization of the transmitter antenna is not the same as the receiver antenna, an efficient communication may not be achieved. Circular or either vertical and horizontal polarization are used in many applications. To maximize system performance of the applications, the difference between polarization should be known.

The instantaneous electric field of a wave that has a propagation in the negative z direction is;

$$\overrightarrow{\xi}(z;t) = \overrightarrow{a}_x \xi_x(z;t) + \overrightarrow{a}_y \xi_y(z;t) \tag{2.5}$$

The instantaneous ξ is counterpart of the complex field $\boldsymbol{E}$ and it is time harmonic variations of the e^{jwt}. The instantaneous electric field can be written as

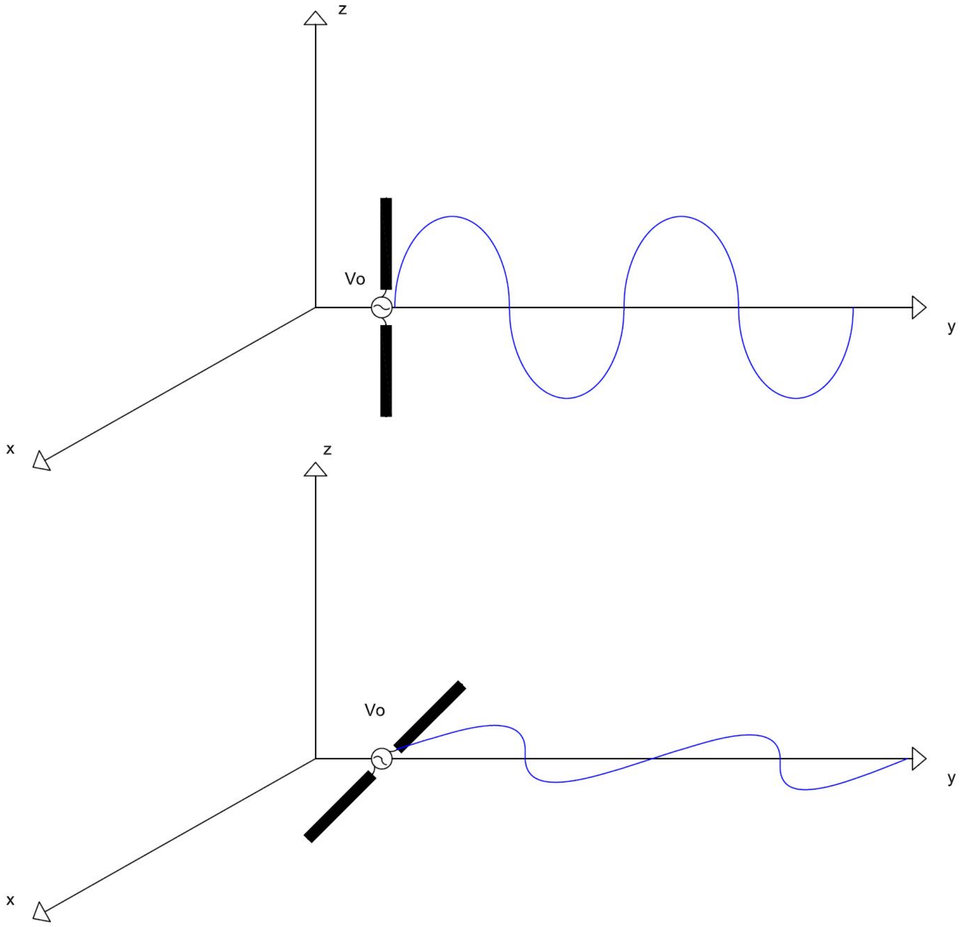

Figure 2.7 The antenna polarization according to antenna position

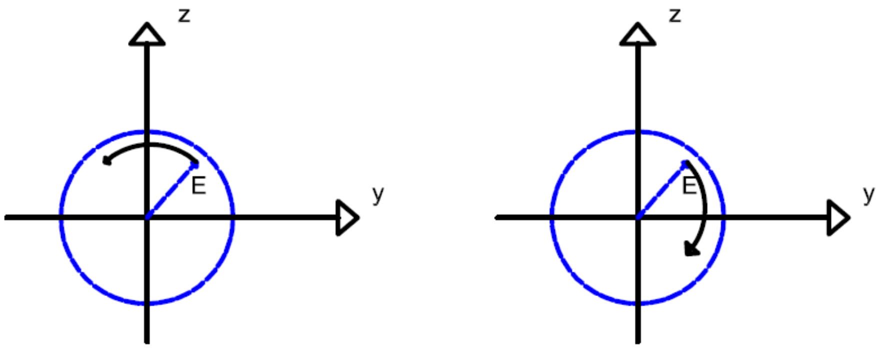

Figure 2.8 Right-hand and left-hand polarization

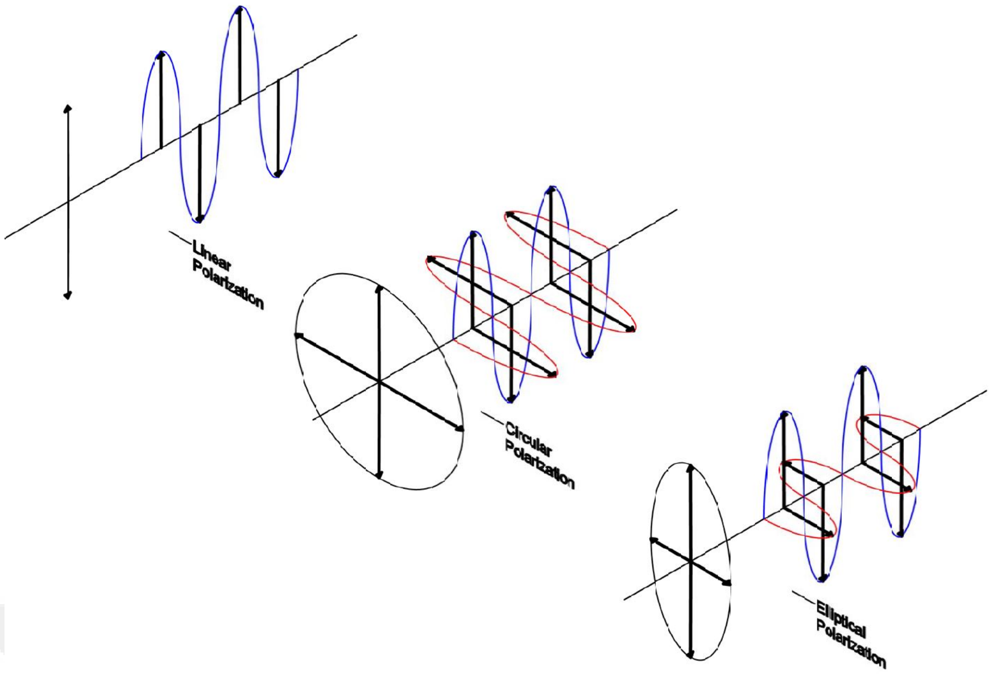

Figure 2.9 Linear, circular and elliptical polarization

$$\xi_x(z;t) = Re[E_x^- e^{j(wt+kz)}] = Re[E_{x0} e^{j(wt+kz+\phi_x)}] \tag{2.6}$$

$$= E_{x0}\cos(wt + kz + \phi_x) \tag{2.7}$$

$$\xi_y(z;t) = Re[E_y^- e^{j(wt+kz)}] = Re[E_{y0} e^{j(wt+kz+\phi_y)}] \tag{2.8}$$

$$= E_{y0}\cos(wt + kz + \phi_y) \tag{2.9}$$

E_{x0} is the the maximum magnitude of the x component and E_{y0} is the maximum magnitude of the y component.

2.2.7.1 Linear Polarization

The polarization equation must include only one component or phase difference between two orthogonal components must be multiples of 180 degrees [11].

$$\Delta\phi = \phi_y - \phi_x = n\pi, \quad n = 0, 1, 2, ... \tag{2.10}$$

2.2.7.2 Circular Polarization

In circular polarization, the electric field propagates in the direction of the x-y axes and it is perpendicular to the direction of the z axes. The polarization equation must include two components. These two components must have same magnitude and phase difference between them must be 90 degrees [11]. The axial ratio of the circular polarization is 1.

$$|\xi_x| = |\xi_y| \Rightarrow E_{x0} = E_{y0} \tag{2.11}$$

$$\Delta\phi = \phi_y - \phi_x = \begin{cases} +(\frac{1}{2}+2n)\pi, n = 0.1.2,... & \text{for } CW \\ -(\frac{1}{2}+2n)\pi, n = 0.1.2,... & \text{for } CCW \end{cases} \tag{2.12}$$

2.2.7.3 Elliptical Polarization

The polarization equation must include two components. These two components must have different magnitude and phase difference between them must be 90 degrees or not equal to 90 degrees [11]. The axial ratio of the circular polarization is $1 \leq AR \leq \infty$.

$$|\xi_x| \neq |\xi_y| \Rightarrow E_{x0} \neq E_{y0} \tag{2.13}$$

$$\Delta\phi = \phi_y - \phi_x = \begin{cases} +(\frac{1}{2}+2n)\pi, n = 0.1.2,... & \text{for } CW \\ -(\frac{1}{2}+2n)\pi, n = 0.1.2,... & \text{for } CCW \end{cases} \tag{2.14}$$

or

$$\Delta\phi = \phi_y - \phi_x \neq \pm\frac{n}{2}\pi \begin{cases} > 0 & \text{for } CW \\ < 0 & \text{for } CCW \end{cases} \tag{2.15}$$

2.3 Microstrip Antennas

Nowadays, small, light, economic antenna types are needed for the advanced technologies such as satellite, spacecraft, etc [11]. The microstrip antennas can be chosen for this purpose. Due to the fact that it is planar configuration, simple to design, suitable integration and small, this antenna has been subjected to research and investigation. Basically, a microstrip antenna has a dielectric layer that is covered with metal. The one side of the dielectric substrate is grounded and the other side has a patch. The basic microstrip patch antenna structure is shown in Figure 2.10.

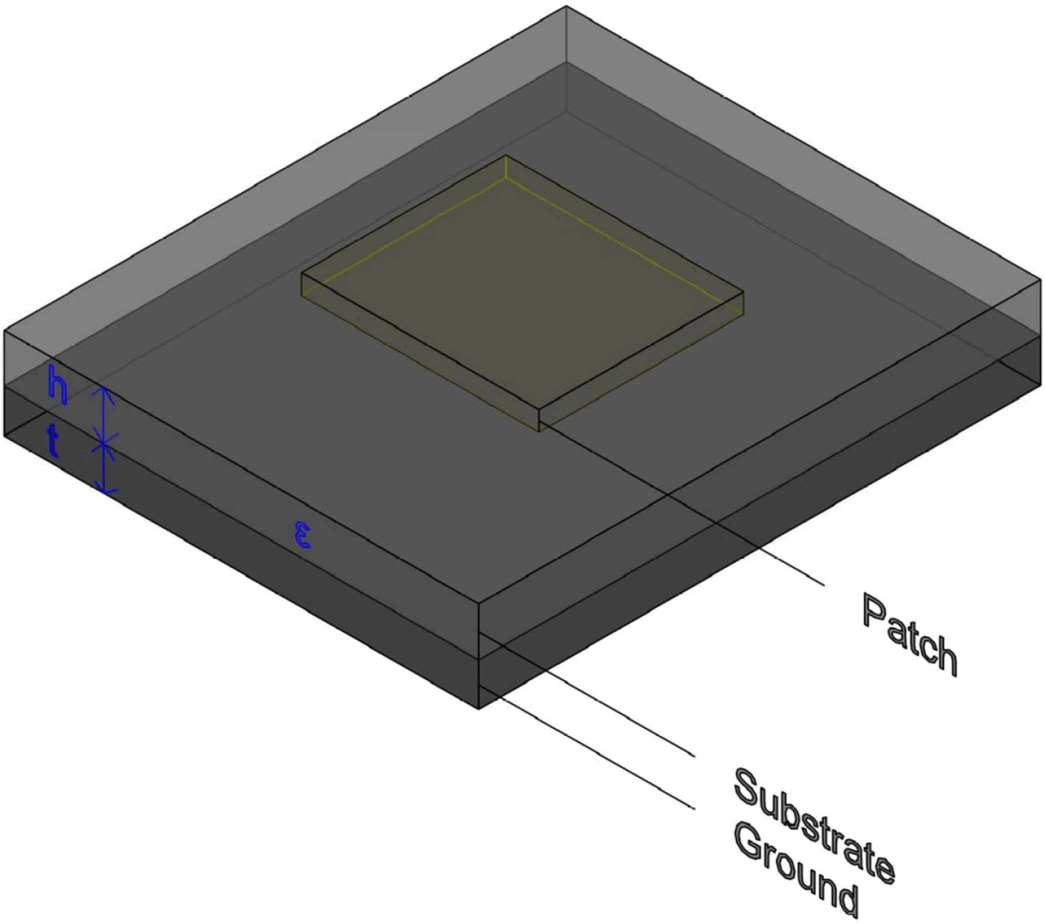

Figure 2.10 The basic microstrip antenna structure

The microstrip antenna is also called as patch antenna [11]. The patch allows the antenna to radiate. The patch can different shapes. It can be rectangular, square, circular, triangular, circular ring, elliptical. The shapes of patch are illustrated in Figure 2.11. In the figure, commonly used patches can be seen. The square patch was used in this project.

The length of the patch is generally between the $\lambda/3$ and $\lambda_0/2$. The height of patch is much less than free space wavelength ($t \ll \lambda_0$). The height of the dielectric substrate is much less than free space length ($h \ll \lambda_0$). It is generally between the 0.003λ and $0.005\lambda_0$. The dielectric constants of the dielectric (ε_r) are generally between the 2.2 and 12. The substrate is selected by deciding the properties such as cost, dielectric constant and thickness. Thick substrate and lower dielectric constant are desirable for the antennas which has larger element size. Because thick substrate and lower dielectric constant provide larger bandwith and better efficiency for radiation. Thin substrate and higher dielectric constant are preferred for the microwave applications which have small element sizes. Because thin substrate and higher dielectric provide

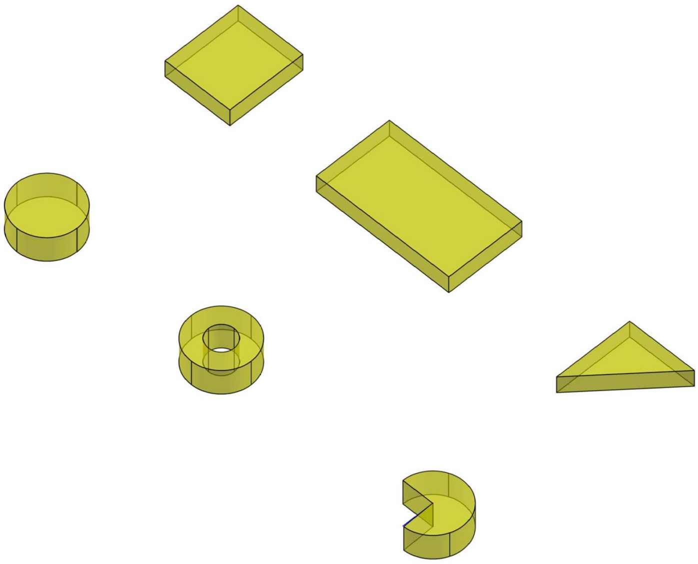

Figure 2.11 The patch shapes

tightly bound fields. In this way, undesired radiation and coupling are minimized. Thin substrate and higher dielectric cause losses. For this reason, efficiency is reduced and bandwith is relatively less [11].

2.3.1 Feeding Techniques

There are many methods to feed a microstrip antenna. In this section the most common techniques will be mentioned. These are microstrip line, aperture coupling, coaxial probe and proximity coupling [11]. The feeding techniques can be divided in two parts; contact feeding and contactless feeding. In contact feeding techniques, feed line is connected directly to the patch. An example of this is the microstrip line and coaxial probe. In contactless feeding techniques, energy is transferred by the electromagnetic coupling between the feed line and patch. An example of this is the aperture and proximity coupling. Feeding technique that will be used depends on the antenna structure and its intended use. Impedance matching must be provided.

2.3.1.1 Microstrip Line Feed

The microstrip line is located on the same substrate as the patch, so that the planar structure is preserved [14]. According to other feeding techniques, this method is the easiest to match, design and fabricate. The basic structure is shown in Figure 2.12.

The width of the feed line is smaller than the width of the patch. By increasing dielectric substrate thickness, the surface waves and parasitic radiation increases. So, the bandwidth is narrow [15].

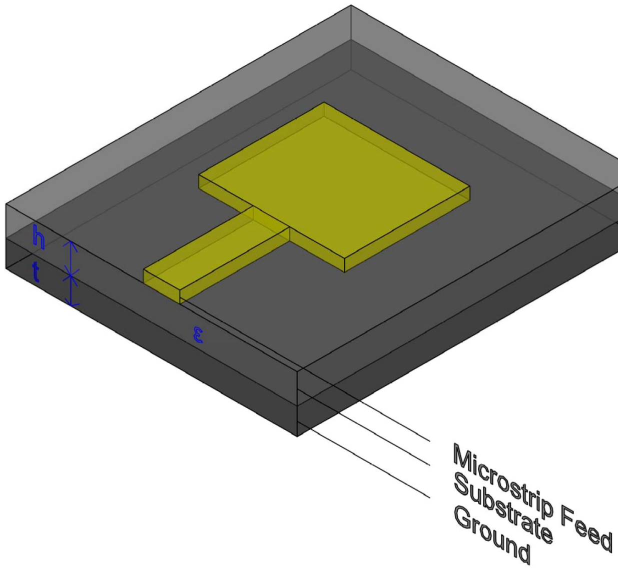

Figure 2.12 Microstrip line feed

2.3.1.2 Coaxial Probe Feed

The coaxial cable is fed by connecting the coaxial cable's inner conductor to the patch and outer conductor is attached to the ground. To make this structure, a hole is opened on the ground plane and dielectric substrate. The inner conductor of the coaxial cable is passed through this hole and connected to the patch. The outer conductor is connected to the ground without passing through this hole [15]. The basic coaxial probe feed is in Figure 2.13.

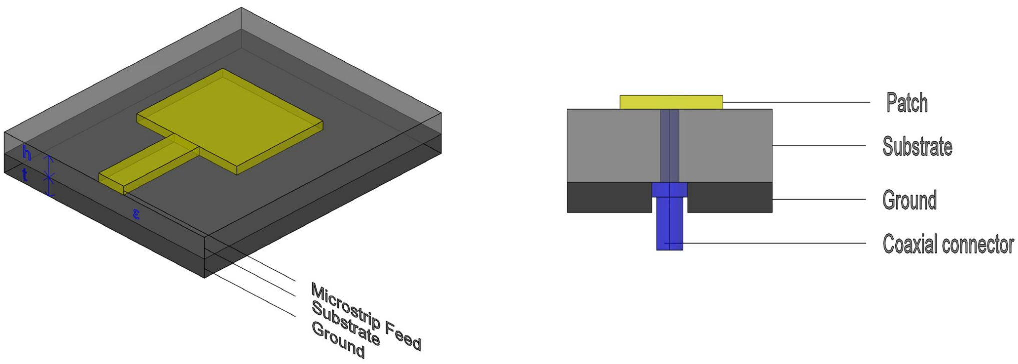

Figure 2.13 Coaxial probe feed

Impedance matching can be achieved with the alignment probe to the desired location inside the patch. It is easy to design and manufacture this structure with less dielectric substrate thickness. Since the length of probe is longer in thicker structures, the input impedance becomes inductive and the impedance matching problems occur. For this reason, design and manufacture of this structure becomes difficult. Although this method causes narrow bandwidth, the parasitic radiation is low [15].

2.3.1.3 Aperture-coupled feed

In this method, the feed line and the ground plane are located between two dielectric substrates, respectively. The patch is placed on the dielectric substrate. An aperture is used on the ground plane. The energy of the feed line is coupled to the patch from this aperture [11]. The basic structure is in Figure 2.14.

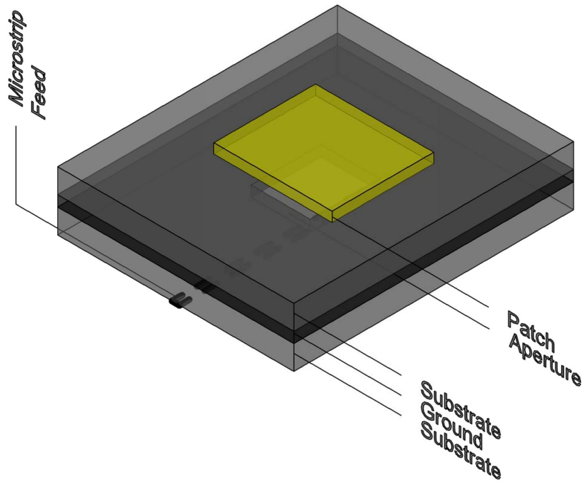

Figure 2.14 Aperture-coupled feed

The patch and feed line are separated by ground plane, so the parasitic radiation is minimized. Generally, to optimize radiation from patch, a high dielectric substrate is used for the bottom substrate and a low dielectric substrate is used for the top substrate. In this feeding technique, the multiple layers increase the antenna thickness. For this reason, manufacture of this design is difficult.

2.3.1.4 Proximity-coupled feed

The proximity-coupled feed is also known as electromagnetic coupling scheme. In this method, the feed line is placed between two dielectric substrates. The patch is on the top of the upper substrate and ground is below of the bottom substrate. The patch and feed line are separated by dielectric substrate, so the parasitic radiation is minimized. The two dielectric layers must be combined properly. For this reason, manufacture of this design is difficult. The basic proximity-coupled feed structure is shown in Figure 2.15.

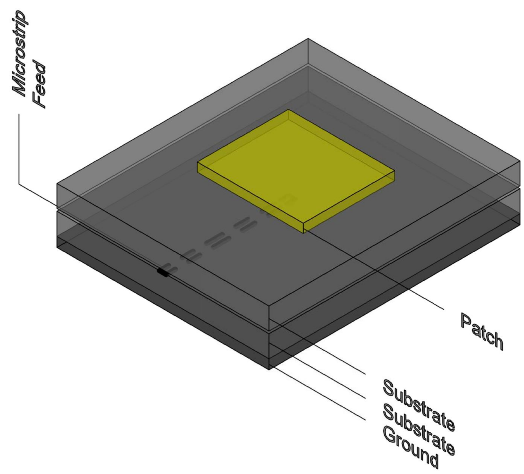

Figure 2.15 Proximity-coupled feed

2.3.2 Advantages and Disadvantages

2.3.2.1 Advantages of Microstrip Antennas

Microstrip antennas have various advantages compared to other microwave antennas. The advantages of microstrip antennas are listed as below [14]

- They have small volume and lightweight structure.
- They have low production cost.
- They are very useful due to their planar structure.
- They have low radar cross-section.
- They can be used for multiple frequency bands (dual,triple frequency) project.
- Various types of patches can be etched easily.
- They do not disrupt the aerodynamics structure of spacecraft because they can be designed very thin.
- They are suitable for mobile communication.

2.3.2.2 Disadvantages of Microstrip Antennas

The disadvantages of patch antennas are listed as below.

- They have narrow bandwidth.
- They have lower gain.

- They radiate from junction points.
- They have low power-handling capability.
- They have lower gain.

2.4 Antennas Array

The high antennas are needed in the long distance communication applications. To achieve this, the electrical size of the single-element is increased. Increasing the dimension of the antenna leads to more directional antenna with higher directivity thus long distance communication can be achieved. The other method to increase the antenna's dimension with no changing a single-element dimension is to combine more than one antenna in order. This antenna type is called as array. Generally, array's unit elements are selected as identical. Because, it is more sufficient and practical. The unit elements can be selected as wires, microstrip, dipole etc. The triangular array of dipoles is shown in the Figure 2.16.

Figure 2.16 Triangular array of dipoles [11]

Assuming the coupling is neglected and the current in each unit element is same as the isolated element, the field of the array is vector addition of the fields which are radiated by the unit elements individually. The fields radiated from the unit elements are added with each other in the desired direction, and they absorb each other in the undesired direction.

The performance of an array can be determined by five design factors. These are listed as follows [11].

- The geometric shape of the antenna array. This shape can be linear, circular, rectangular, spherical etc.

- The distance between unit elements in the array.
- The excitation amplitude of the unit elements.
- The excitation phase of the unit elements.
- The excitation radiation pattern of the unit elements.

2.4.1 The Principles of Pattern Multiplication

To understand the effect of individual antennas on array, let's examine the two antennas in Figure 2.17.

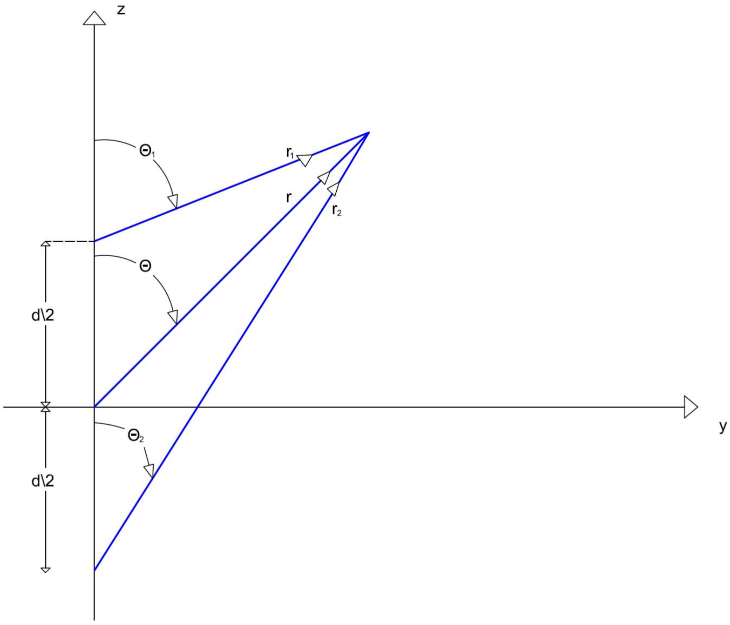

Figure 2.17 Dipole antennas

These two antennas are infinitesimal horizontal dipoles and they are located at the z-axis. The fields radiated by the dipole 1 and 2 are given by

$$\boldsymbol{E}_1 = \boldsymbol{a}_\theta j\eta \frac{kI_0 l}{4\pi}\{\frac{e^{-j[kr_1-(\beta/2)]}}{r_1}\cos\theta_1\} \tag{2.16}$$

$$\boldsymbol{E}_2 = \boldsymbol{a}_\theta j\eta \frac{kI_0 l}{4\pi}\{\frac{e^{-j[kr_2-(\beta/2)]}}{r_1}\cos\theta_2\} \tag{2.17}$$

The total field radiated by the two dipoles is given by

$$\boldsymbol{E}_t = \boldsymbol{E}_1 + \boldsymbol{E}_2 = \boldsymbol{a}_\theta j\eta \frac{kI_0 l}{4\pi}\{\frac{e^{-j[kr_1-(\beta/2)]}}{r_1}\cos\theta_1 + \frac{e^{-j[kr_2-(\beta/2)]}}{r_2}\cos\theta_2\} \tag{2.18}$$

where $\boldsymbol{k}$ is the propagation number, $\boldsymbol{\eta}$ is the medium's intrinsic impedance of and β is the difference in phase excitation between the antennas. The excitation magnitude of the unit elements is identical. For far-field acceptances are given by

$$\theta_1 \simeq \theta_2 \simeq \theta \tag{2.19}$$

$$r_1 \simeq r - \frac{d}{2}\cos\theta \tag{2.20}$$

$$r_2 \simeq r + \frac{d}{2}\cos\theta \tag{2.21}$$

$$r_1 \simeq r_2 \simeq r \tag{2.22}$$

with these acceptances equation 2.9 reduces to

$$\boldsymbol{E}_t = \boldsymbol{a}_\theta j\eta \frac{kI_0 l e^{-jkr}}{4\pi r}\cos\theta[e^{\frac{+j(kd\cos\theta+\beta)}{2}} + e^{\frac{-j(kd\cos\theta+\beta)}{2}}] \tag{2.23}$$

Eular's Formula

$$\cos\theta = \frac{e^{j\theta} + e^{-j\theta}}{2} \tag{2.24}$$

By using Euler's Formula equation 2.14 reduces to

$$\boldsymbol{E}_t = \boldsymbol{a}_\theta j\eta \frac{kI_0 l e^{-jkr}}{4\pi r}\cos\theta\{2\cos[\frac{1}{2}(kd\cos\theta+\beta)]\} \tag{2.25}$$

Equation 2.16 shows that multiplying the field of an unit element by a factor gives the total field of array. This factor is called as array factor. Array factor for two-dipole array is given by

$$AF = 2\cos\frac{1}{2}(kd\cos\theta+\beta) \tag{2.26}$$

The array's total field is adjusted by changing the d and β between the antennas. The total field radiated by the 2 antennas is given by

$$\boldsymbol{E}(total) = [\boldsymbol{E}(\text{unit element at reference point})] \times [\text{array factor}] \tag{2.27}$$

This is called as pattern multiplication. The principles of pattern multiplication are used to find the total field radiated by array antenna. For this reason, an identical single element of array is multiplied by array factor.

2.5 Feed Network

The array feed network can be series-feed network, corporate-feed network and parallel-series feed network [11, 13]. These networks are illustrated in Figure 2.18.

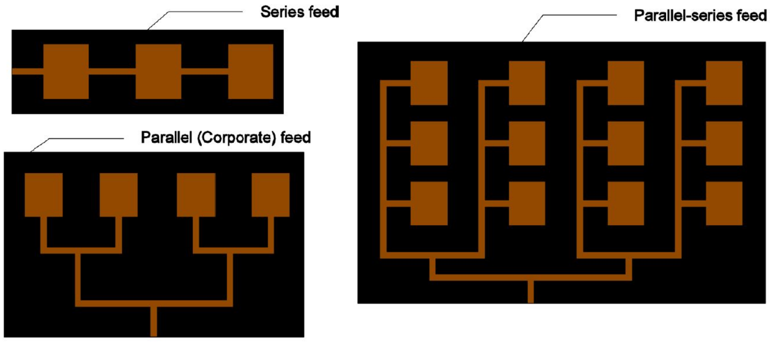

Figure 2.18 The array feed networks

The other name of the corporate-feed network is parallel feed. As the distance to each unit element is equal, a symmetric network and mutual coupling effects are formed. Thanks to this structure, each unit element can be fed with equal phase and amplitude. Also, the corporate-feed network can be used as power divider as shown in Figure 2.19. Although the series-feed network is a simple structure, it has some disadvantages that caused loss and complex structure. The series-parallel network is also called as hybrid feed and it is usually used [11, 13].

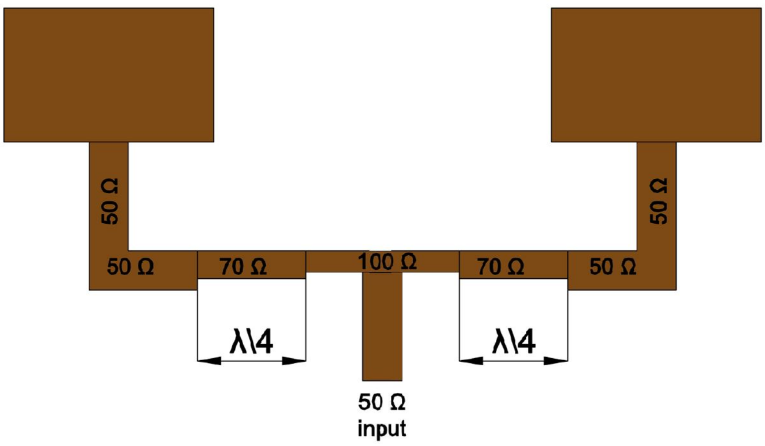

Figure 2.19 Tapered lines and $\lambda/4$ transformers

2.6 Satellite Orbits

The orbits are defined as paths which are travelled by satellites. The shape of these paths are elliptical. The farthest point from the earth is called as apogee and the closest point to the earth is called as perigee. The orbits can be divided into three categories [16].

- Orientation of the orbital plane
- Eccentricity
- Distance from Earth

2.6.1 Orientation of the Orbital Plane

The type of the satellite's orbital plane varies by angle between the satellite's orbital plane and equatorial plane of Earth. Orientation of the orbital plane is divided into three which are equatorial orbit, inclined orbit and polar orbit. These are shown in Figure 2.20. If the angle between satellite's orbital plane and and equatorial plane of Earth is zero, this satellite orbit type is equatorial orbit. If the angle between satellite's orbital plane and and equatorial plane of Earth is 90°, this satellite orbit is polar orbit. If the angle between satellite's orbital plane and and equatorial plane of Earth is 0° $\sim$ 180°, this satellite orbit is inclined orbit.

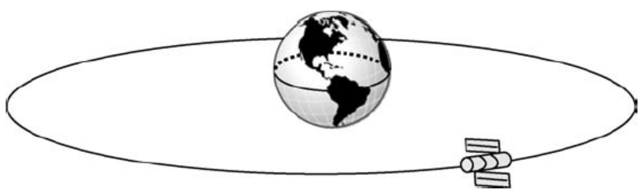

(a) Equatorial Orbit

(b) Polar Orbit

(c) Inclined Orbit

Figure 2.20 Orientation of the Orbital Plane [16]

2.6.2 Eccentricity of the Orbit

The eccentricity of orbital classification includes two types of orbits, elliptical and circular. If the orbit eccentricity is between 0 and 1, the eccentricity of the orbit is elliptical. If the orbit eccentricity is zero, the eccentricity is the circular. These are shown in Figure 2.21.

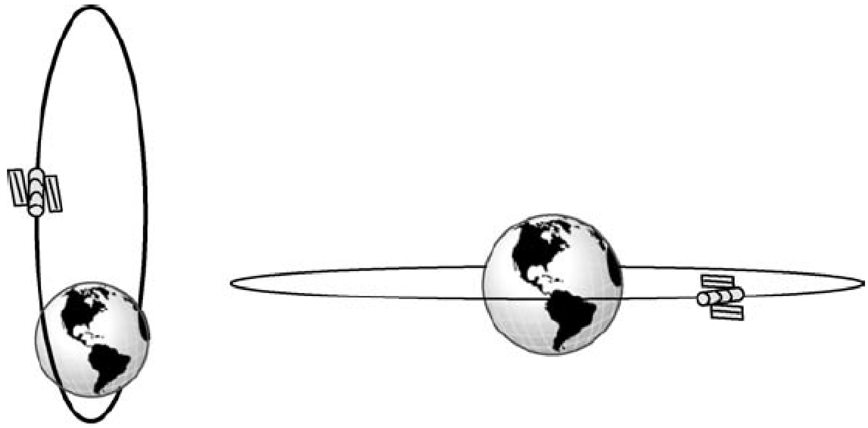

(a) Elliptical Orbit **(b)** Circular Orbit

Figure 2.21 Eccentricity of the Orbit [16]

2.6.3 Distance from Earth

Satellite orbits can be defined according to distance from Earth. These are Low Earth Orbit (LEO), Medium Earth Orbit (MEO) and Geostationary Orbit (GEO). That are illustrated in Figure 2.22.

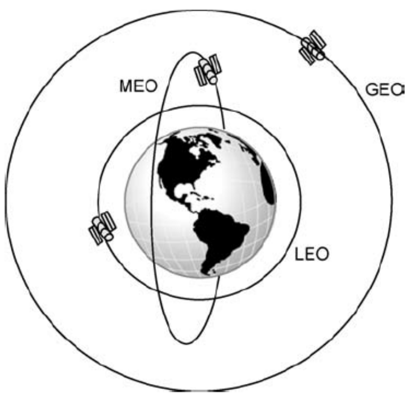

Figure 2.22 Satellite's position relative to the distance from Earth's [16]

2.6.3.1 Low Earth Orbit (LEO)

LEO is used for spaceflight,for collecting weather data, making observations and military purposes. In addition, the International Space Station is also located in LEO.

The altitude of the LEO from the Earth's surface is around 160 to 2000 km. Satellites of LEO are closer to the Earth, so they have shorter orbital periods. Their orbital periods are approximately 1,5 hours. They have small signal propagation delays, so they are good at communication applications. The path of orbit is less, so the power needed by satellite is also less. Thus, the size of the materials used is smaller and cheaper [16].

There are some disadvantages of the LEO. Being so close to the Earth surface causes atmospheric drag. As a result, the speed of the satellite may decrease and its orbit may decay. The other disadvantage of LEO is being so fast. Since the satellites on the LEO are moving very fast, they spend very short time on any part of the Earth [16].

2.6.3.2 Medium Earth Orbit (MEO)

MEO is used for communication and navigation. The altitude of the MEO from the Earth's surface is around 10 000km to 20 000km. Satellites of MEO are far from the world, they have long orbital periods.Their orbital periods are approximately 6 to 12 hours. There are more propagation delays than LEO satellites.

2.6.3.3 Geostationary Orbit (GEO)

Due to the covering most of area by GEO satellites consistently, GEO are preferable for communication, collecting weather data, TV broadcast and military. The altitude of the GEO from the Earth's surface is around 36 000km. Their orbital period is approximately 24 hours.

2.7 Isoflux Pattern

As the elevation angle of the satellite increases from the horizon, the communication range increases. Thus, free space loss also increases. The isoflux radiation pattern is used to compensate the free space loss with the gain that varies with the antenna elevation angle. The goal of the isoflux pattern is to provide constant power density over the ground along the surface curvature of the earth covered by the antenna radiation pattern[17]. Isoflux is sometimes named as saddle-shaped, M-shaped or bowl-shaped [7]. The isoflux is shown as in Figure 2.23.

The distance from the earth and to the satellite can be expressed as $R(\theta)$. Due to the distance varies by surface curvature of the earth, R depends on the θ variable. The angle of θ is the angle between distance R and the observation point on the ground at the edge of the coverage (EOC). If the observation point on the ground at the EOC is located at the sub-satellite (nadir direction), the distance between Earth and satellite

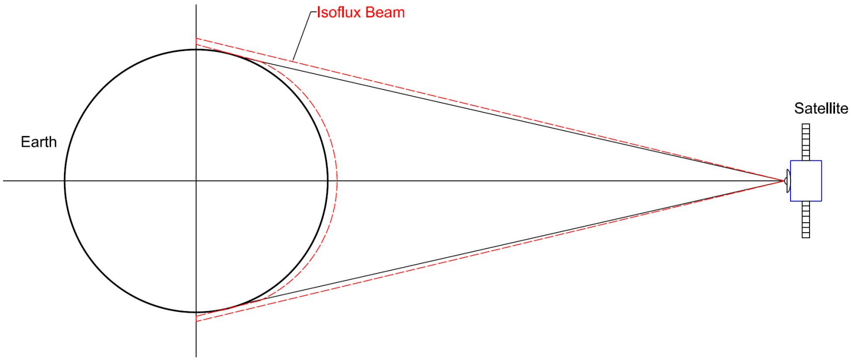

Figure 2.23 The isoflux radiation pattern for the earth coverage

is minimum and angle of the θ is $0°$. The minimum distance is indicated by $H = R(0)$ with $\theta = 0°$ and is shown as in Figure2.24 [17].

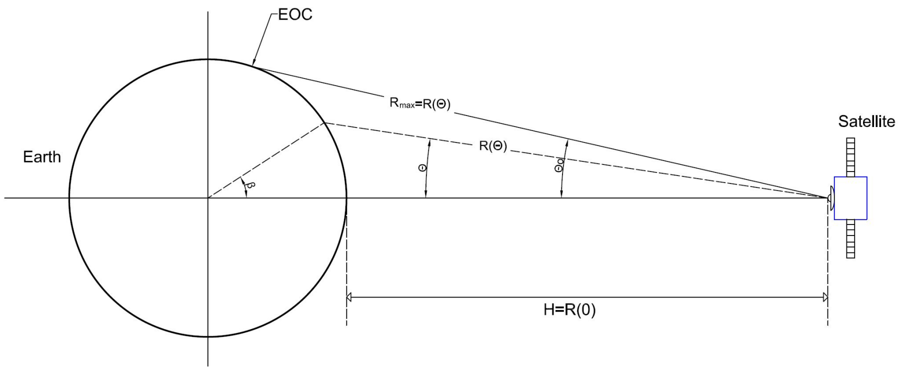

Figure 2.24 The geometry of the earth-satellite

The $P(\theta)$ is radiation intensity and $S(\theta)$ radiation power density;

$$P(\theta) = R^2 S(\theta) \tag{2.28}$$

If $\theta = 0°$;

$$S(\theta) = S(\theta = 0) \tag{2.29}$$

The equation 2.28 can be rewritten as

$$P(\theta) = R^2 S(\theta = 0) \tag{2.30}$$

$$S(\theta = 0) = \frac{P(\theta)}{R(\theta)^2} \tag{2.31}$$

$$\frac{P(\theta=0)}{R(0)^2} = \frac{P(\theta)}{R(\theta)^2} \tag{2.32}$$

$$\frac{P(\theta=0)}{H^2} = \frac{P(\theta)}{R(\theta)^2} \tag{2.33}$$

$$\frac{P(\theta)}{P(\theta=0)} = \frac{R(\theta)^2}{H^2} \tag{2.34}$$

So, the antenna pattern without considering atmospheric attenuation is as follows

$$P(\theta) \approx \left\{\frac{R(\theta)}{H}\right\}^2 \tag{2.35}$$

If the atmospheric attenuation is not neglected, the antenna pattern is as follows

$$P(\theta) \approx \left\{\frac{R(\theta)}{H}\right\}^2 A(\theta) \tag{2.36}$$

For determining the atmospheric attenuation, we solve the problem in Figure 2.25 with Cosine Rule

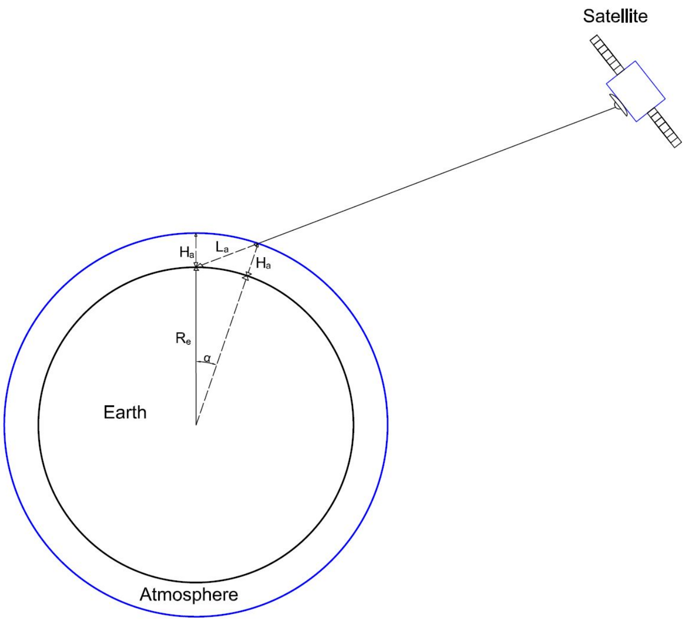

Figure 2.25 The atmospheric path

L_a is the path length of the earth's atmosphere.

$$L_a = \sqrt{(R_e + H_a)^2 + R_e^2 - 2R_e(R_e + Ha)\cos\alpha} \tag{2.37}$$

$$L_a = H_a\sqrt{(R_e/H_a + 1)^2 + (\frac{R_e}{H_a})^2 - 2(\frac{R_e^2}{{H_a}^2} + (\frac{R_e}{Ha})\cos\alpha} \tag{2.38}$$

$$L_a = H_a\sqrt{1 + 4(\frac{R_e^2}{H_a^2} + \frac{R_e}{H_a})\sin^2(\alpha/2)} \tag{2.39}$$

If we considere $R_e/H_a \gg 1$

$$L_a \approx H_a\sqrt{1 + 4\frac{R_e^2}{H_a^2}\sin^2(\alpha/2)} \tag{2.40}$$

$$\alpha = 90^\circ - \phi - \sin^{-1}\left\{\left(\frac{R_e + H}{R_e + H_a}\right)\sin\theta\right\} \tag{2.41}$$

$$R = \sqrt{R_e^2 + (R_e + H)^2 - 2R_e(R_e + H)\cos\beta} \tag{2.42}$$

$$R = H\sqrt{1 + 4[(R_e/H)^2 + R_e/H]\sin^2(\beta/2)} \tag{2.43}$$

which is $\beta = 90^\circ - \theta - \phi$, and

$$\phi = cos^{-1}[(1 + H/R_e)\sin\theta] \tag{2.44}$$

If the equation 2.44 is rearranged, the edge of the coverage can formed as shown below.

$$\theta = \sin^{-1}[R_e\cos\phi_0/(R_e + H)] \tag{2.45}$$

As seen in equation 2.45,the satellite altitude is inversely proportional to edge of the coverage θ_0. When the satellite altitude decreases, the edge of the coverage θ_0 increases. ϕ_0 is the minimum satellite elevation. It is generally less than 20° for satellite applications. If we consider the altitude of the LEO from the Earth's surface is around 160 to 2000 km with radius of the earth as $R_e = 6378$ km and the minimum satellite elevation as 15°, the edge of the coverage can be calculated;

for 160 km;

$$\theta = \sin^{-1}[R_e \cos\phi_0/(R_e + H)] = 70.4° \quad (2.46)$$

for 2000 km;

$$\theta = \sin^{-1}[R_e \cos\phi_0/(R_e + H)] = 47.3° \quad (2.47)$$

So, the edge of the coverage for the LEO should be between 47.3° and 70.4°

3
Design and Implementation of the Isoflux Microstrip Patch Antenna Array and Implementation

3.1 Design of the Isoflux Microstrip Patch Antenna Array and Feed Network

3.1.1 Design of the Unit Element

The antenna shown in the Figure 3.1 was used as an unit element. The square patch is used in design, so the width and length of the patch are 7.65 mm. The dimension of the unit element is as shown in Figure 3.1 (c).

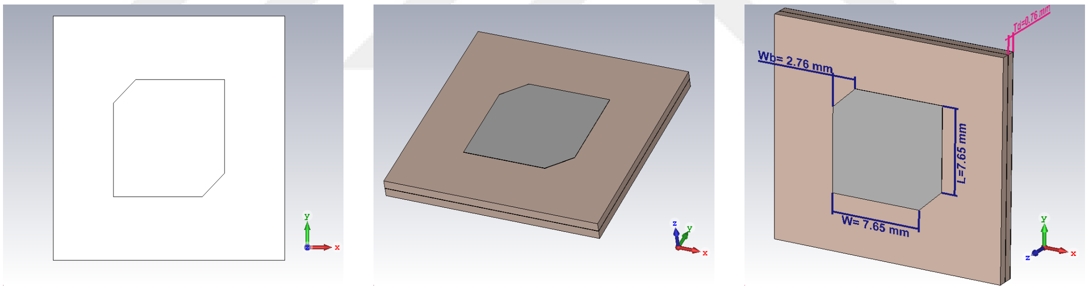

(a) Top view of the Unit Element

(b) Isometric view of the Unit Element

(c) Isometric view of the Unit Element

Figure 3.1 The unit element

The RO3003 is used as dielectric substrate. The dielectric constant (ϵ_r) is 3. The dissipation factor ($\tan\delta$) is 0.0010 mm. The thickness of the top and bottom copper cladding is 0.035 mm. These copper claddings are used as ground and feed network.

The opposite sides of the patch are bent to create circular polarization. The inverse axial ratio is 0 dB in theoretical for circular polarization, but in practice it can be between 0 and -10 dB.The inverse axial ratio of the array antenna for the ϕ values of 90°, 22.5° and 0° are shown in Figure 3.4, Figure 3.5 and Figure 3.6 respectively. The proximity-coupled feed technique is selected for the antenna feeding technique. For the 8 GHz and 8.4 GHz frequency range, S_{11} should be below -14 dB for microstrip patch antenna in Figure 3.2.

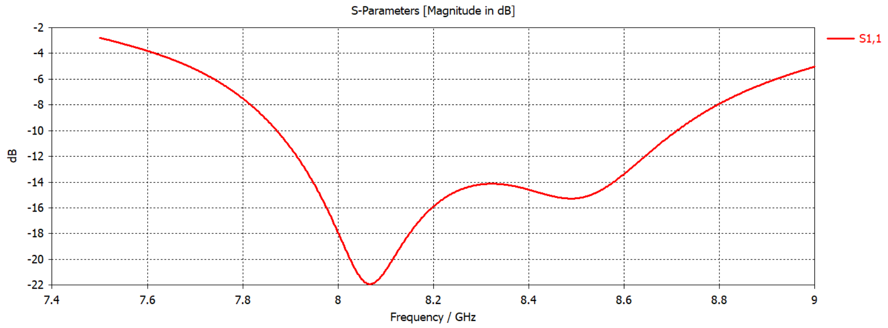

Figure 3.2 The S parameter of the unit element

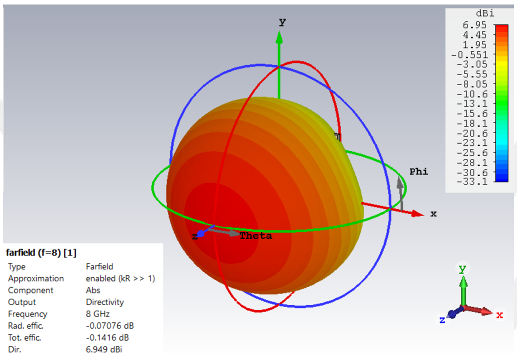

(a) 8 GHz

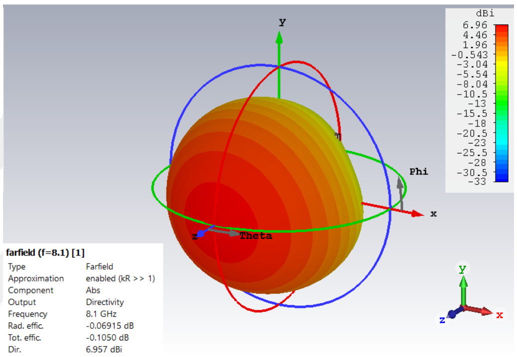

(b) 8.1 GHz

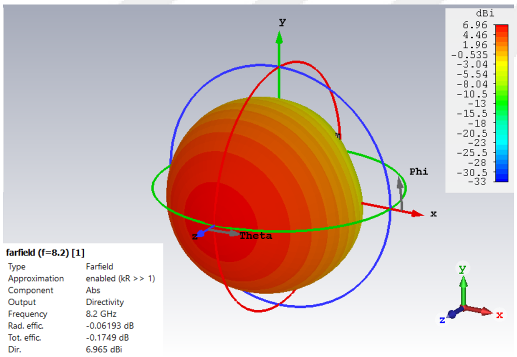

(c) 8.2 GHz

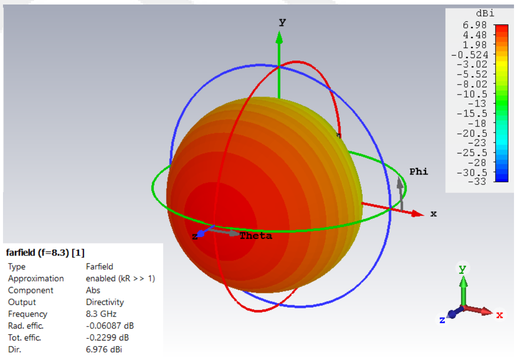

(d) 8.3 GHz

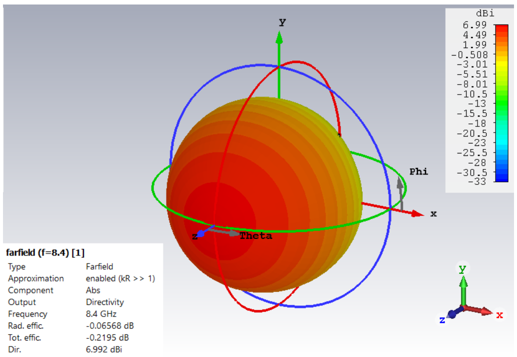

(e) 8.4 GHz

Figure 3.3 The 3D Radiation Patterns of the Unit Element

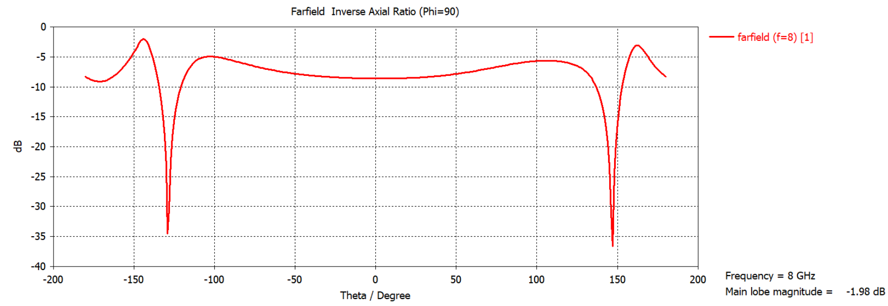

(a) 8 GHz

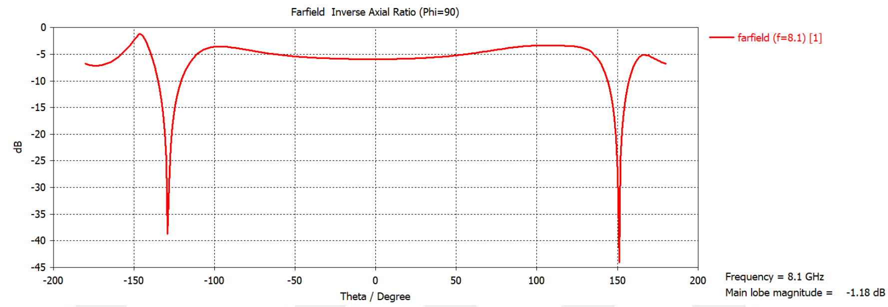

(b) 8.1 GHz

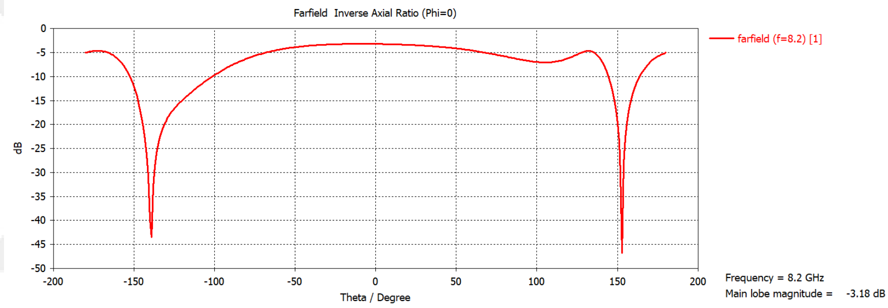

(c) 8.2 GHz

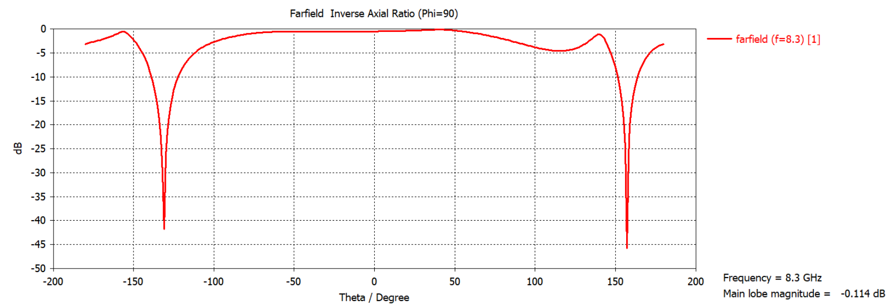

(d) 8.3 GHz

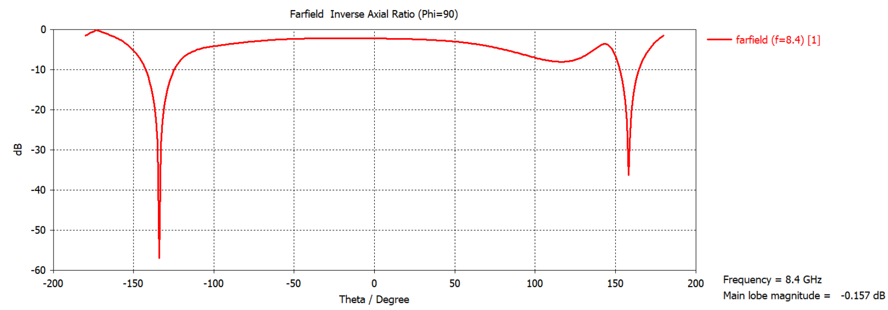

(e) 8.4 GHz

Figure 3.4 The Inverse Axial Ratios of the Unit Element (ϕ=90°)

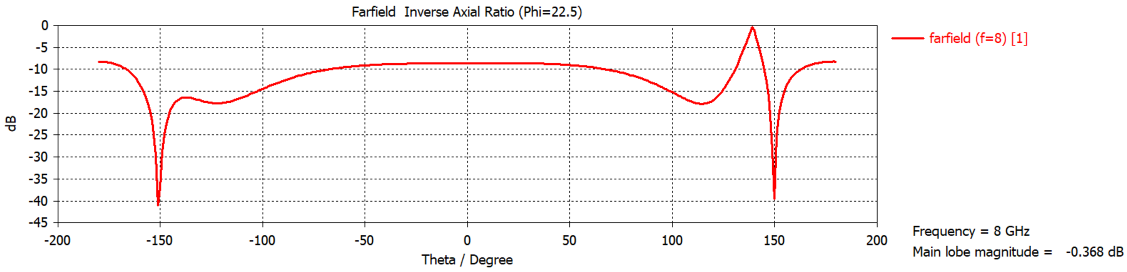

(a) 8 GHz

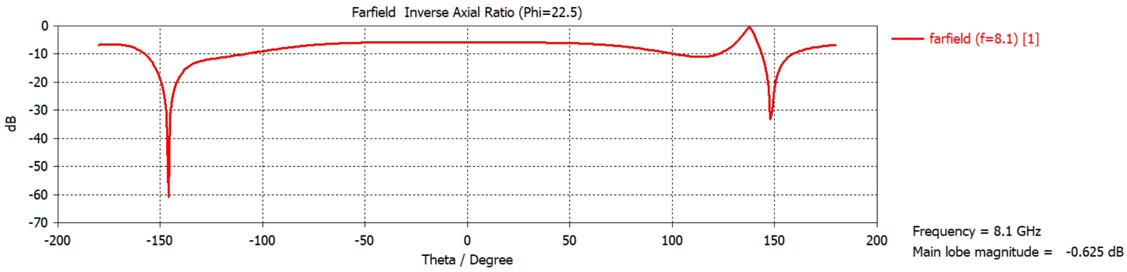

(b) 8.1 GHz

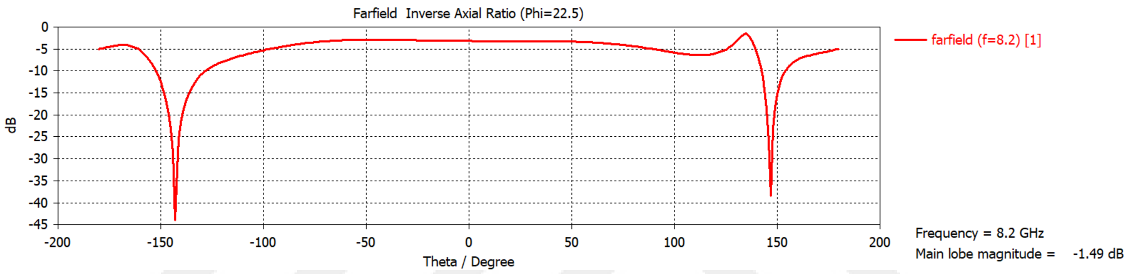

(c) 8.2 GHz

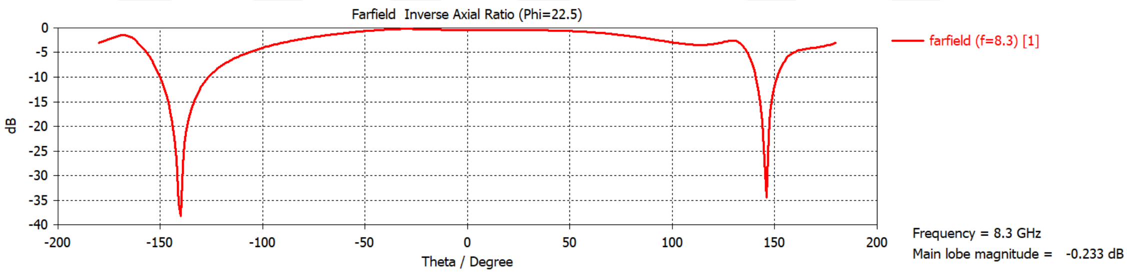

(d) 8.3 GHz

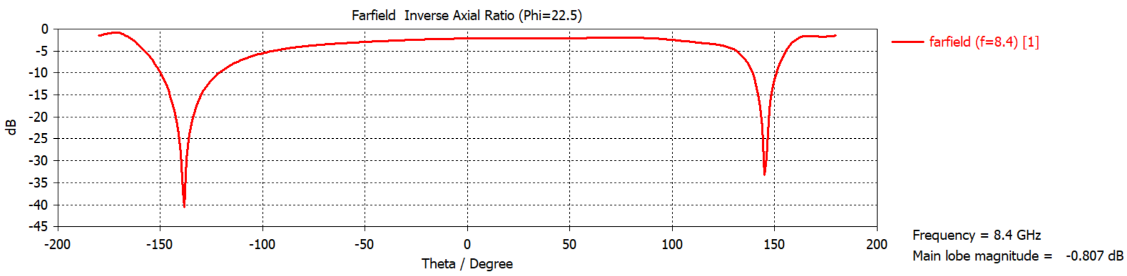

(e) 8.4 GHz

Figure 3.5 The Inverse Axial Ratios of the Unit Element (ϕ=22.5°)

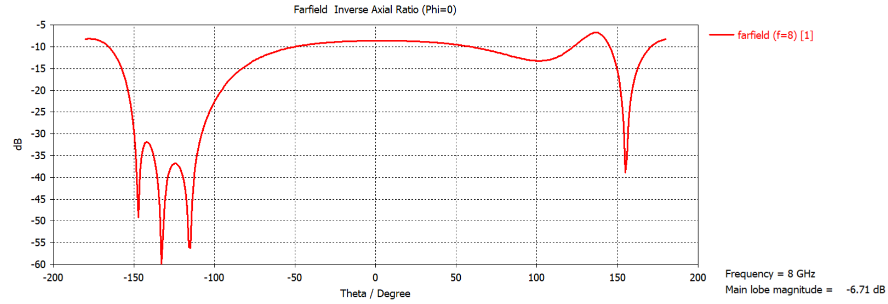

(a) 8 GHz

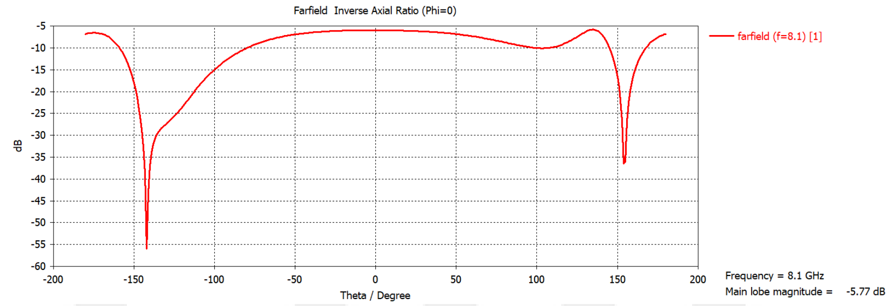

(b) 8.1 GHz

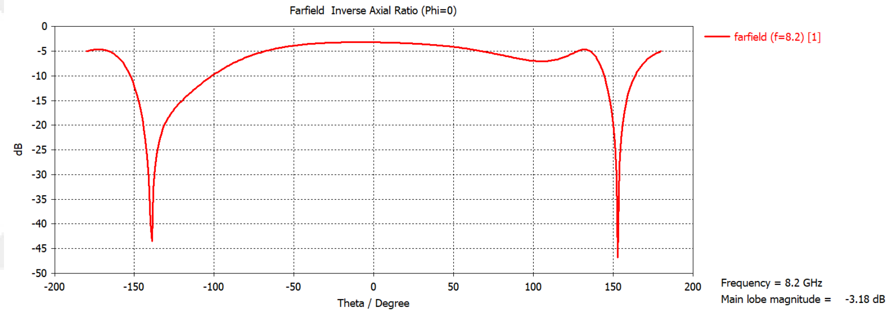

(c) 8.2 GHz

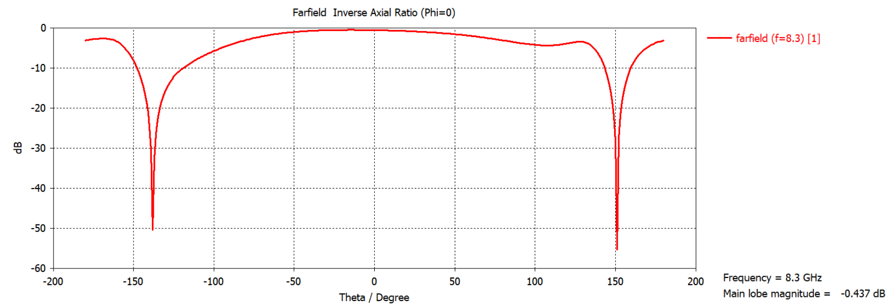

(d) 8.3 GHz

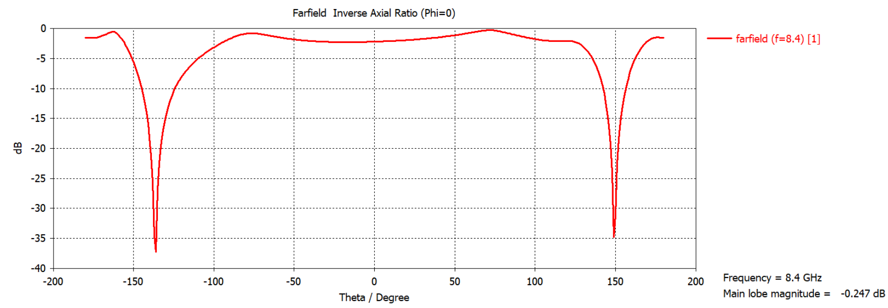

(e) 8.4 GHz

Figure 3.6 The Inverse Axial Ratios of the Unit Element (ϕ=0°)

3.1.2 Design of the 8-16 Antenna Array

The 8-16 Antenna Array is shown in Figure 3.7 and the dimension of the array is shown in Figure 3.8.

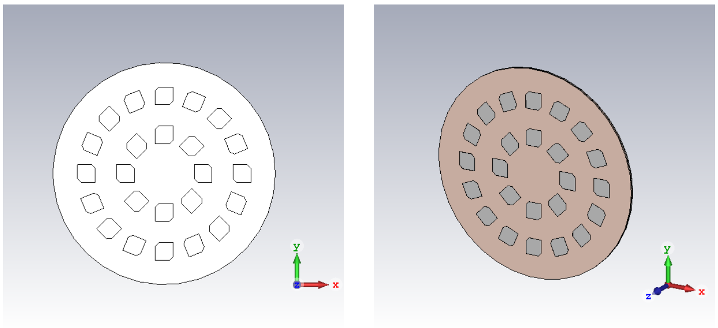

(a) Top view of the 8-16 Antenna Array

(b) Isometric view of the 8-16 Antenna Array

Figure 3.7 8x16 Antenna Array

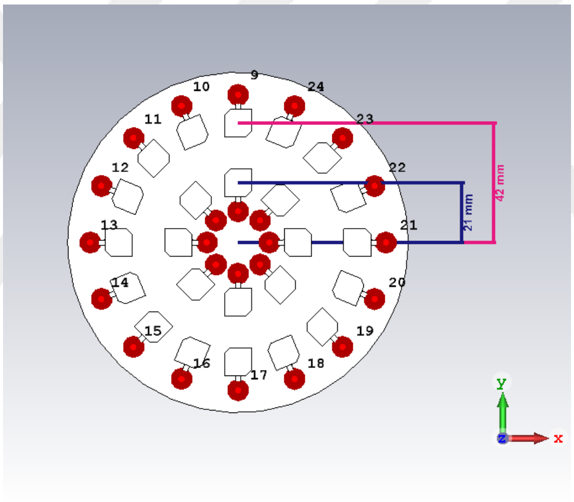

Figure 3.8 The dimension of the 8-16 Antenna Array

The following steps were taken to create the 8-16 microstrip patch antenna array.

- In this design 8 (eight) microstrip patch antennas for the first ring and 16 (sixteen) microstrip patch antennas for the second ring are used.
- To create the best isoflux pattern that shown in Figure 3.9, the radius of the first ring and the second ring are simulated as 21 mm and 42 mm respectively. The patch antennas are equally spaced by 22.5° (180°/8) in the first ring and 11.25° (180°/16) in the second ring as shown in Figure 3.8. The patch antennas and feed lines in the first and second row rings are arranged in opposite directions as shown in Figure 3.8 so that the feeding network can be designed easily. The amplitude of the first ring and second ring are 1 (one) and 0.5 (zero point five)

respectively. The phase shift of the first ring and second ring are 0 (zero), so the phase difference between the first and second ring are 180° because of the feed line arrangement.

- The targeted inverse axial ratio to create circular polarization is between 0 and -10 dB. The inverse axial ratio of the array antenna for the ϕ values of 90°, 22.5° and 0° are shown in Figure 3.10, Figure 3.11 and Figure 3.12 respectively.

- In order to use the satellite antenna in LEO, the edge of the coverage for the LEO should be between 47.3° and 70.4° . So, the targeted minimum of the theta value is between $-47.3°$ and $47.3°$. The targeted maximum of the theta value is between $-70.4°$ and $70.4°$.

- The Cartesian Radiation Pattern for the ϕ values of 90°, 22.5° and 0° are shown in Figure 3.13, Figure 3.14 and Figure 3.15 respectively.

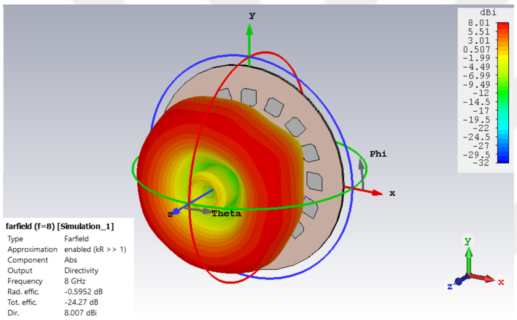

(a) 8 GHz

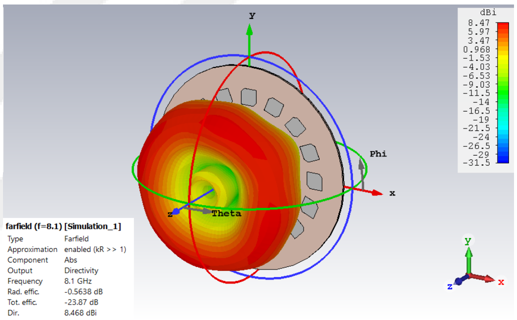

(b) 8.1 GHz

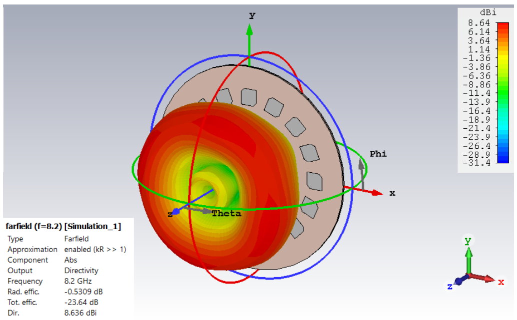

(c) 8.2 GHz

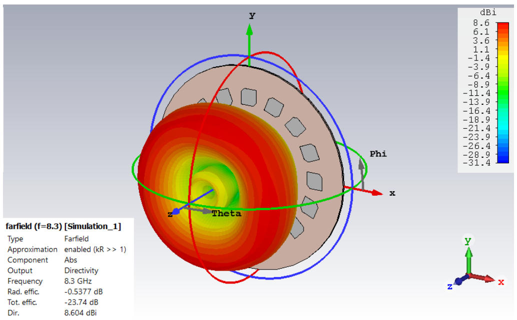

(d) 8.3 GHz

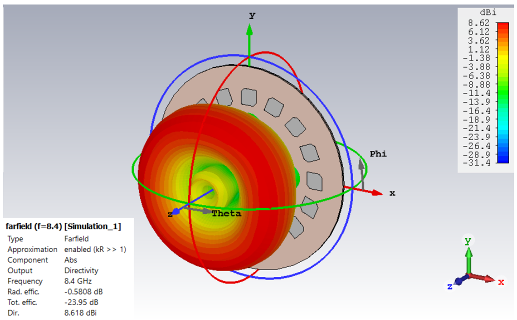

(e) 8.4 GHz

Figure 3.9 The 3D Radiation Patterns of 8-16 Antenna Array

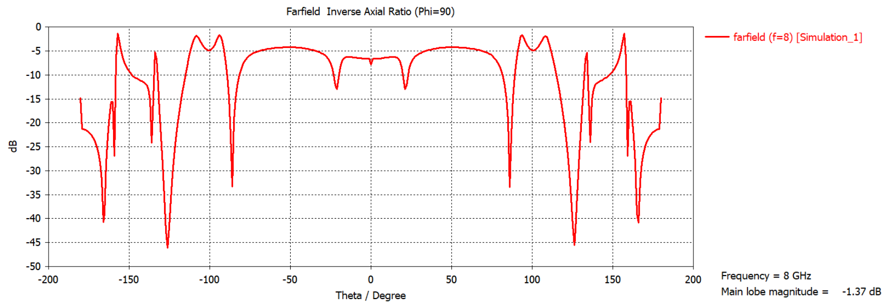

(a) 8 GHz

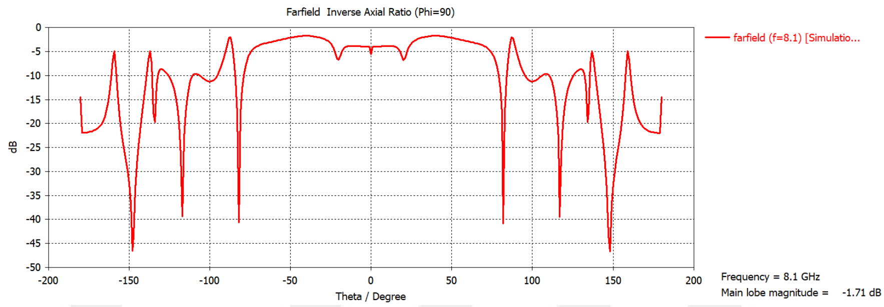

(b) 8.1 GHz

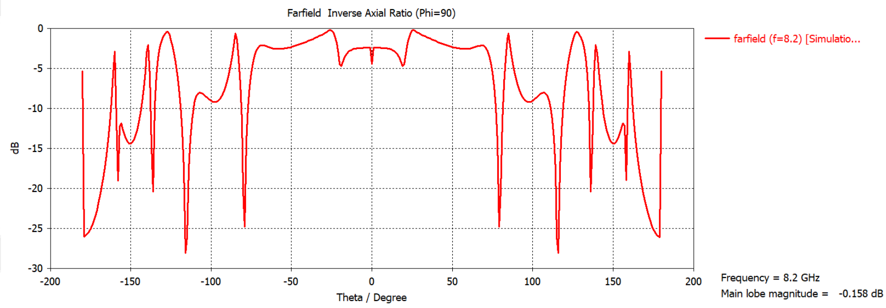

(c) 8.2 GHz

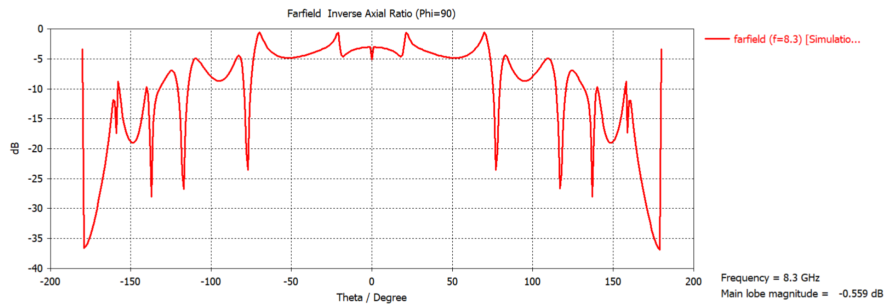

(d) 8.3 GHz

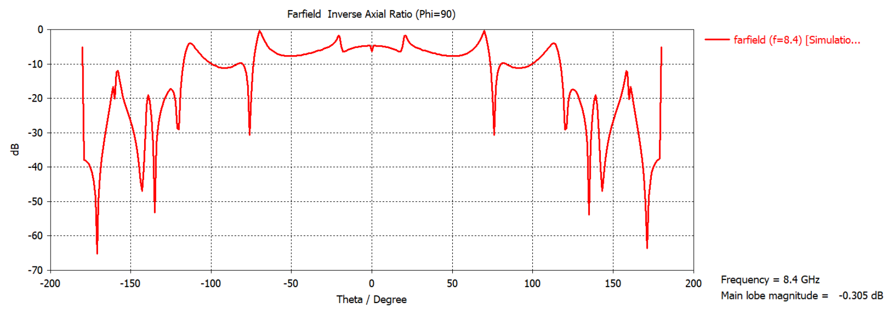

(e) 8.4 GHz

Figure 3.10 The Inverse Axial Ratios of 8-16 Antenna Array (ϕ=90°)

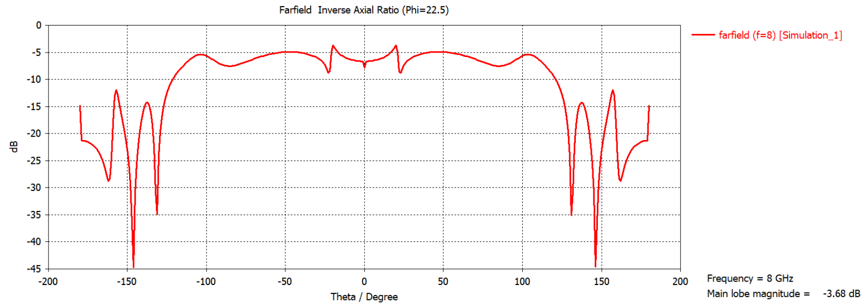

(a) 8 GHz

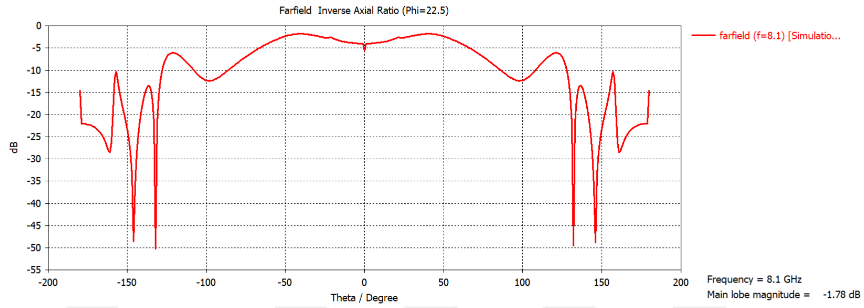

(b) 8.1 GHz

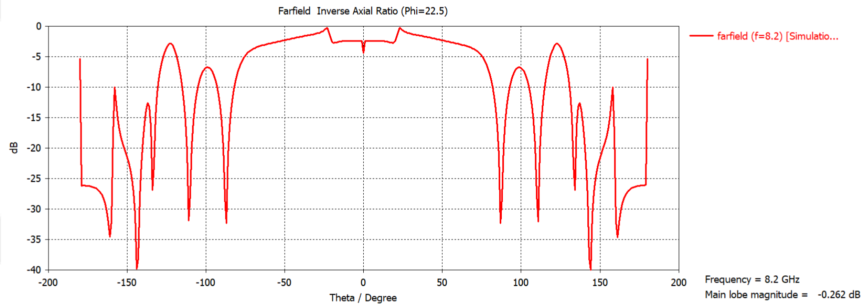

(c) 8.2 GHz

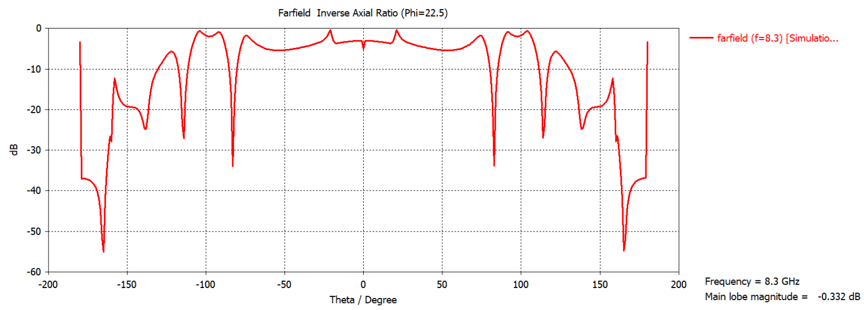

(d) 8.3 GHz

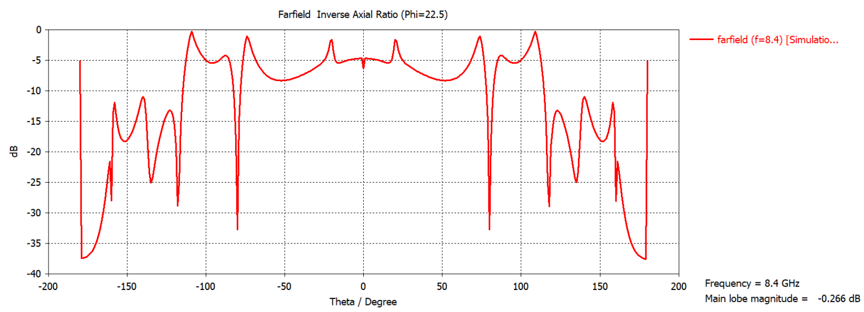

(e) 8.4 GHz

Figure 3.11 The Inverse Axial Ratios of 8-16 Antenna Array (ϕ=22.5°)

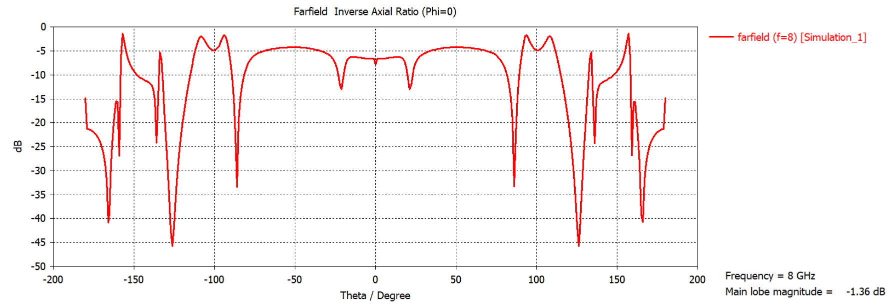

(a) 8 GHz

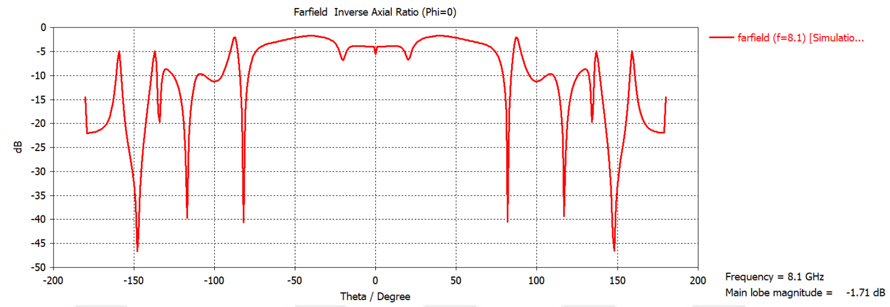

(b) 8.1 GHz

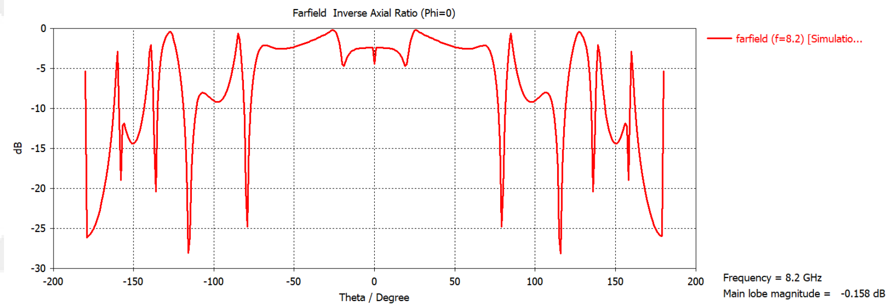

(c) 8.2 GHz

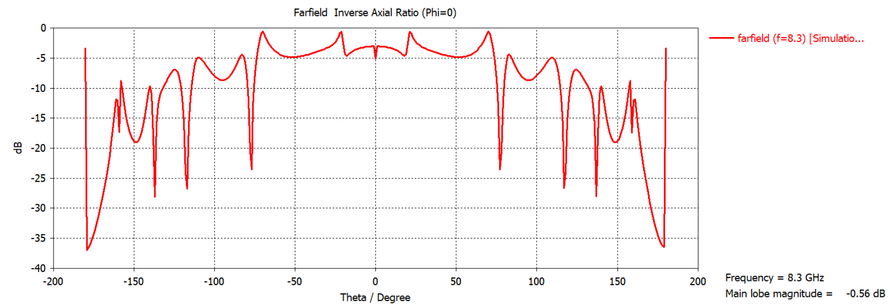

(d) 8.3 GHz

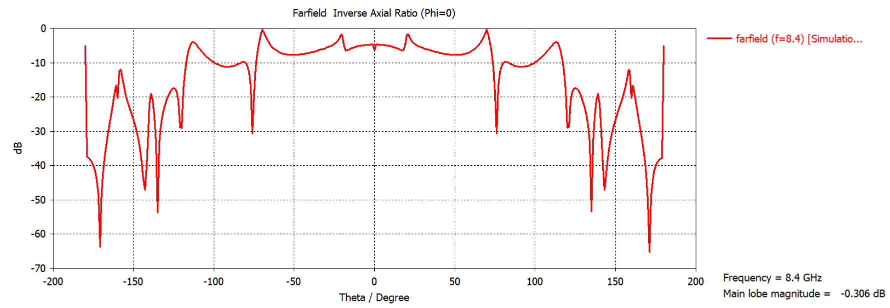

(e) 8.4 GHz

Figure 3.12 The Inverse Axial Ratios of 8-16 Antenna Array (ϕ=0°)

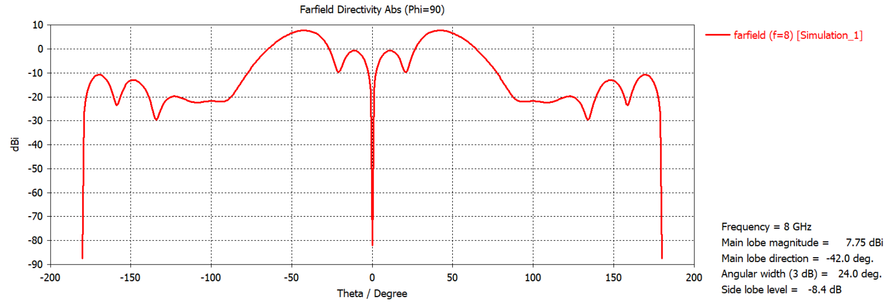

(a) 8 GHz

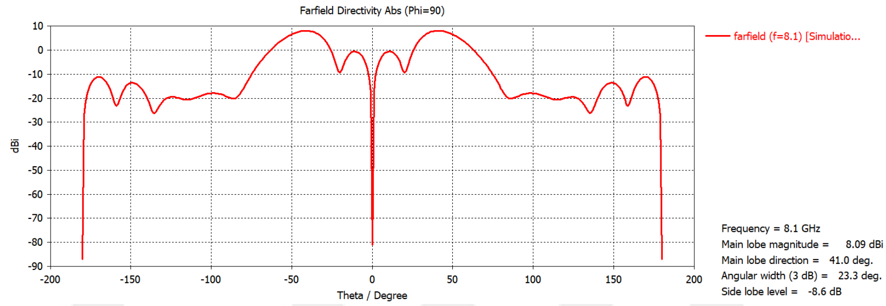

(b) 8.1 GHz

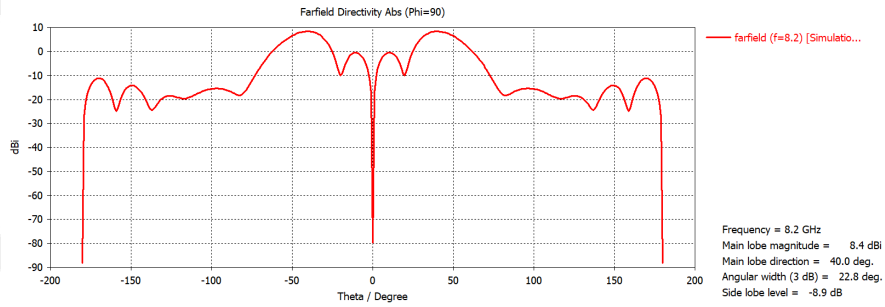

(c) 8.2 GHz

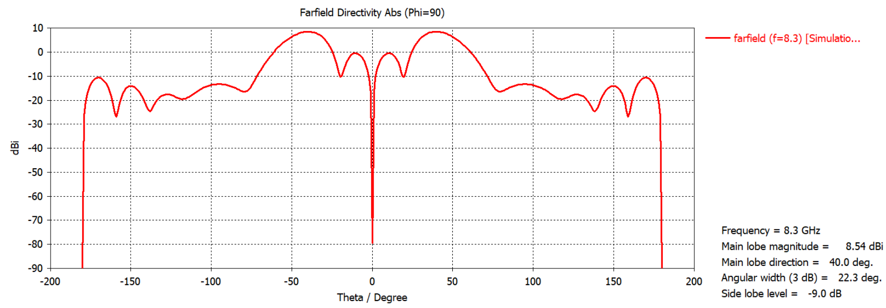

(d) 8.3 GHz

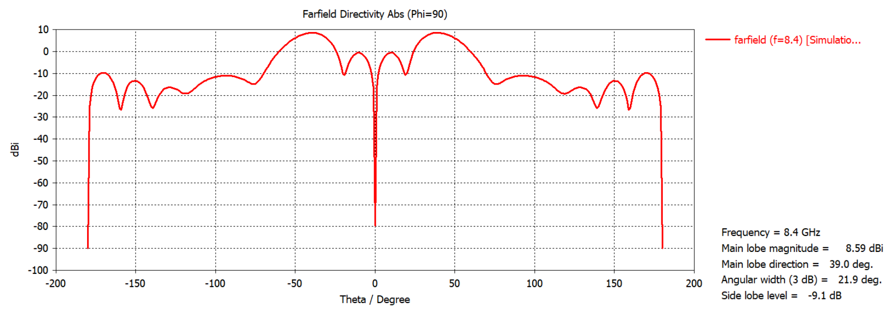

(e) 8.4 GHz

Figure 3.13 The Cartesian Radiation Patterns of 8-16 Antenna Array (ϕ=90°)

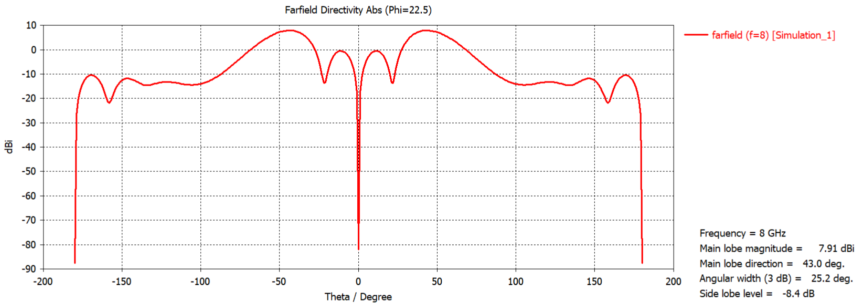

(a) 8 GHz

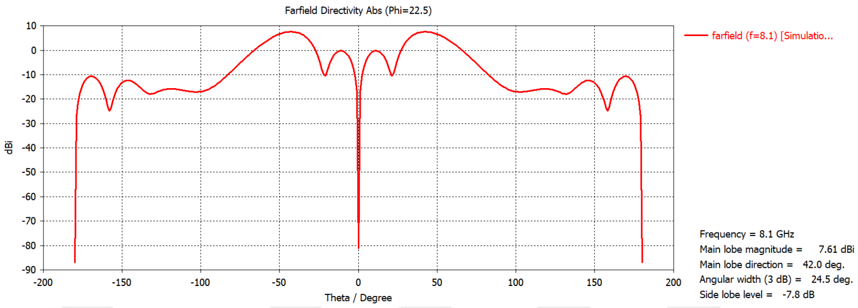

(b) 8.1 GHz

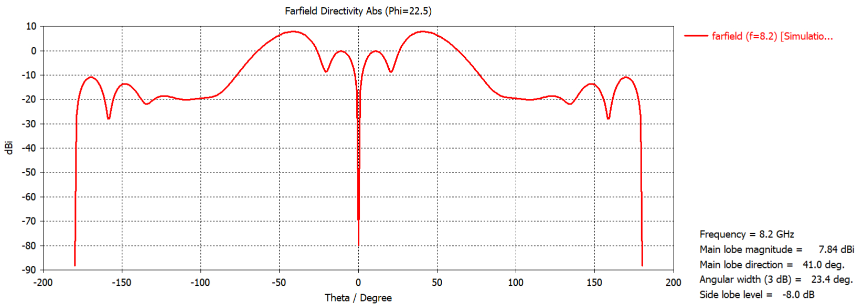

(c) 8.2 GHz

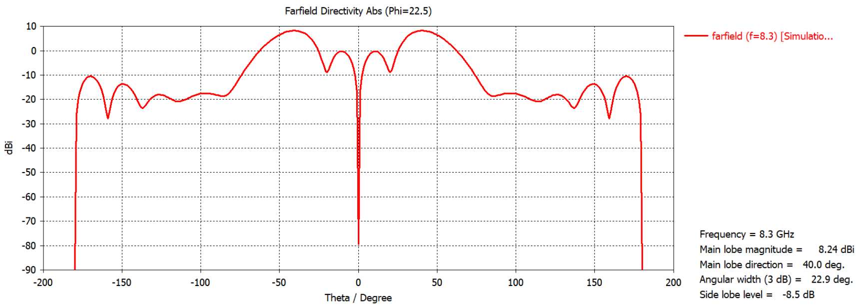

(d) 8.3 GHz

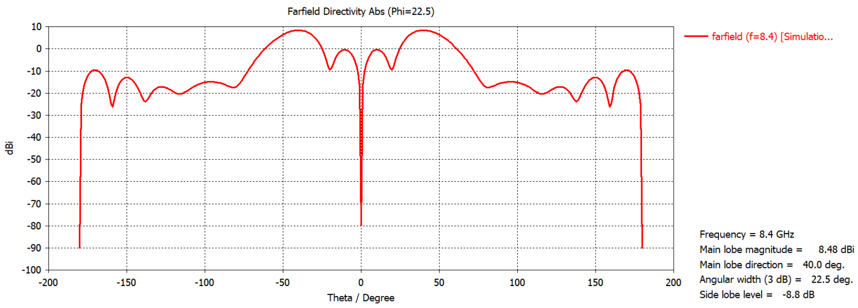

(e) 8.4 GHz

Figure 3.14 The Cartesian Radiation Patterns of 8-16 Antenna Array (ϕ=22.5°)

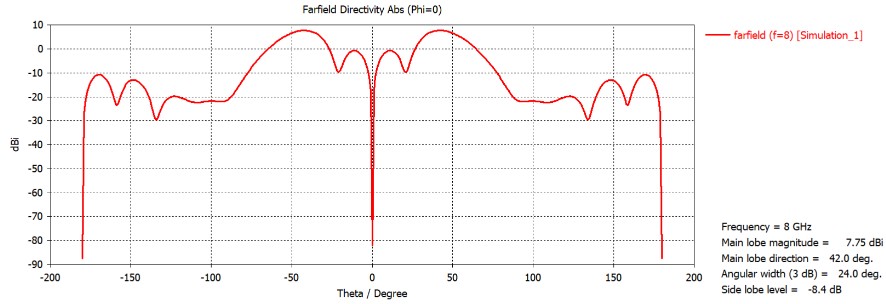

(a) 8 GHz

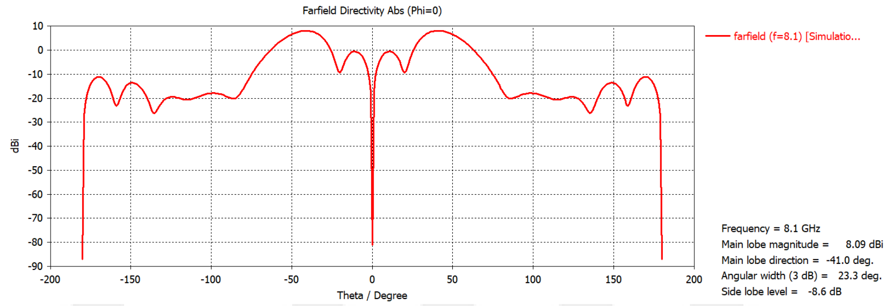

(b) 8.1 GHz

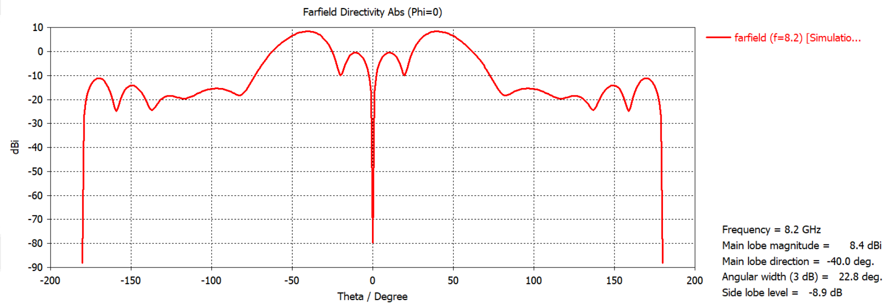

(c) 8.2 GHz

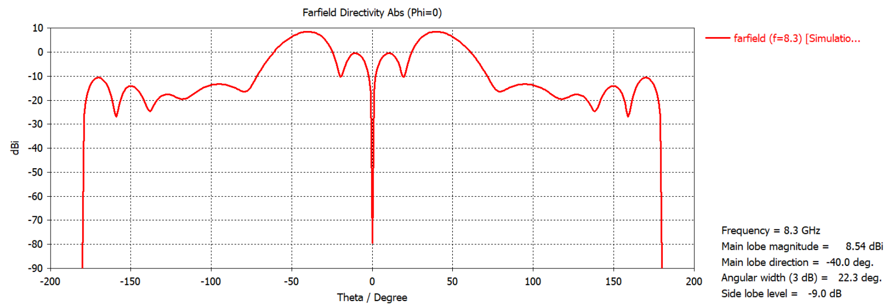

(d) 8.3 GHz

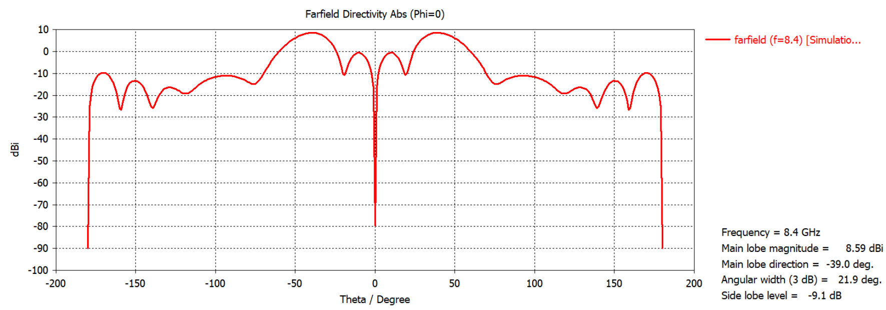

(e) 8.4 GHz

Figure 3.15 The Cartesian Radiation Patterns of 8-16 Antenna Array (ϕ=0°)

3.1.3 Design of the 4-8 Antenna Array without Feed Network

The 4-8 Antenna Array is shown in Figure 3.16 and the dimension of the array is shown in Figure 3.17.

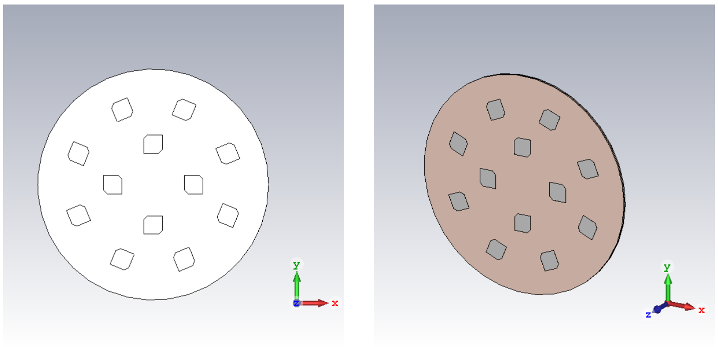

(a) Top view of the 4-8 Antenna Array

(b) Isometric view of the 4-8 Antenna Array

Figure 3.16 4-8 Antenna Array

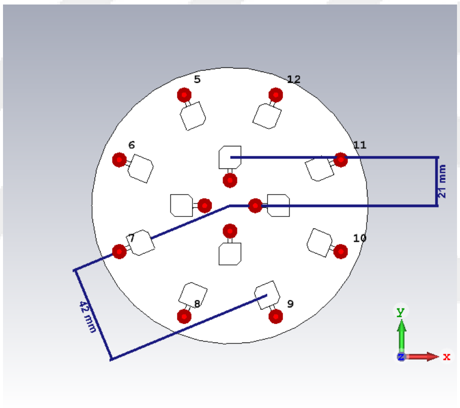

Figure 3.17 The dimension of the 4-8 Antenna Array

The following steps were taken to create the 4x8 microstrip patch antenna array.

- In this design 4 (four) microstrip patch antennas for the first ring and 8 (eight) microstrip patch antennas for the second ring are used.
- To create the isoflux pattern that shown in Figure 3.18, the radius of the first ring and the second ring are simulated as 21 mm and 42 mm respectively. The patch antennas are equally spaced by 45° (180°/4) in the first ring and 22.5° (180°/8) in the second ring as shown in Figure 3.17. The patch antennas and feed lines in the first and second row rings are arranged in opposite directions as shown in Figure 3.17 so that the feeding network can be designed easily. The amplitude of the first ring and second ring are 1 (one) and 0.5 (zero point five) respectively. The phase shift of the first ring and second ring are 0 (zero), so the phase difference between the first and second ring are 180° because of the feed line arrangement.

- The targeted inverse axial ratio to create circular polarization is between 0 and -10 dB. The inverse axial ratio of the array antenna for the ϕ values of 90°, 22.5° and 0° are shown in Figure 3.19, Figure 3.20 and Figure 3.21 respectively.
- In order to use the satellite antenna in LEO, the edge of the coverage for the LEO should be between 47.3° and 70.4° . So, targeted the minimum of the theta value is between $-47.3°$ and $47.3°$. The targeted maximum of the theta value is between $-70.4°$ and $70.4°$.
- The Cartesian Radiation Patterns for the ϕ values of 90°, 22.5° and 0° are shown in Figure 3.22, Figure 3.23 and Figure 3.24 respectively.

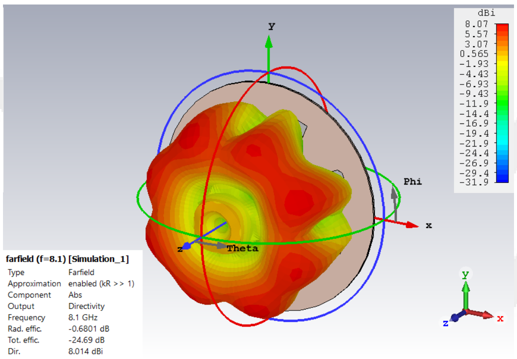

(a) 8 GHz

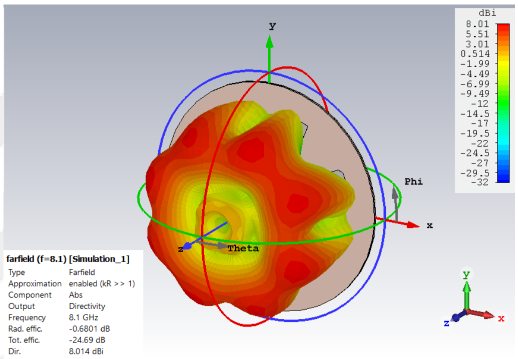

(b) 8.1 GHz

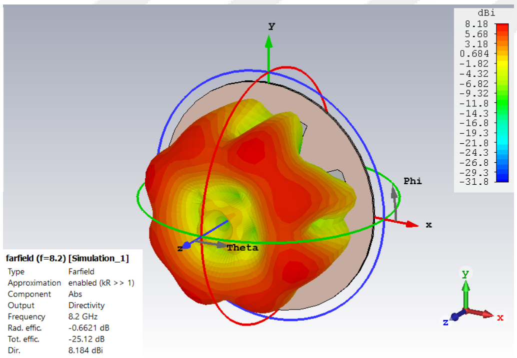

(c) 8.2 GHz

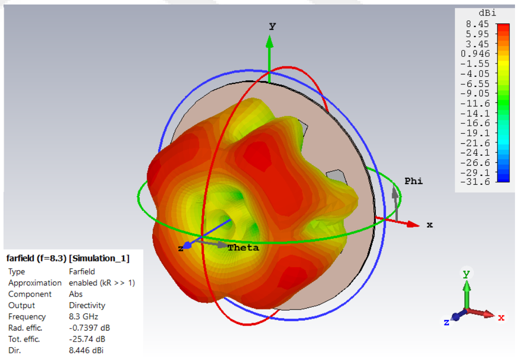

(d) 8.3 GHz

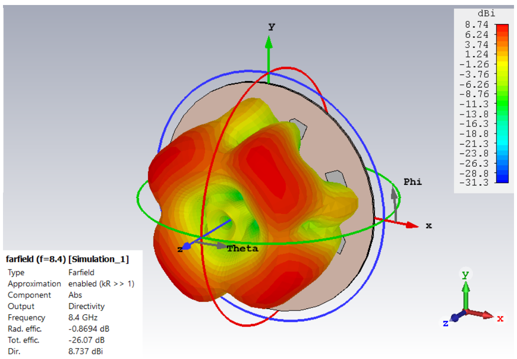

(e) 8.4 GHz

Figure 3.18 The 3D Radiation Patterns of 4-8 Antenna Array

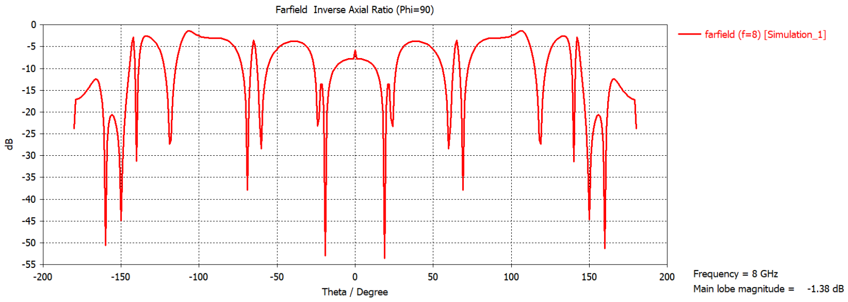

(a) 8 GHz

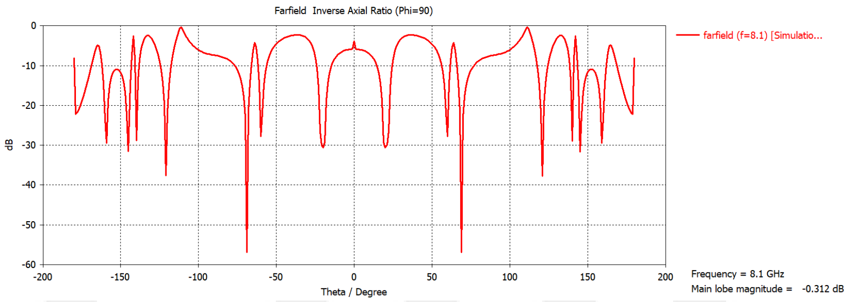

(b) 8.1 GHz

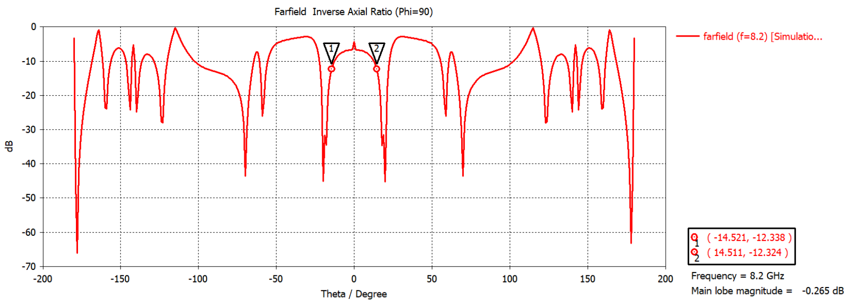

(c) 8.2 GHz

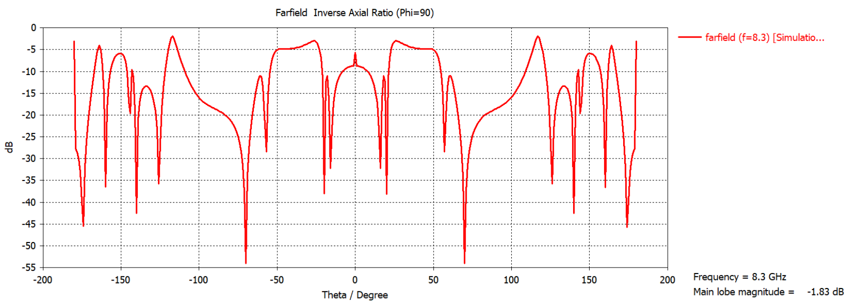

(d) 8.3 GHz

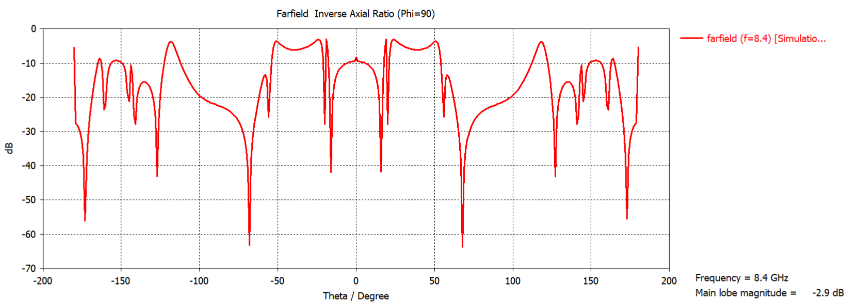

(e) 8.4 GHz

Figure 3.19 The Inverse Axial Ratios of 4-8 Antenna Array (ϕ=90°)

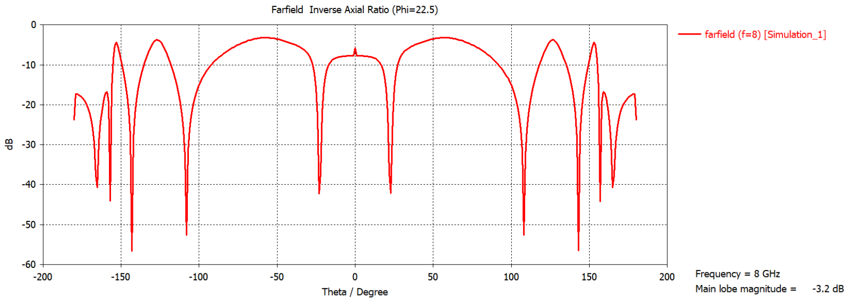

(a) 8 GHz

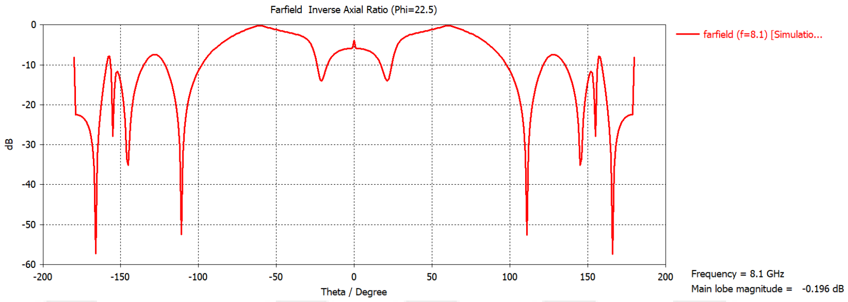

(b) 8.1 GHz

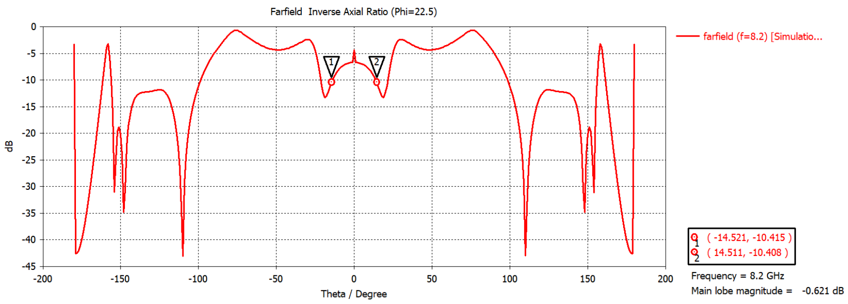

(c) 8.2 GHz

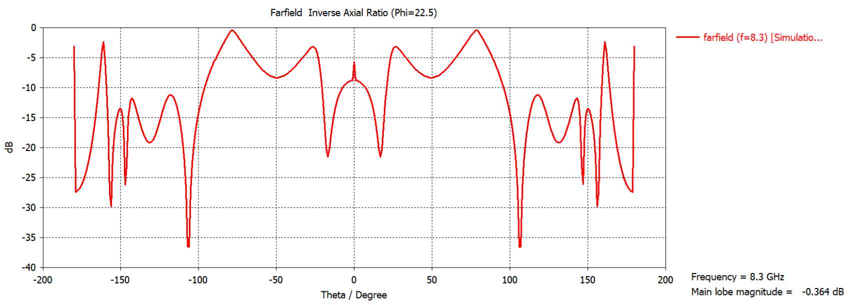

(d) 8.3 GHz

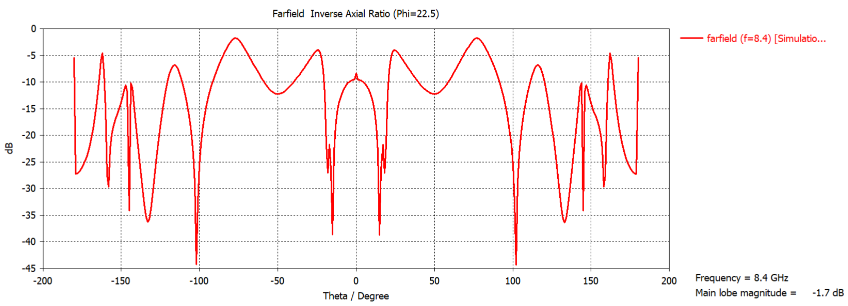

(e) 8.4 GHz

Figure 3.20 The Inverse Axial Ratios of 4-8 Antenna Array (ϕ=22.5°)

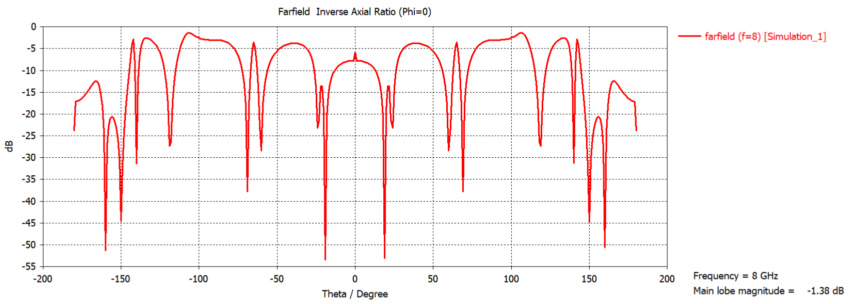

(a) 8 GHz

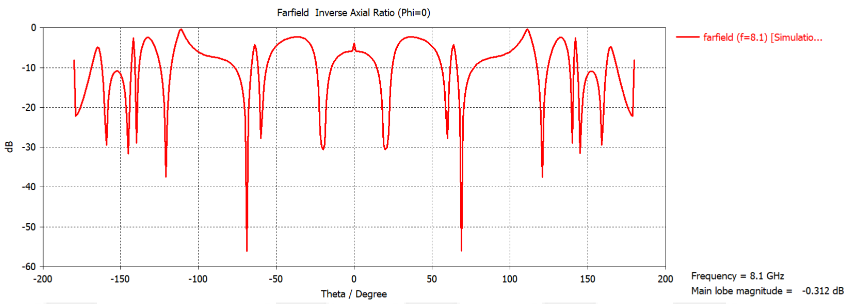

(b) 8.1 GHz

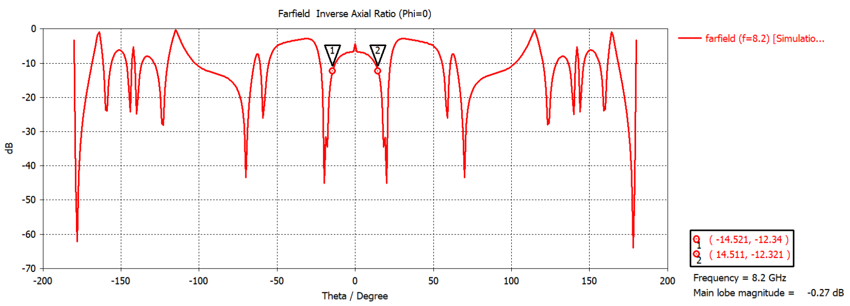

(c) 8.2 GHz

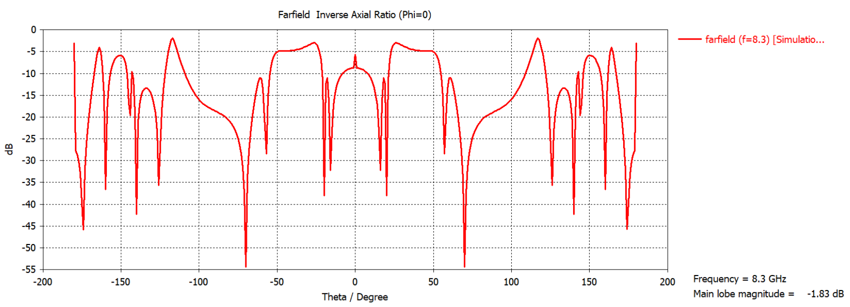

(d) 8.3 GHz

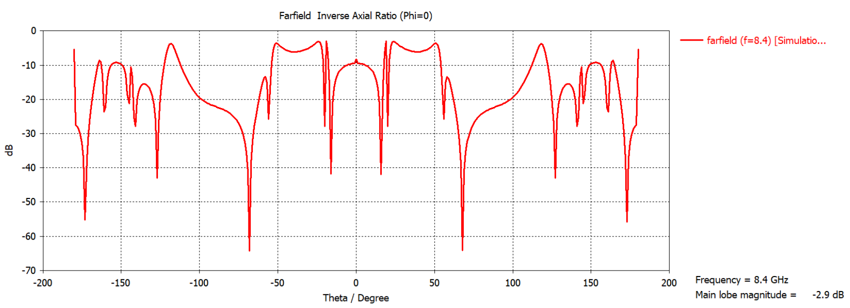

(e) 8.4 GHz

Figure 3.21 The Inverse Axial Ratios of 4-8 Antenna Array (ϕ=0°)

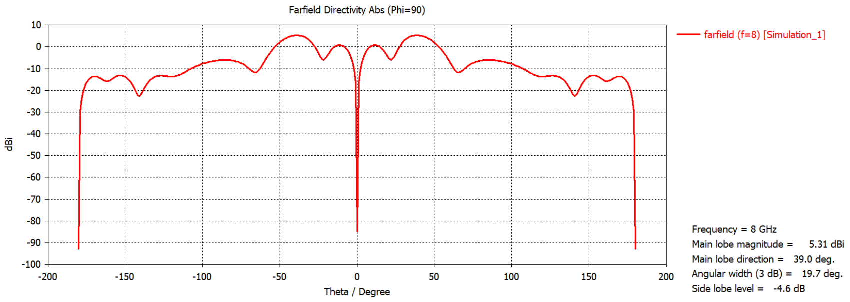

(a) 8 GHz

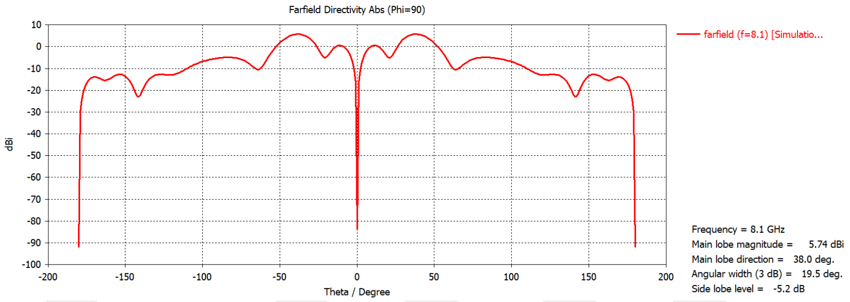

(b) 8.1 GHz

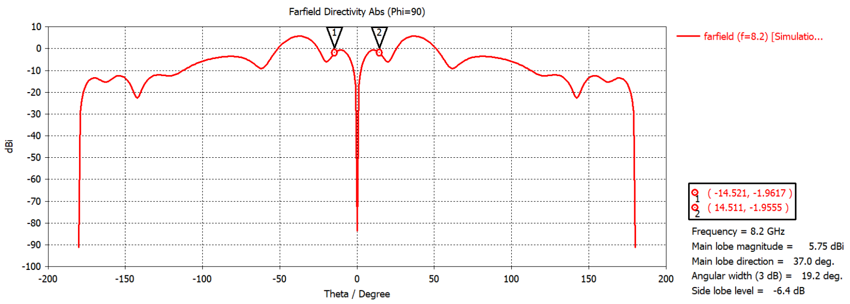

(c) 8.2 GHz

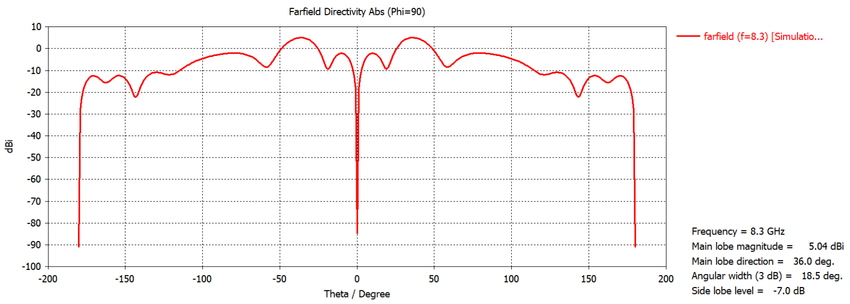

(d) 8.3 GHz

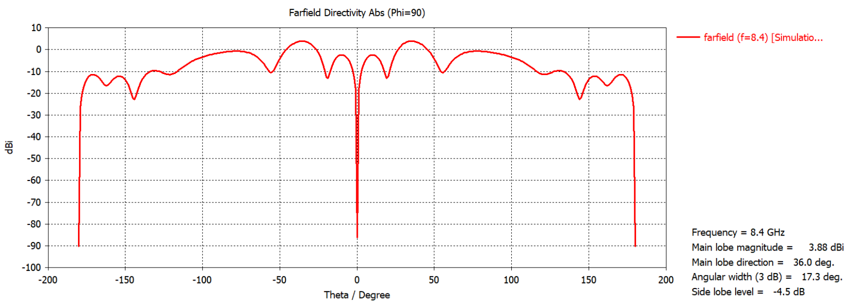

(e) 8.4 GHz

Figure 3.22 The Cartesian Radiation Patterns of 4-8 Antenna Array (ϕ=90°)

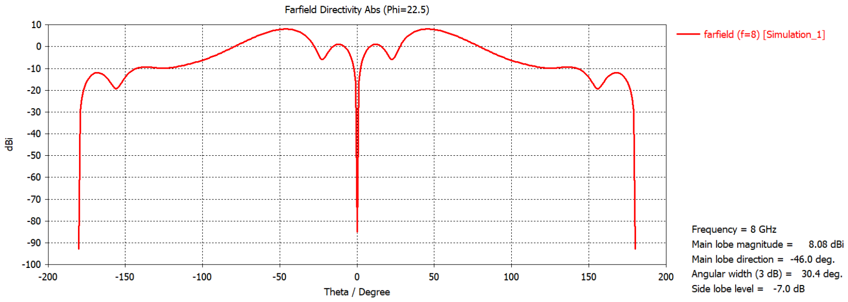

(a) 8 GHz

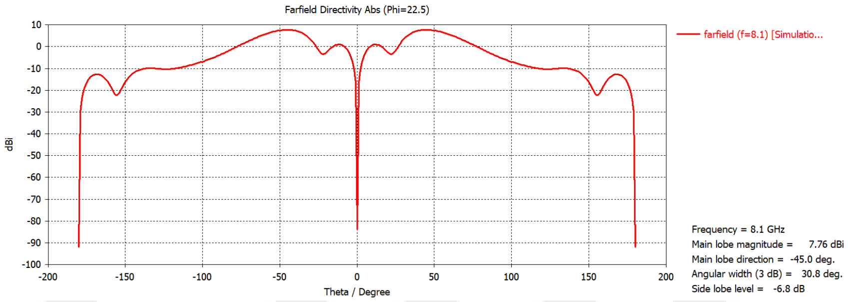

(b) 8.1 GHz

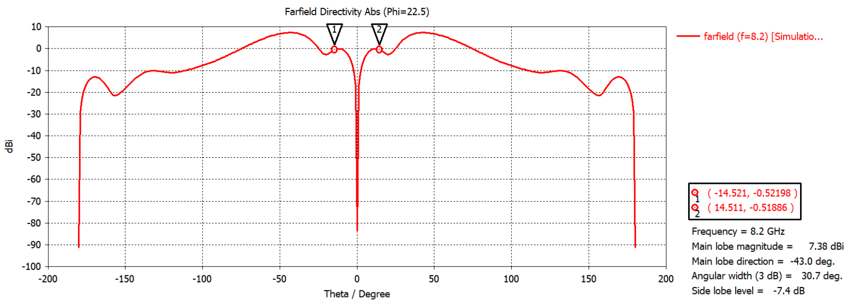

(c) 8.2 GHz

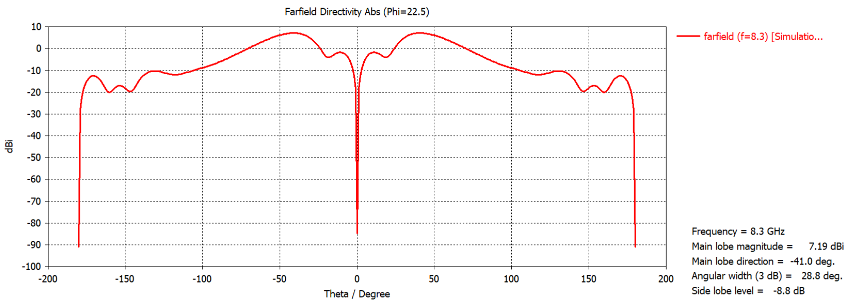

(d) 8.3 GHz

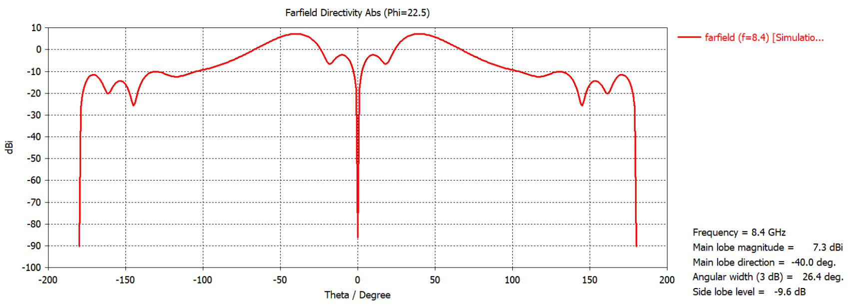

(e) 8.4 GHz

Figure 3.23 The Cartesian Radiation Patterns of 4-8 Antenna Array (ϕ=22.5°)

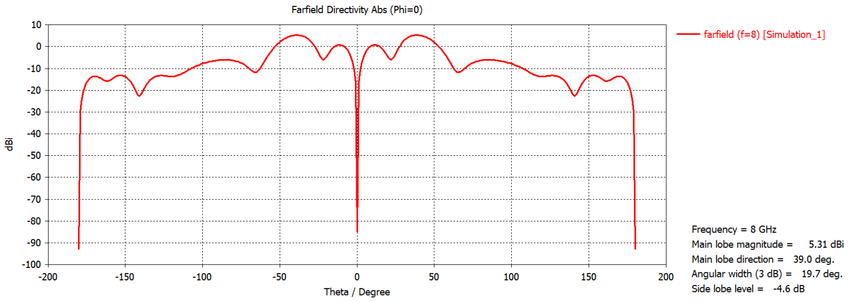

(a) 8 GHz

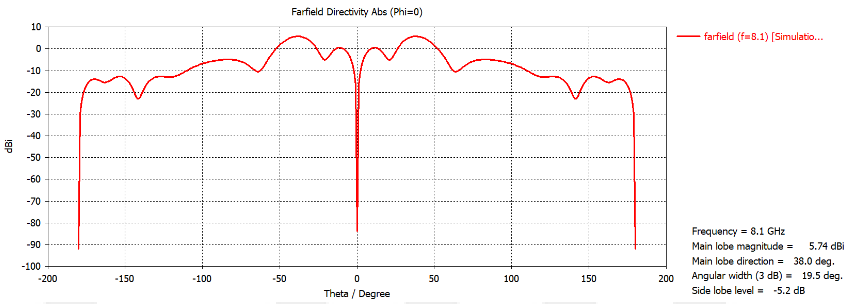

(b) 8.1 GHz

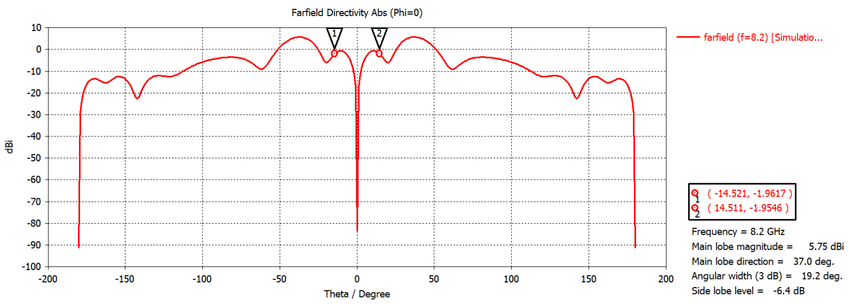

(c) 8.2 GHz

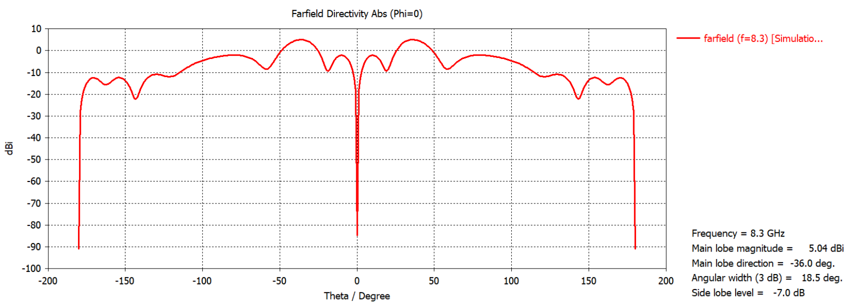

(d) 8.3 GHz

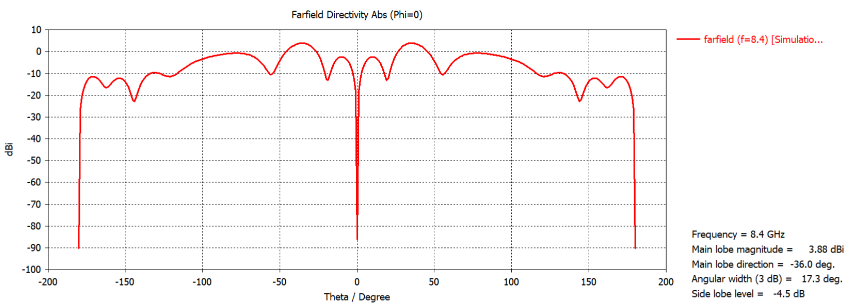

(e) 8.4 GHz

Figure 3.24 The Cartesian Radiation Patterns of 4-8 Antenna Array (ϕ=0°)

3.1.4 Design Feed Network for the 4-8 Antenna Array

Due to the size constraint of the RO3003, the paths of the feed network were designed as short as possible. However, the path connected to the power divider of ports 2, 3 and ports 4,5 and the path connected to the power divider of ports 6,7 and ports 8,9 in the Figure 3.26 were designed longer because of the coupling. Also, the path connected to the inner ring from the port 1 power divider were designed long because of the coupling.

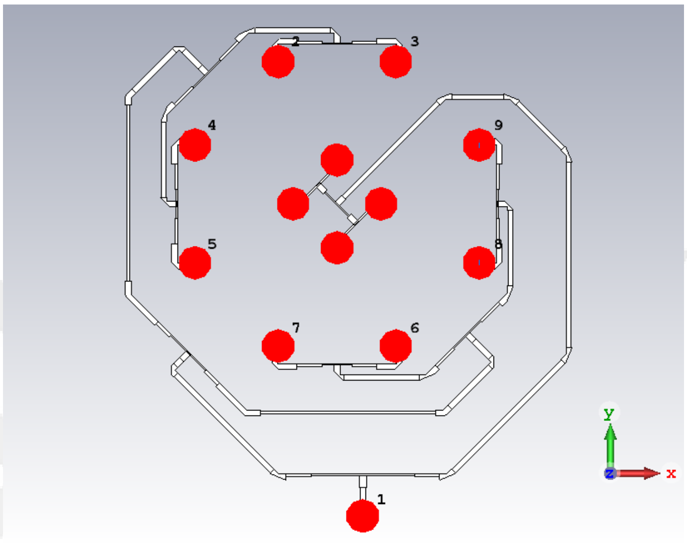

Figure 3.25 Top view of Feed Network

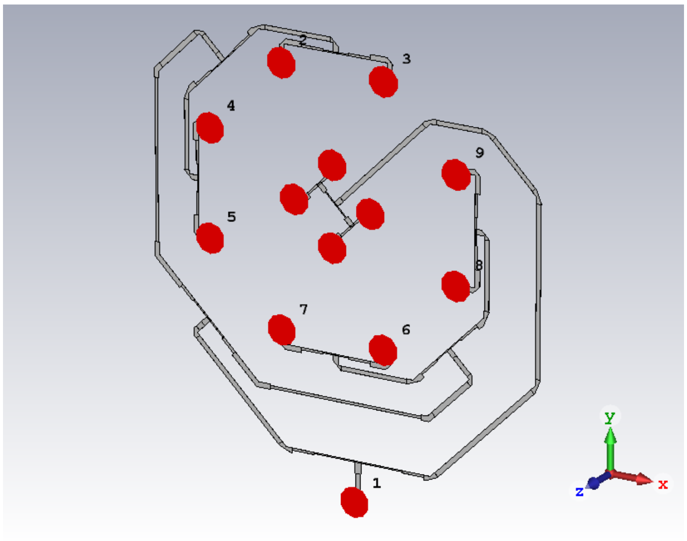

Figure 3.26 Isometric view of Feed Network

The phase difference between patches on the inner ring and outer ring should be 0 (zero). For this reason, the paths from patches on the inner ring to the port 1 power divider and the path from the patches on the outer ring to the port 1 power divider are adjusted as same. The phase difference between the patches is shown as in Figure 3.27.

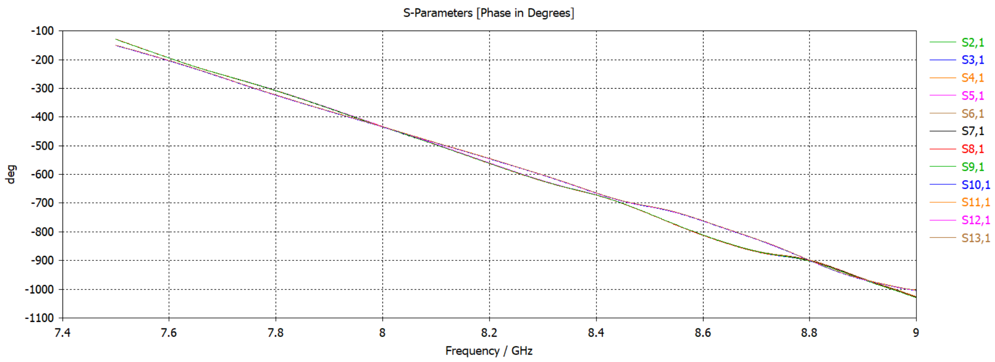

Figure 3.27 S parameter of the inner and outer patch antennas (Phase in Degrees)

The amplitude of the patches on the inner ring 1 (one) and the outer ring should be 0.5 (zero point five). For this reason, difference between inner and outer patches magnitude is approximately -3 dB as shown in Figure 3.28.

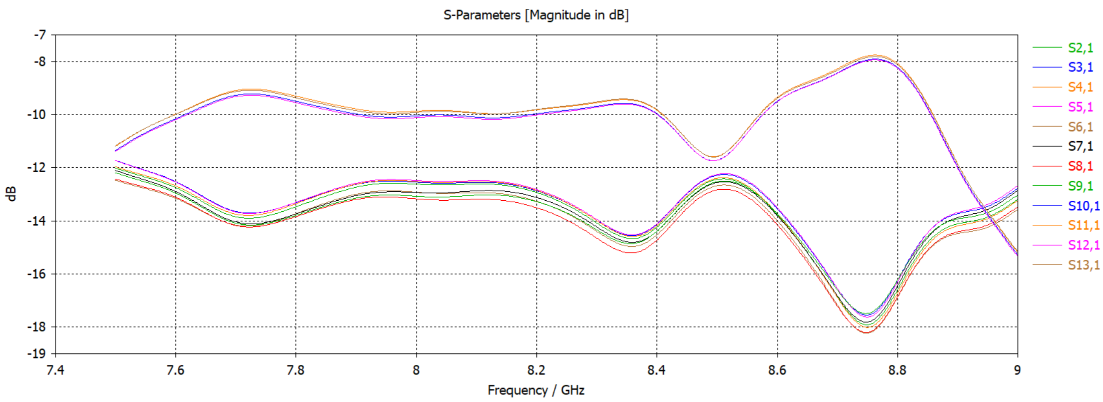

Figure 3.28 S parameter of the inner and outer patch antennas (Magnitude in dB)

The main purpose of the feed network is to adjust the magnitude and phase difference among the patch antennas and feed them one port. Therefore, the S parameter of the feed network shown in the Figure 3.29 is adjusted with the patch antennas.

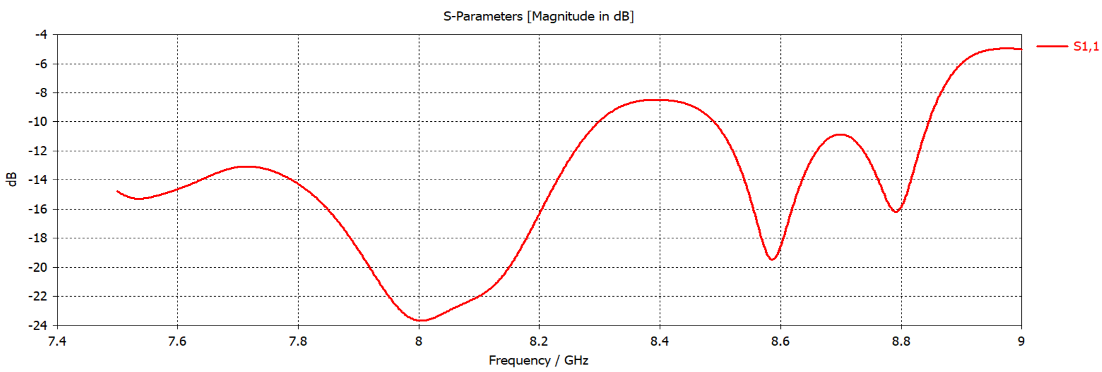

Figure 3.29 S parameter of the 4x8 Feed Network

3.1.5 Design of the 4-8 Antenna Array with Feed Network

For understanding the structure well, the 4-8 Antenna Array with Feed Network is shown in Figure 3.30 without the second dielectric layer between the patch antennas and feed network. By design of the feed network, the antenna is fed from a single port. The S parameter of the structure is shown in Figure3.31

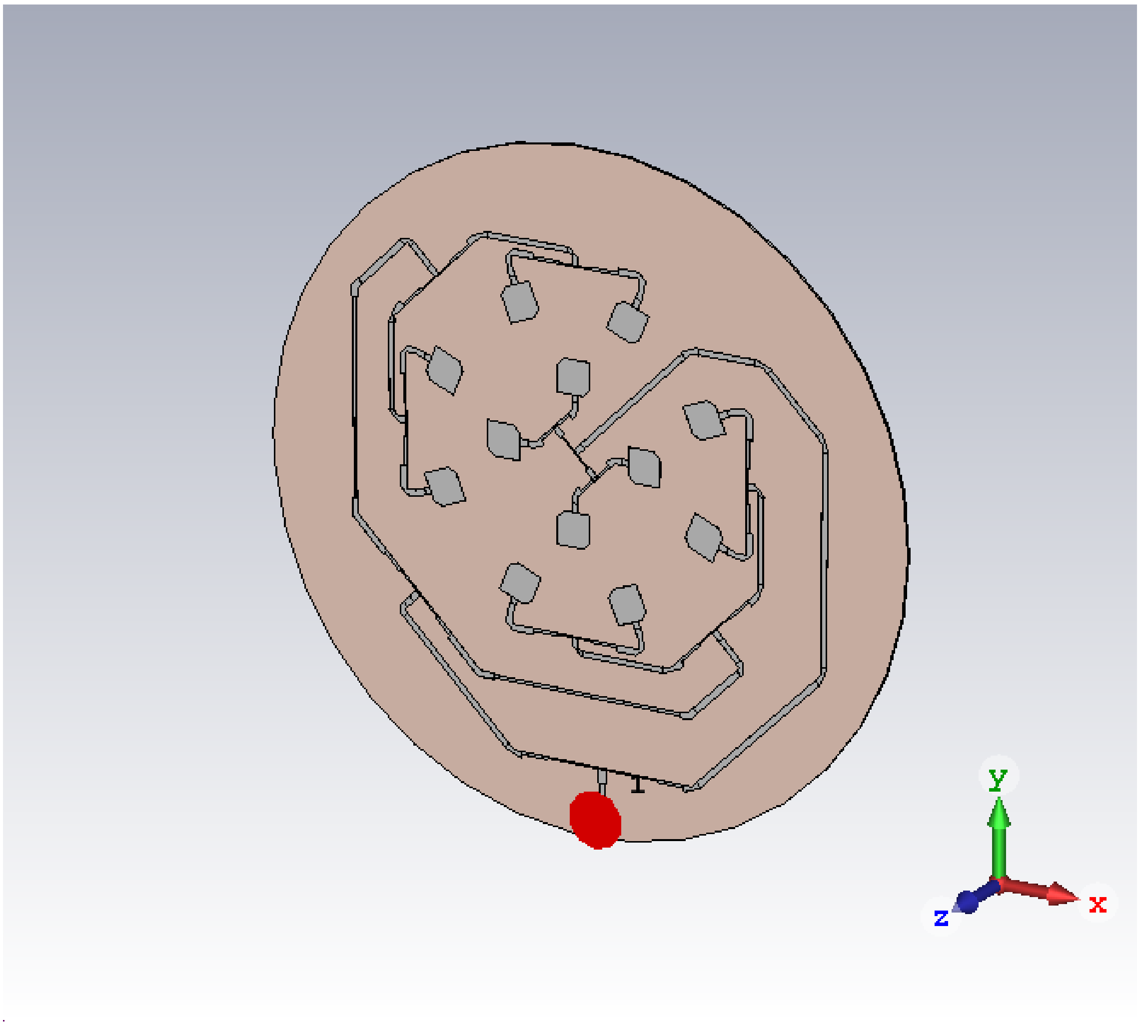

Figure 3.30 4x8 Antenna Array with Feed Network

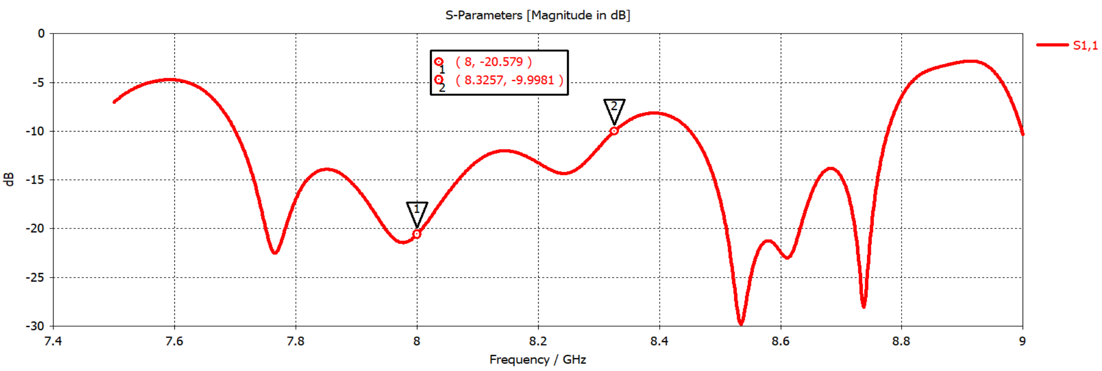

Figure 3.31 S parameter of the 4-8 Antenna Array with Feed Network

The isoflux pattern is distorted in some region due to the feed network and coupling as shown in Figure 3.32. The inverse axial ratios of the array antenna for the ϕ values of 90°, 22.5° and 0° are shown in Figure 3.33, Figure 3.34 and Figure 3.35 respectively. In order to use the satellite antenna in LEO, the edge of the coverage for the LEO should be between 47.3° and 70.4° . So, targeted the minimum of the theta value is between $-47.3°$ and 47.3°. The targeted maximum of the theta value is between $-70.4°$ and 70.4°.The Cartesian Radiation Patterns for the ϕ values of 90°, 22.5° and 0° are shown in Figure 3.36, Figure 3.37 and Figure 3.38 respectively.

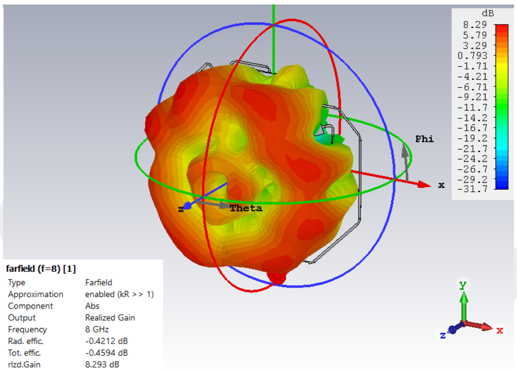

(a) 8 GHz

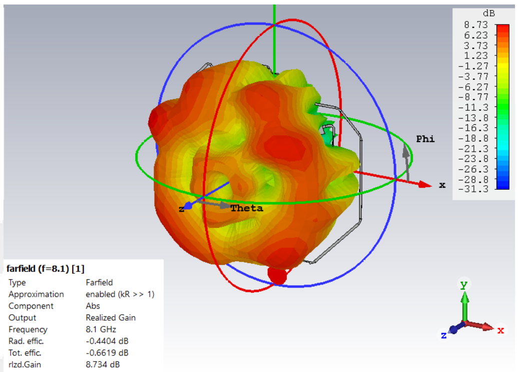

(b) 8.1 GHz

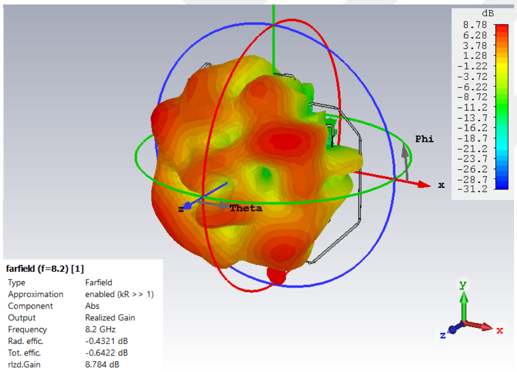

(c) 8.2 GHz

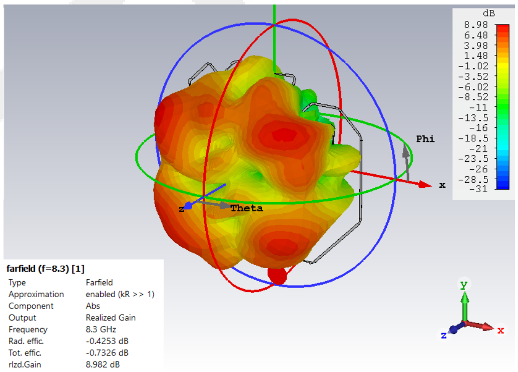

(d) 8.3 GHz

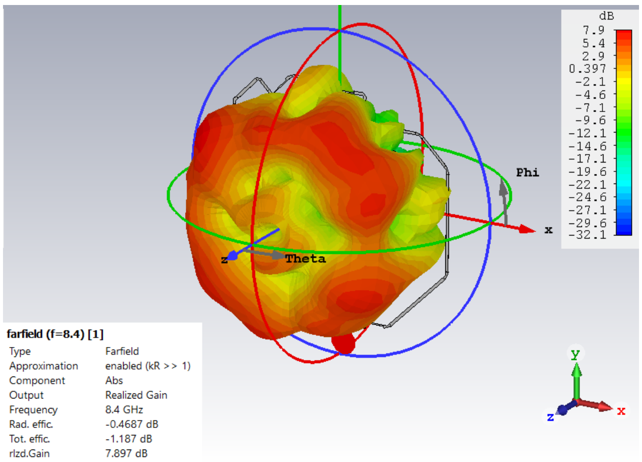

(e) 8.4 GHz

Figure 3.32 The 3D Radiation Patterns of 4-8 Antenna Array with Feed Network

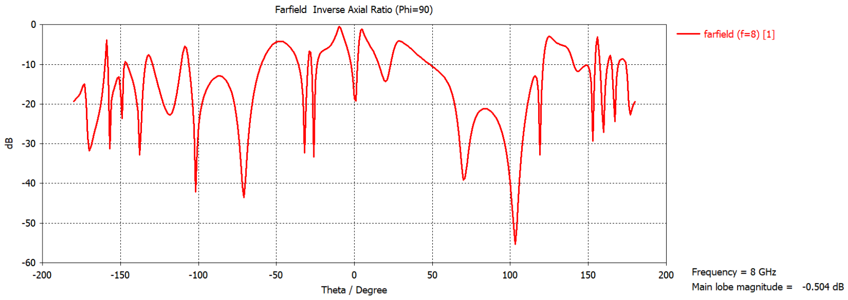

(a) 8 GHz

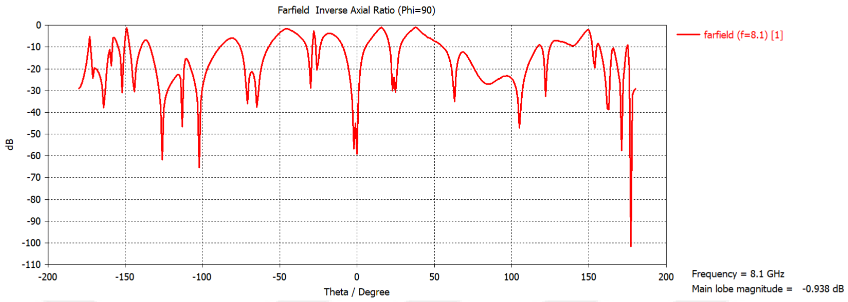

(b) 8.1 GHz

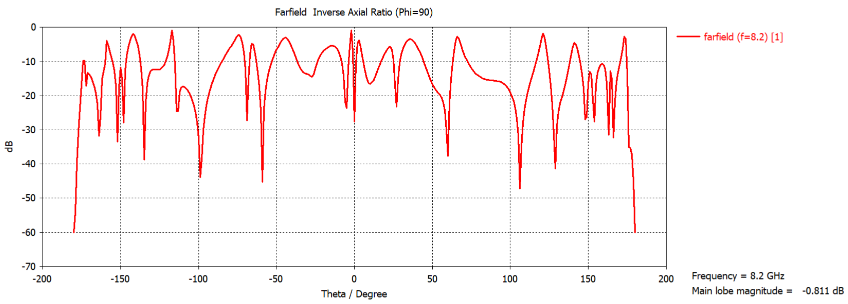

(c) 8.2 GHz

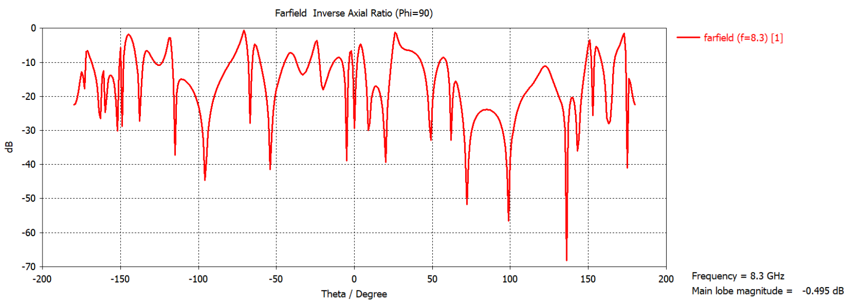

(d) 8.3 GHz

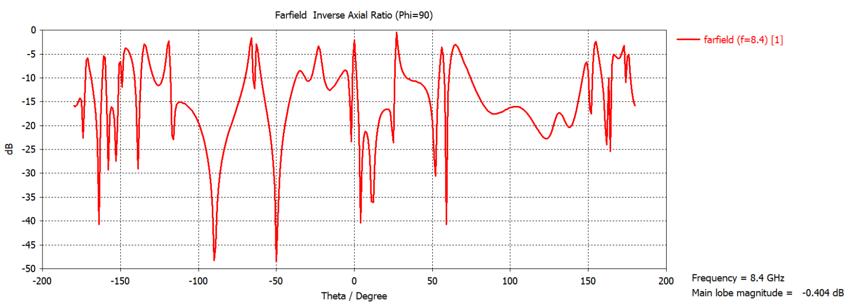

(e) 8.4 GHz

Figure 3.33 The Inverse Axial Ratios of 4-8 Antenna Array with Feed Network (ϕ=90°)

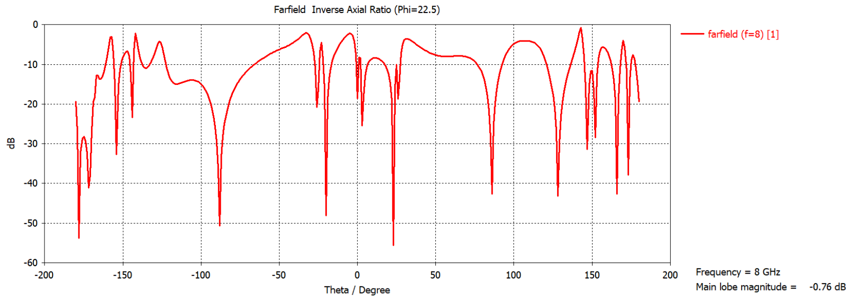

(a) 8 GHz

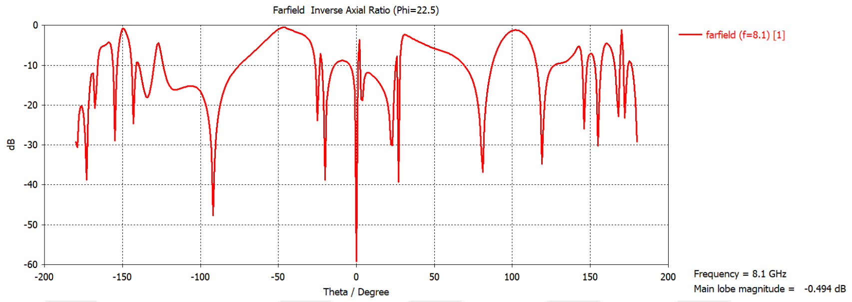

(b) 8.1 GHz

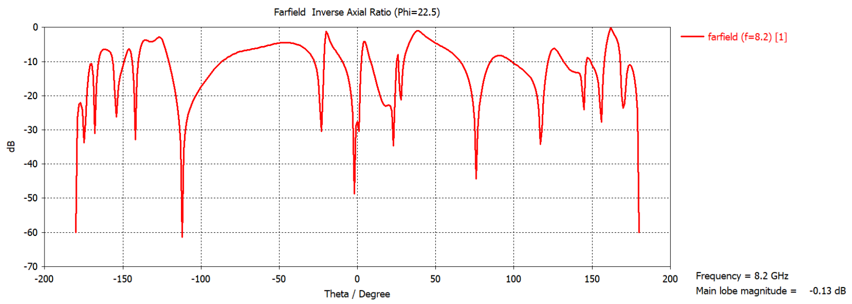

(c) 8.2 GHz

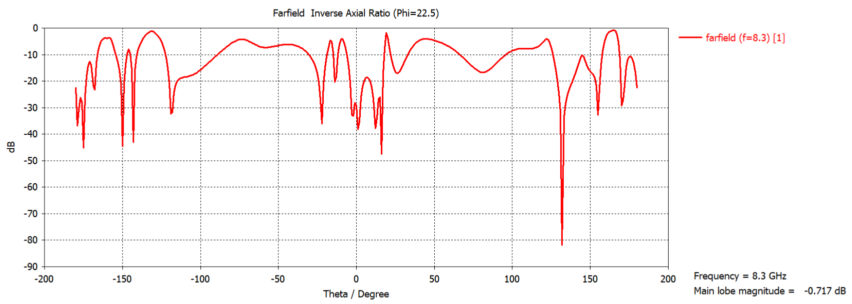

(d) 8.3 GHz

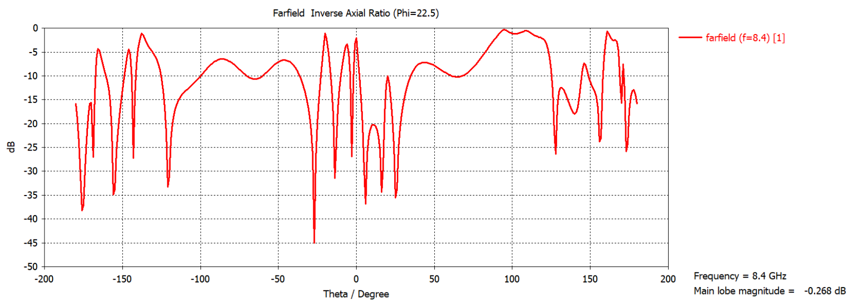

(e) 8.4 GHz

Figure 3.34 The Inverse Axial Ratios of 4-8 Antenna Array with Feed Network (ϕ=22.5°)

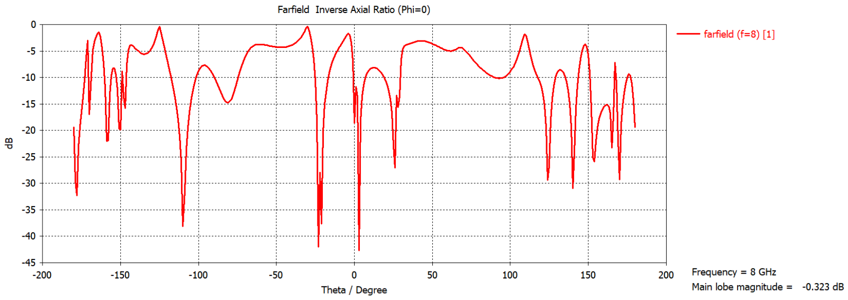

(a) 8 GHz

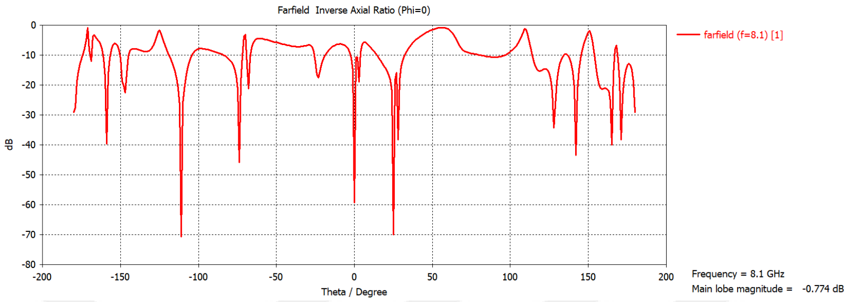

(b) 8.1 GHz

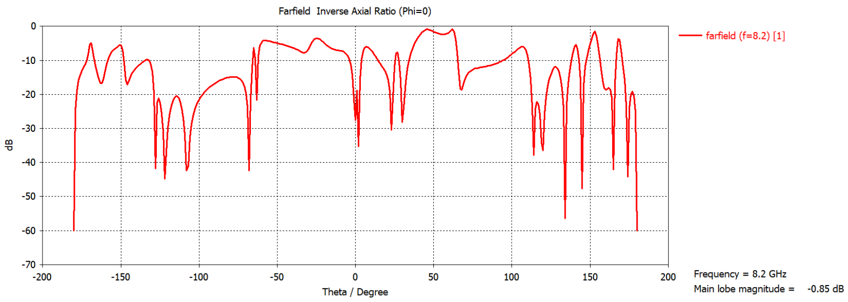

(c) 8.2 GHz

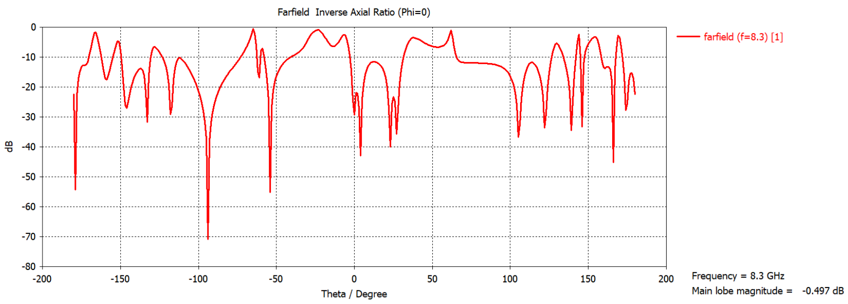

(d) 8.3 GHz

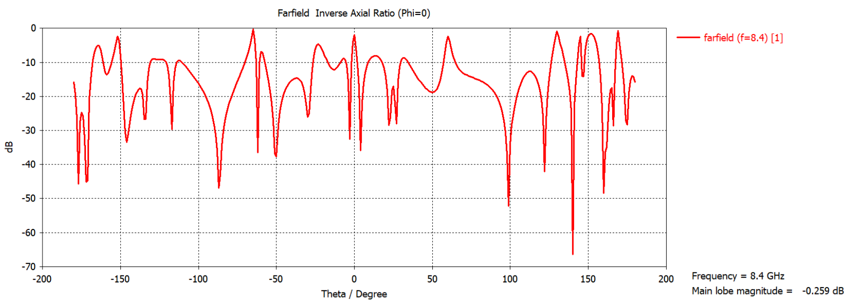

(e) 8.4 GHz

Figure 3.35 The Inverse Axial Ratios of 4-8 Antenna Array with Feed Network (ϕ=0°)

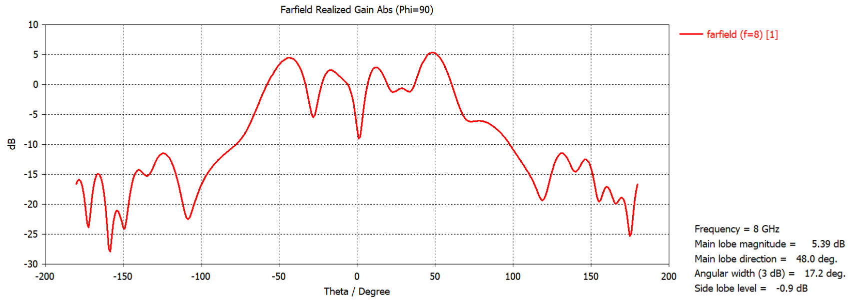

(a) 8 GHz

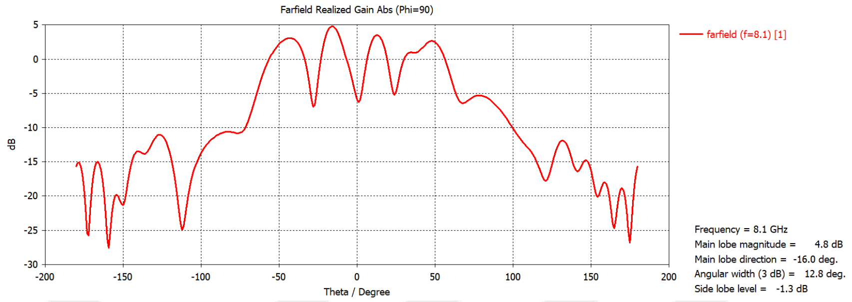

(b) 8.1 GHz

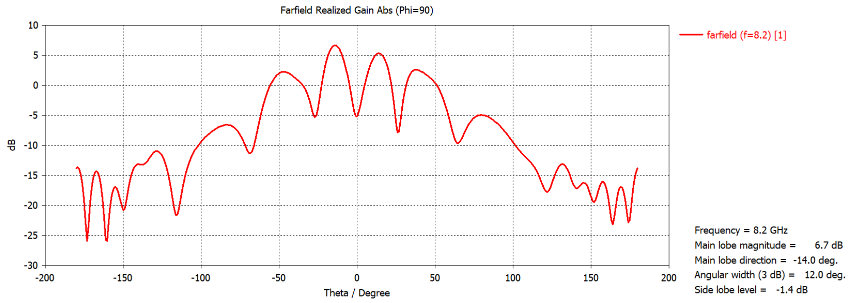

(c) 8.2 GHz

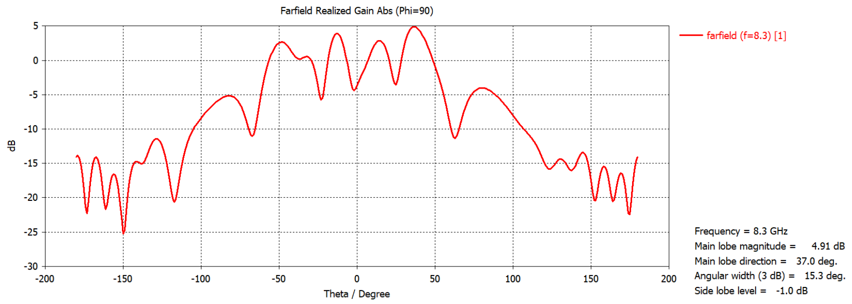

(d) 8.3 GHz

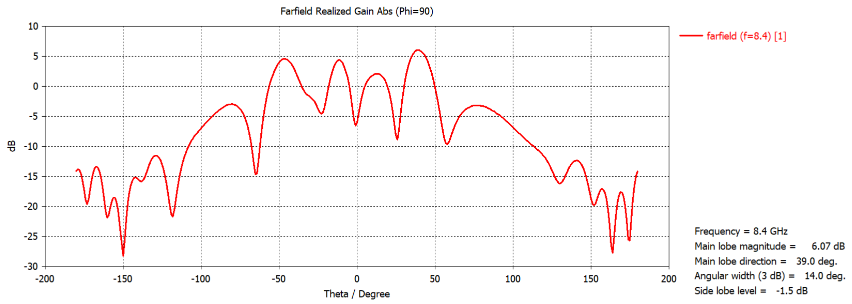

(e) 8.4 GHz

Figure 3.36 The Cartesian Radiation Patterns of 4-8 Antenna Array with Feed Network (ϕ=90°)

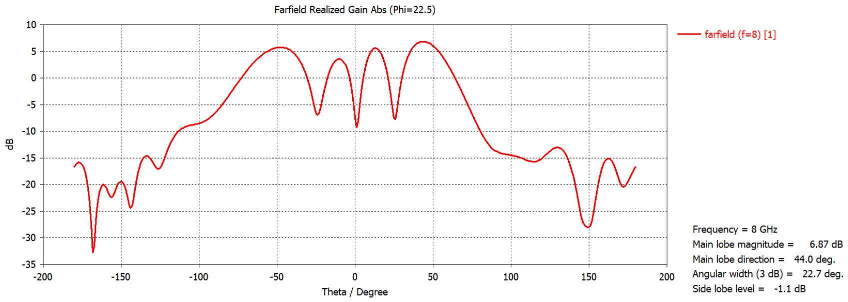

(a) 8 GHz

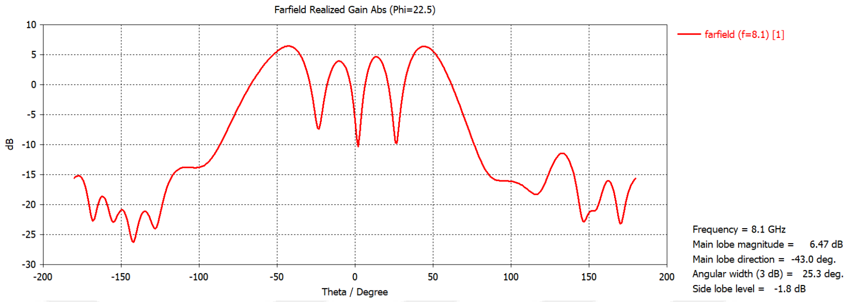

(b) 8.1 GHz

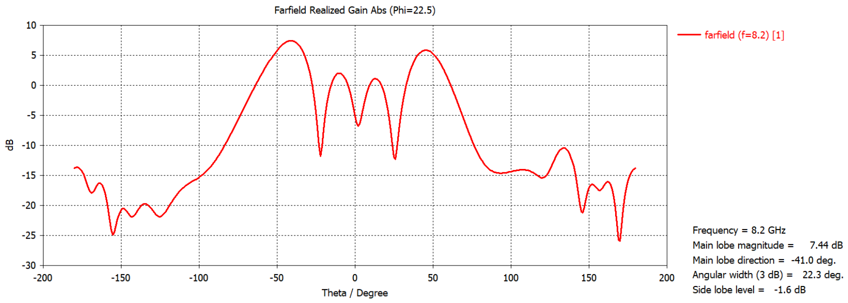

(c) 8.2 GHz

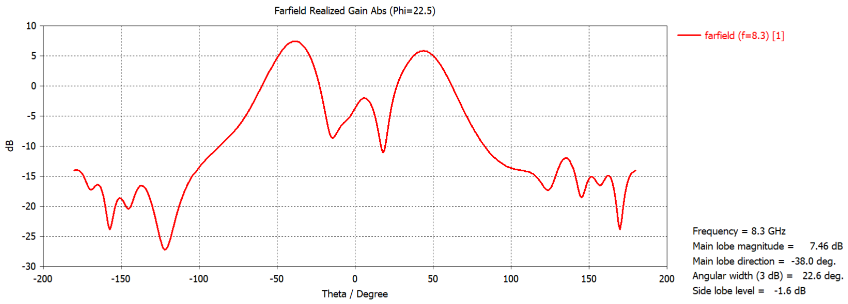

(d) 8.3 GHz

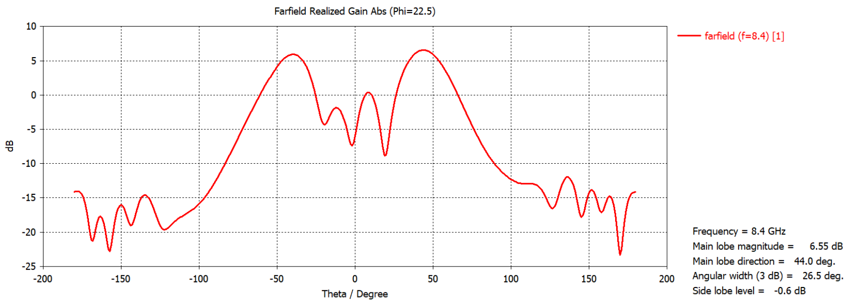

(e) 8.4 GHz

Figure 3.37 The Cartesian Radiation Patterns of 4-8 Antenna Array with Feed Network (ϕ=22.5°)

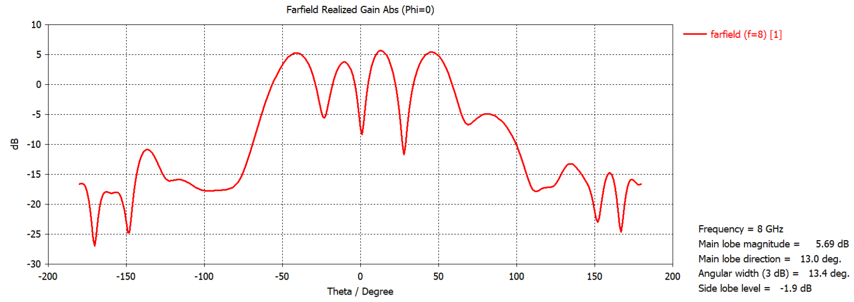

(a) 8 GHz

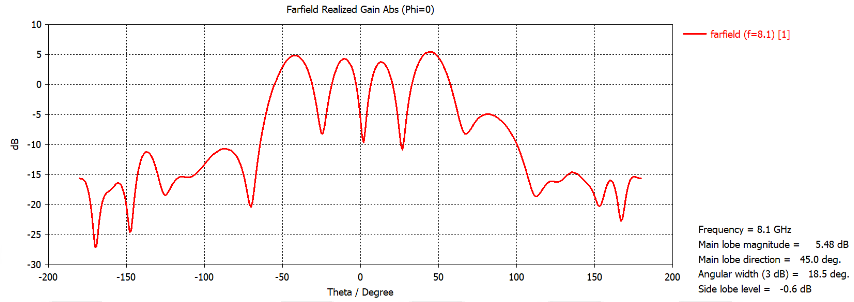

(b) 8.1 GHz

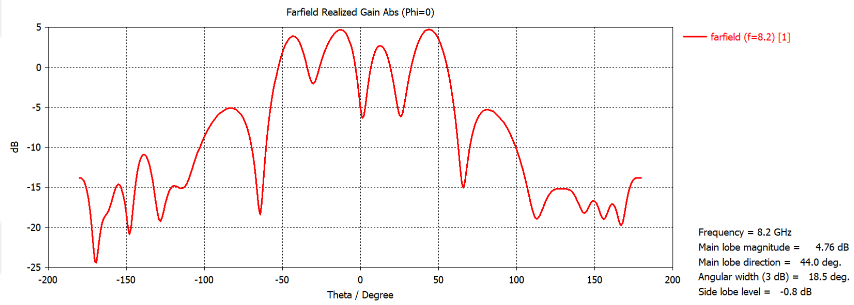

(c) 8.2 GHz

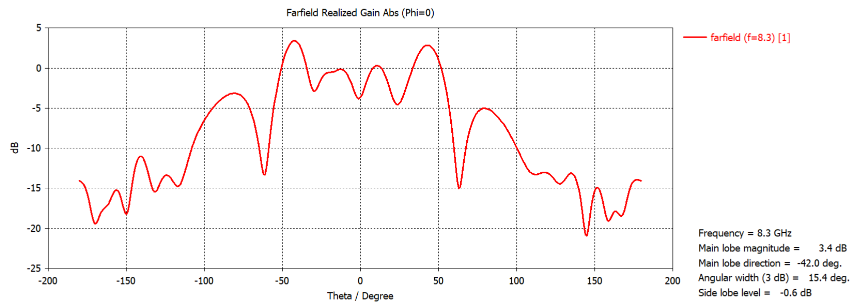

(d) 8.3 GHz

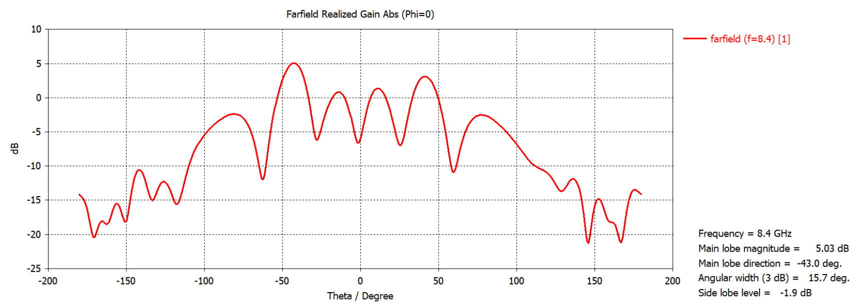

(e) 8.4 GHz

Figure 3.38 The Cartesian Radiation Patterns of 4-8 Antenna Array with Feed Network (ϕ=0°)

3.2 Simulated and Measured Result

The patch and feed network were produced individually as shown in Figure 3.42. After that, they were combined by the double-sided tape. The prototype 4x8 microstrip patch antenna array was produced and the results of the simulation and the measured values were compared. The radiation patterns and S_{11} parameter are measured at Laboratory of the RF-Microwave R&D [Yıldız Technical University RF LAB]. The measurements are obtained by the test arrangement as shown in Figure 3.39. By connecting SMA connector to the antenna as shown in Figure 3.40, the S_{11} parameter and radiation patterns were measured by spectrum analyzer which is illustrated in Figure 3.40. The reference antenna with linear polarization was used during the test. Therefore, our circular polarizing tested antenna has been tested like a linear antenna. Since our antenna array is a circular antenna array, therefore the measurement results were compared to the Ludwig 3 Horizontal and Ludwig 3 Vertical results found in the CST software in Figure 3.43 and Figure 3.44. The measured S-parameter has some differences according to the simulated S-parameter shown in Figure 3.41. The production and measurement errors can be the reason of these differences. They can also caused by the errors that occurred during the combining of the two layers. The path and feed network are on the different layers. Therefore there can be minor manufacturing errors when the two dielectric layers are combined.

(a) 1 **(b)** 2

Figure 3.39 The test arrangement

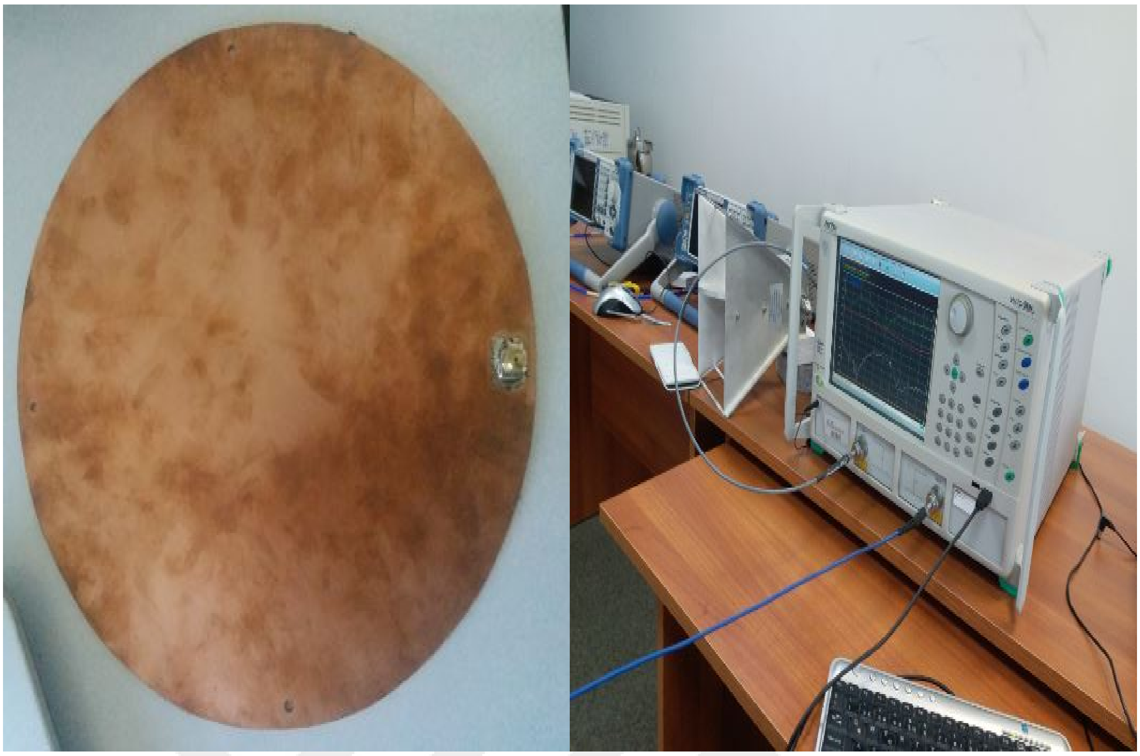

(a) The 50Ω SMA connector **(b)** The spectrum analyzer and reference antenna

Figure 3.40 The materials for the test equipment

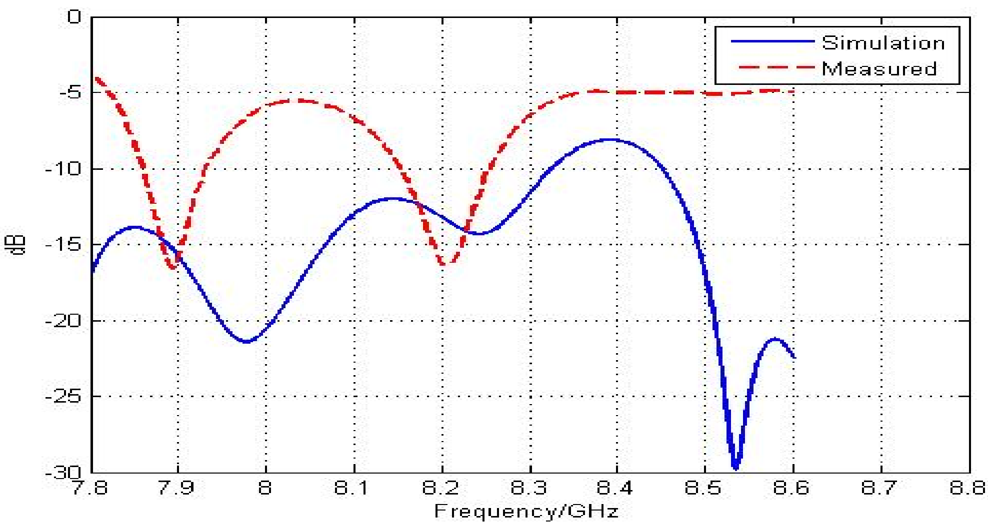

Figure 3.41 Comparison of the measurement and simulated S parameter

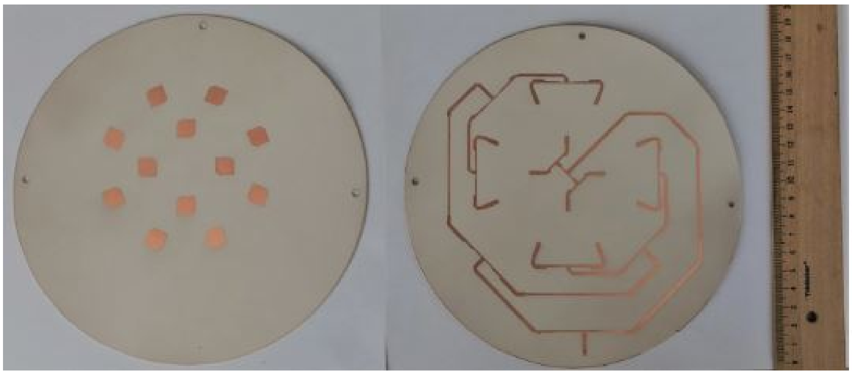

(a) Top view of the Patch and Feed Network

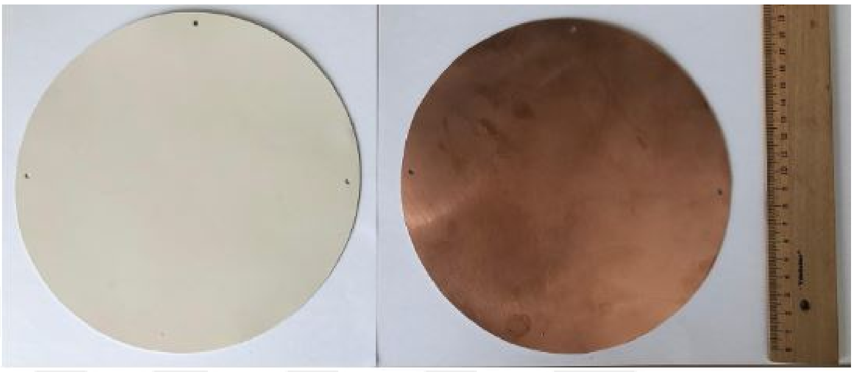

(b) Bottom view of the Patch and Feed Network

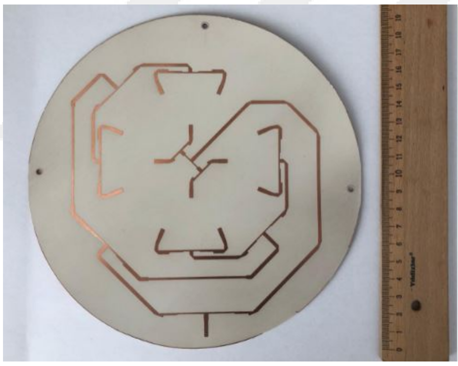

(c) Top view of the Patch

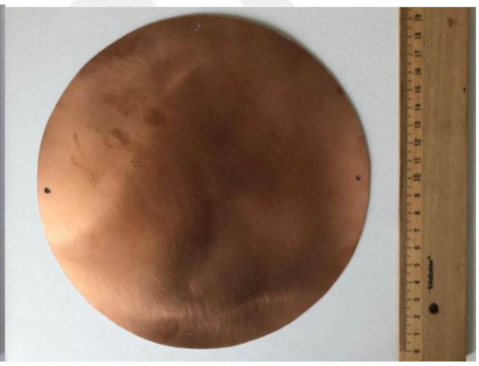

(d) Bottom view of the Patch

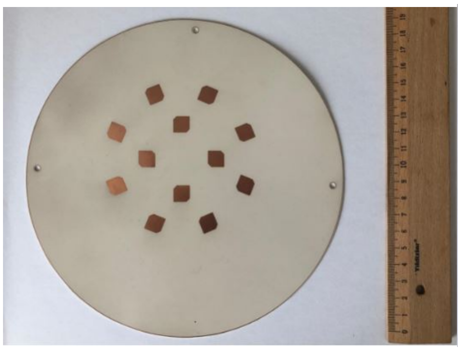

(e) Top view of the Feed Network

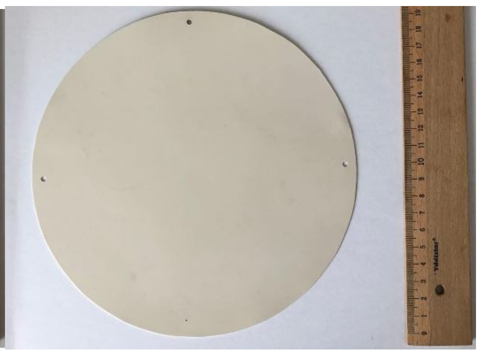

(f) Bottom view of the Feed Network

Figure 3.42 The Patch and Feed Network

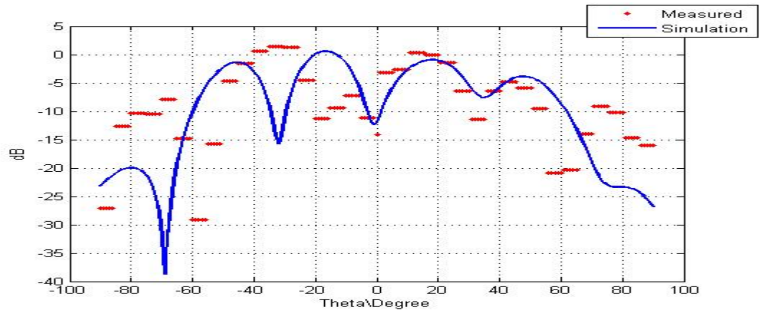

(a) The Ludwig 3 Horizontal at 8 GHz

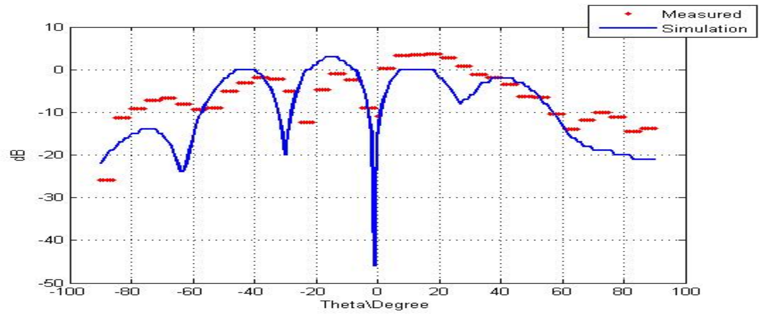

(b) The Ludwig 3 Horizontal at 8.1 GHz

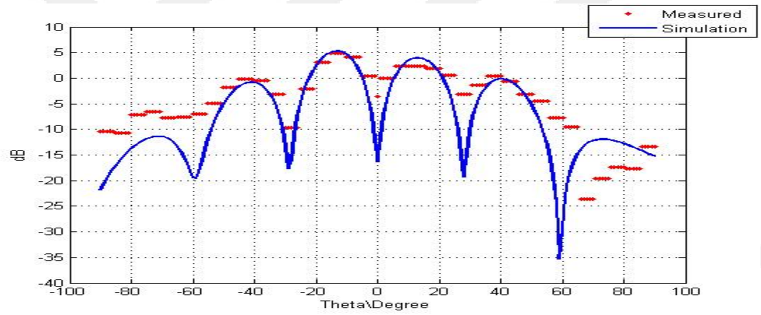

(c) The Ludwig 3 Horizontal at 8.2 GHz

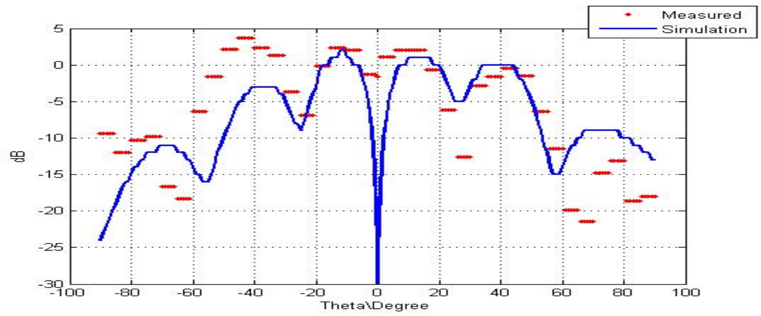

(d) The Ludwig 3 Horizontal at 8.3 GHz

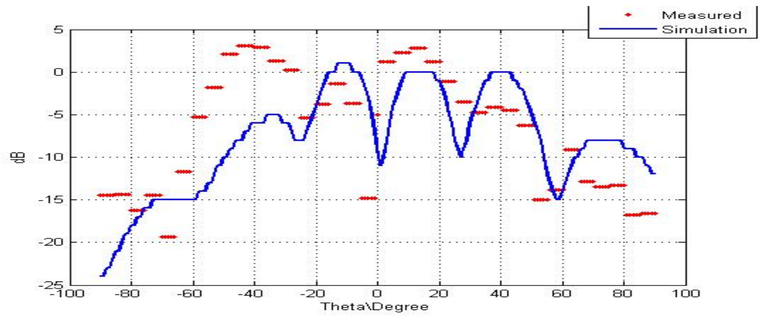

(e) The Ludwig 3 Horizontal at 8.4 GHz

Figure 3.43 The Ludwig 3 Horizontal

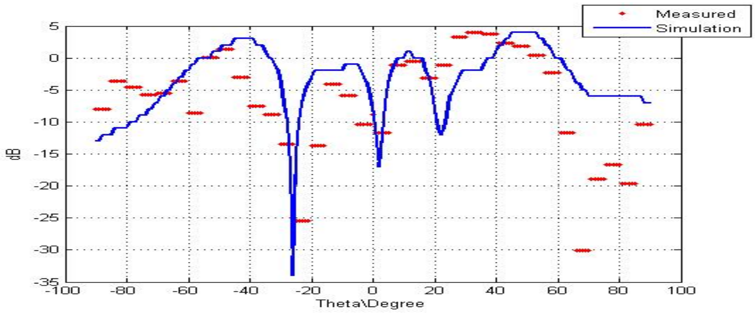

(a) The Ludwig 3 Vertical at 8 GHz

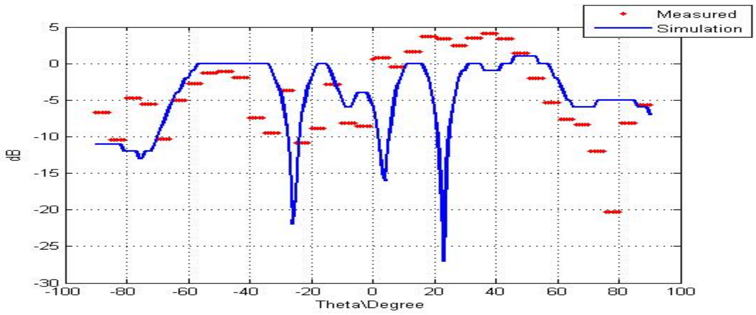

(b) The Ludwig 3 Vertical at 8.1 GHz

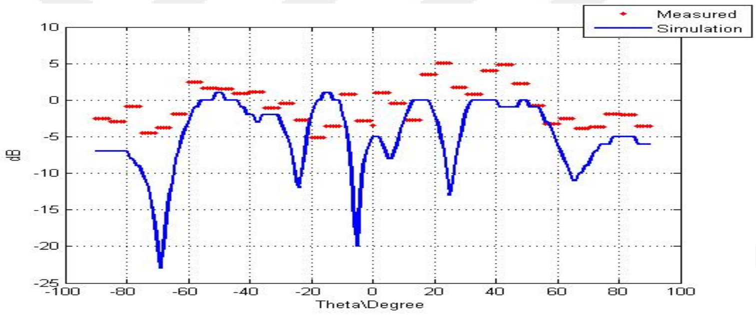

(c) The Ludwig 3 Vertical at 8.2 GHz

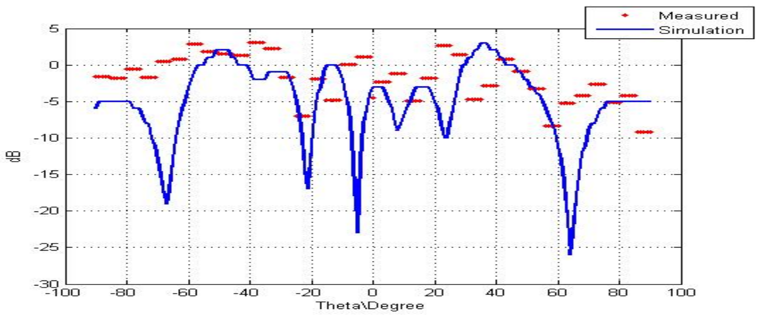

(d) The Ludwig 3 Vertical at 8.3 GHz

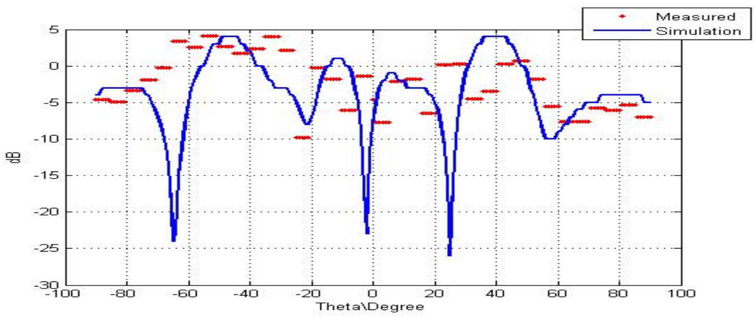

(e) The Ludwig 3 Vertical at 8.4 GHz

Figure 3.44 The Ludwig 3 Vertical

4
Conclusion and Discussions

The main purpose of this thesis is to provide an isoflux pattern operating at X-Band frequency. The antenna array design has been made by considering antenna parameters such as return loss, bandwidth, gain and polarization. The RO3003 is used as dielectric substrate for the wide bandwidth. In this project, the proposed array antenna is designed to operate in the 8 - 8.32 GHz band and can be used in LEO. The antenna array is designed as 8-16 and thus the isoflux radiation pattern is created. The following steps were taken to create the Isoflux pattern.

- The amplitude of the patches on the inner ring and the outer ring are designed to be 1 (one) and 0.5 (zero point five) respectively. For this reason, difference between inner and outer patches magnitude is approximately -3 dB.
- The phase difference between patches on the inner ring and outer ring are designed to be 0 (zero).
- The inverse axial ratio to create circular polarization is designed to be between 0 and -10 dB.
- In order to use the satellite antenna in LEO, the edge of the coverage for the LEO should be between 47.3° and 70.4° . Therefore, theta values are designed to be between $-47.3°$ and 47.3°.

After forming the desired radiation pattern, the design of the 4-8 antenna array and its feed network are made for the prototype. The 4-8 antenna array with feed network is manufactured . Since the number of the antennas are decreased, the pattern characteristics of some ϕ values are not as desired. The pattern where the axial ratio is good is also good. The measurement errors and S_{11} differences have been occurred in this thesis because of the two dielectric substrate layers. The isoflux pattern is achieved by less number of the microstrip antennas.

References

[1] W. Nawaz and A. S. Ali, “Improvement of gain in dual fed x band isoflux choke horn antenna for use in leo satellite mission,” in *2015 Fourth International Conference on Aerospace Science and Engineering (ICASE)*, IEEE, 2015, pp. 1–4.

[2] J.-W. Kim and J.-M. Woo, “A design of isoflux radiation pattern microstrip patch antenna for leo medium-sized satellites,” *The Journal of The Korea Institute of Intelligent Transport Systems*, vol. 14, no. 2, pp. 24–29, 2015.

[3] J. Fouany, M. Thévenot, E. Arnaud, F. Torres, T. Monediere, N. Adnet, R. Manrique, L. Duchesne, J. Baracco, and K. Elis, “Circurlaly polarized isoflux compact x band antenna for nano-satellites applications,” in *2015 European Radar Conference (EuRAD)*, IEEE, 2015, pp. 381–384.

[4] J. Wettergren, P. Dimming, J. F. Johansson, and M. Öhgren, “A high gain x-band isoflux helix antenna,” in *2016 10th European Conference on Antennas and Propagation (EuCAP)*, IEEE, 2016, pp. 1–4.

[5] H. Zhu, S. Cheung, K. L. Chung, and T. I. Yuk, “Linear-to-circular polarization conversion using metasurface,” *IEEE Transactions on Antennas and Propagation*, vol. 61, no. 9, pp. 4615–4623, 2013.

[6] M. A. El-Hassan, K. Hussein, A. Farahat, and K. Awadalla, “Performance assessment of straight and l-shaped probe fed u-slotted patch antenna arrays for sar applications,” in *2017 Intl Conf on Advanced Control Circuits Systems (ACCS) Systems & 2017 Intl Conf on New Paradigms in Electronics & Information Technology (PEIT)*, IEEE, 2017, pp. 232–238.

[7] S. M. Mousavi and S. A. Mirtaheri, “Design, implementation and test of a broadband isoflux beam reflectarray antenna for geo satellites,” *Journal of ElEctromagnEtic WavEs and applications*, vol. 30, no. 5, pp. 626–636, 2016.

[8] A. Reyna, M. A. Panduro, and C. del Rio Bocio, “A new reconfigurable wide coverage pattern by optimizing a microstrip patch antenna array,” in *2013 IEEE Antennas and Propagation Society International Symposium (APSURSI)*, IEEE, 2013, pp. 1440–1441.

[9] A. Reyna Maldonado, M. A. Panduro, C. del Rio Bocio, and A. L. Mendez, “Design of concentric ring antenna array for a reconfigurable isoflux pattern,” *Journal of Electromagnetic Waves and Applications*, vol. 27, no. 12, pp. 1483–1495, 2013.

[10] M. Ibarra, A. Reyna, M. A. Panduro, and C. del Rio-Bocio, “Design of aperiodic planar arrays for desirable isoflux radiation in geo satellites,” in *2011 IEEE International Symposium on Antennas and Propagation (APSURSI)*, IEEE, 2011, pp. 3003–3006.

[11] C. A. Balanis, *Antenna theory: analysis and design*. John wiley & sons, 2016.

[12] F. T. Ulaby, E. Michielssen, and U. Ravaioli, "Fundamentals of applied electromagnetics 6e," *Boston, Massachussetts: Prentice Hall*, 2010.

[13] W. L. Stutzman and G. A. Thiele, *Antenna theory and design*. John Wiley & Sons, 2013.

[14] G. Kumar and K. P. Ray, *Broadband microstrip antennas*. Artech house, 2003.

[15] S. Bisht, S. Saini, D. Prakash, and B. Nautiyal, "Study the various feeding techniques of microstrip antenna using design and simulation using cst microwave studio," 2014.

[16] A. K. Maini and V. Agrawal, *Satellite technology: principles and applications*. John Wiley & Sons, 2011.

[17] M. Oliaei, R. A. Sadeghzadeh, and Y. M. B. Ekhtiar, "Small size dropping cross dipole antenna with isoflux pattern in c band for leo satellites," in *2015 Loughborough Antennas & Propagation Conference (LAPC)*, IEEE, 2015, pp. 1–3.

Publications From the Thesis

Contact Information: alpaguelif@gmail.com

Conference Papers

1. 1. Uluslararası Avrasya Uygulamalı Bilimler Kongresi syf 10. 30 Kasım – 2 Aralık 2018